



A University of Sussex PhD thesis

Available online via Sussex Research Online:

<http://sro.sussex.ac.uk/>

This thesis is protected by copyright which belongs to the author.

This thesis cannot be reproduced or quoted extensively from without first obtaining permission in writing from the Author

The content must not be changed in any way or sold commercially in any format or medium without the formal permission of the Author

When referring to this work, full bibliographic details including the author, title, awarding institution and date of the thesis must be given

Please visit Sussex Research Online for more information and further details

The Flavour Of Warped Extra Dimensions

Andrew Granger

Submitted for the degree of Doctor of Philosophy
University of Sussex
September 2015

Acknowledgements

I would like to thank all the members of the Theoretical Particle Physics Group at Sussex who have helped make my PhD enjoyable, informative and stimulating. I have greatly enjoyed the many interesting talks, seminars, lunchtime and coffee conversations, of which I have had the privilege to be a part. I would like to thank my supervisor Sebastian Jäger for ongoing guidance, encouragement and personally teaching me much of the physics I have learnt during my time at Sussex, Stephan Huber for always being ready to give an opinion, guidance and help with both physics and bureaucratic matters.

I have also benefited greatly from informal discussions with, in particular, Barry Dillon, Agamemnon Sfondilis, Jan Schröder, Mike Atkins and Jorge Camalich. I also must thank Paul Archer, for being willing to answer several questions by email regarding his work, despite having already moved on from Sussex.

UNIVERSITY OF SUSSEX

ANDREW GRANGER, DOCTOR OF PHILOSOPHY

THE FLAVOUR OF WARPED EXTRA DIMENSIONS

Summary

Models with warped extra dimensions offer a promising solution to the hierarchy problem. However, it is known that flavour changing neutral currents arise at tree level in models with warped extra dimensions, which can lead to fatally large corrections to rare processes in the standard model. Since the introduction of the warped mechanism in 1999 by Randall and Sundrum, modifications of the original AdS_5 geometries have been considered, having different phenomenologies. In particular, it has been previously shown that CP-violation in the $K - \bar{K}$ mixing system can be suppressed in what is known as the soft-wall model, in which the extra dimension is effectively compactified via a background scalar dilaton field. Prior to the work presented in this thesis, however, this study had been limited to a background geometry with a specific form. A detailed study of bosonic propagators in soft-wall models has been conducted as part of this research, yielding some novel results, which permit the study of particle interactions throughout an extended family of warped 5D backgrounds in a practicable way. This methodology has then been applied, via the development of numerical routines, to an investigation of K and B meson phenomenology in a range of geometries in this family. The relevant and necessary technical prerequisites are reviewed and discussed, including (but not limited to) some of the general properties of warped extra dimensions, the application of Kaluza-Klein theory in warped 5D, topics in flavour physics and quark mixing and the application of effective field theory methods in perturbative calculations of flavour observables. It is found that there is indeed a significant interplay between the structure of the extra dimension and flavour phenomenology at a scale of 1-10 TeV. Although it turns out that the previously studied construction was already quite well-optimised with regard to flavour constraints, it is demonstrated that one can do more to ameliorate these via deformations to the background geometry and modifications to the power law dependence of the fermion masses on the extra dimension.

Contents

1	Introduction	8
1.1	Motivations	8
1.1.1	The Hierarchy Problem, Naturalness and NP at $\mathcal{O}(\text{TeV})$	9
1.1.2	The Flavour Mass Hierarchy	10
1.1.3	WEDs As A Solution To The Hierarchy Problem	12
1.2	Historical Developments in WEDs	17
1.3	Synopsis	19
2	The Class of Viable Warped Geometries	21
2.1	Frames and Formulations In The Bottom-Up Perspective	21
2.2	Scalar-Gravity System	24
3	The Model	29
3.1	Fermions	31
3.2	Gauge Bosons	33
3.3	Gauge Fixing and the 5D Action	35
3.4	Canonical Quantisation of Gauge Fields	38
3.5	Gauge Boson Propagators	39

3.5.1	The Hybrid Approach	39
3.5.2	General form of the Bosonic Propagator	42
3.5.3	The Correlation Functions	44
3.5.4	Determining the Correlation Function for Quadratic Dilaton . .	45
4	Flavour Physics Overview	49
4.1	Quark Mixing and the CKM Matrix	49
4.2	Suppression of FCNCs in the SM	52
4.3	Neutral Meson Mixing in the SM	54
4.4	Tree-Level FCNCs in WEDs	59
4.5	Neutral Meson Mixing In WEDs	63
5	Effective Field Theory Methodology	66
5.1	Operator Product Expansion for Tree-Level FCNCs	69
5.1.1	Gluon Mediated	69
5.1.2	Photon Mediated	72
5.1.3	Z Mediated	72
5.2	Effective Operators	73
5.2.1	Gluon Contribution	73
5.2.2	Photon Contribution	74
5.2.3	Z Contribution	75
5.2.4	Wilson Coefficients for Hadronic Processes	76
5.3	Bosonic Correlation Function for General Dilaton	76
5.3.1	Photon/Gluon (Massless Case)	77
5.3.2	W/Z (Massive Case)	80

5.3.3	Calculation of $G_{-1,p=0}^{(W/Z)}(z_0, z')$	81
5.3.4	Comparison: KK expansion vs $1/M^2$ expansion.	83
6	Flavour Phenomenology of WEDs	85
6.1	Numerical Methodology	86
6.1.1	Boson Propagators: Coordinate Transformations	86
6.1.2	Boson Propagators: Convergence	87
6.1.3	Boson Propagators: Interpolation	88
6.1.4	Calculation of h_0	90
6.1.5	Fit to Quark Masses	91
6.1.6	Naturalness	91
6.1.7	Yukawa Couplings	92
6.1.8	Input Configurations	93
6.1.9	Computation of Gauge Basis Double Integrals	93
6.1.10	Basis Rotations	94
6.1.11	The Range of α and ν	97
6.1.12	Observables in K and B Mixing	99
6.1.13	Bag Factors	101
6.2	Numerical Results and Analysis	102
6.2.1	$K - \bar{K}$ Mixing	102
6.2.2	$B - \bar{B}$ Mixing	108
7	Summary and Conclusions	116
	Bibliography	119

Chapter 1

Introduction

1.1 Motivations

While the standard model (SM) has seen remarkable success in explaining a huge array of particle phenomena observed in nature, there are several outstanding problems which have yet to be addressed. It is widely believed that there should be a consistent description of quantum gravity, and that the four fundamental forces and matter fields should sit within some unified framework which is valid at all observable energy scales. From a bottom up perspective, however, we can already motivate the search for new physics (NP) at or close to the TeV scale. Presented below is a short discussion of some unsolved problems which require physics beyond the SM. The discussion is by no means exhaustive, rather we shall focus on those topics which bear the greatest relevance to models with warped extra dimensions, i.e. those that serve as direct motivations for such models.

1.1.1 The Hierarchy Problem, Naturalness and NP at $\mathcal{O}(\text{TeV})$

The explanation of the large hierarchy $M_{Pl} \gg M_{EW}$ is one of the greatest outstanding challenges in modern particle physics. With the observed Higgs mass of $m_h = 126\text{GeV}$ [1, 25], the electroweak scale is at $v \sim \mathcal{O}(10^2)\text{GeV}$, while the Planck mass sits some seventeen orders of magnitude higher at $M_{Pl} \sim \mathcal{O}(10^{19})\text{GeV}$ [49]. With the masses of the standard model particles coming from the Higgs, the pertinent question may be phrased: why are the fundamental particles of nature so incredibly light in comparison to the expected scale of unification of the fundamental forces? Equivalently, why do they couple so strongly to the standard model forces but so weakly to gravity? Indeed, naïvely one would expect the Higgs mass to be sensitive to any scale at which the standard model is valid. As such one would expect its mass to be much higher and therefore that gravity would be significant in fundamental particle interactions. To see this, consider a simple model of a massive scalar field, which couples to gauge and fermion fields, and spontaneously acquires a non-zero vev

$$\mathcal{L}_\phi = \frac{1}{2}(D_\mu\phi)^2 - \frac{1}{2}\mu^2\phi^2 - \frac{1}{4}\lambda\phi^4 - y\phi\bar{\psi}\psi. \quad (1.1)$$

At one loop level, the corrections to the bare mass squared m_h^2 coming from scalar self-coupling, fermion and gauge coupling respectively [54] are shown in Figure 1.1, giving an overall quadratic dependence on the cutoff Λ . In the absence of a stabilisation mechanism to remove such loop contributions (and higher orders) at some higher energy scale, one would have to assume that the bare mass (i.e. the vev) is exactly fine-tuned to cancel such divergences all the way up to $\Lambda \sim M_{Pl}$. In the case of the

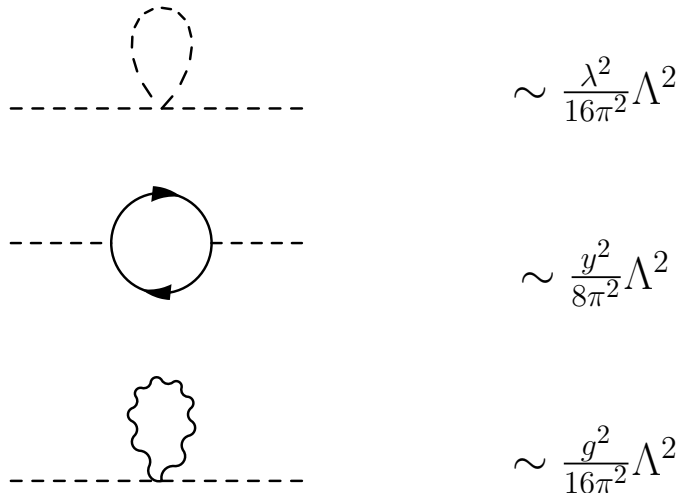


Figure 1.1: One loop corrections to the Higgs mass

standard model Higgs, with the largest contribution coming from the heavy top quark at $\Delta m_h^2 \sim \mathcal{O}(10^{-2})\Lambda^2$, the stabilisation mechanism would have to enter the game at $\mathcal{O}(\text{TeV})$ to achieve the observed EW scale mass.

1.1.2 The Flavour Mass Hierarchy

The large $M_{Pl} \gg M_{EW}$ difference is certainly not the only unexplained hierarchy present in the standard model. In particular, there are smaller, but still puzzling hierarchies visible within the pattern of fermion masses. Most notably, the ratio of the heaviest SM fermion, the top quark, to the lightest, the electron neutrino, is already about $m_t/m_{\nu_e} \geq \mathcal{O}(10^{10})$ [52]. However, since for the remainder of this work we are primarily interested in quark flavour physics, we will focus our attention on the mass structure of the quark sector. Within the quarks alone, the largest observed hierarchy is that of the top to the down, $m_t/m_d \sim \mathcal{O}(10^5)$ [52]. The quark masses are not themselves predicted naturally by the standard model. In the SM, fermion masses arise from coupling to the Higgs. After spontaneous symmetry breaking, the vacuum state of the

m_t	m_b	m_c	m_s	m_u	m_d
173.21 ± 0.51	4.18 ± 0.03	1.275 ± 0.025	0.095 ± 5	$0.0023 \begin{smallmatrix} +0.7 \\ -0.5 \end{smallmatrix}$	$0.0048 \begin{smallmatrix} +0.5 \\ -0.3 \end{smallmatrix}$

Table 1.1: The masses of the SM quarks in GeV. Specifically, the values stated are estimates of the u, d and s “current quark masses” in a mass-independent subtraction scheme (e.g. \overline{MS}) at a scale 2GeV. The c and b masses are the “running” masses in the \overline{MS} scheme. The t quark mass is from direct measurements at the LHC and Tevatron. For further details on the stated values and measurements, see [52] from which the values are taken.

scalar field in (1.1) can be expressed

$$\phi_0 = \frac{1}{\sqrt{2}} \begin{pmatrix} 0 \\ v + h \end{pmatrix}. \quad (1.2)$$

Yukawa terms arising from the scalar-fermion interaction (one for the three up-like quarks and one for the down-like quarks) are of the form

$$\mathcal{L}_{Yuk} = \frac{v}{\sqrt{2}} \lambda'_{ab} \bar{\psi}'^L_a \psi'^R_b + h.c. \quad (1.3)$$

where the indices label generation and the primes indicate that we are working in a basis such that the Yukawa matrix is diagonal. In Section 4, we will look in detail at basis transformations and their importance in quark mixing and flavour physics effects. For now, suffice to say that writing mass terms for the physical quark fields as (1.3), the diagonal Yukawa matrices must be made to contain the simple hierarchies required to produce the quark masses. There is no a priori reason why this should be so. One of the attractive features of extra dimensional models is that, in contrast to the SM, one need not introduce ad hoc hierarchies in the Yukawa couplings. Rather, in a somewhat analogous fashion to the explanation of $M_{Pl} \gg M_{EW}$, one can entirely reproduce the

observed masses through an elegant interplay between the Higgs, fermion fields and background geometry. It turns out that, in contrast to flat extra dimensions, warped extra dimensions provide an automatic suppression of flavour violation known as the RS-GIM mechanism. The details of this are left to Section 4.4.

1.1.3 WEDs As A Solution To The Hierarchy Problem

One approach to stabilising the Higgs mass is to propose that there is a protective symmetry which leads to cancellation of the loop processes at energies $> \mathcal{O}(\text{TeV})$. Such a mechanism is provided, for example, by supersymmetry (SUSY) which naturally introduces, for every loop diagram in 1.1, a corresponding diagram with a superpartner in the loop [47]. Each superparticle loop gives the same contribution but with opposite sign, leading to a direct cancellation of all quadratic corrections above M_{SUSY} , that is, the mass scale of the supersymmetric particles. In such a scenario, one can safely take the cutoff to the Planck scale and the Higgs will only feel corrections below M_{SUSY} . While this is a promising idea, warped extra dimensions provide a very different solution, addressing the hierarchy itself directly. The idea is to suggest that the fundamental scale M_{Pl} could be naturally suppressed in an effective theory down to about $\mathcal{O}(\text{TeV})$, such that in fact it only makes sense to take the cutoff that far. The theory can then be valid for all physical energy scales, free from heavy corrections pushing the Higgs mass higher than M_{EW} , without the need for large fine-tuning. This can be achieved via a mechanism originally due to Randall and Sundrum [56]. Assuming a 5D a gravity action [33]

$$S_{gravity} = \int d^4x \int_{-L}^L dy \sqrt{-g} (M^3 R - \Lambda_{cc}) \quad (1.4)$$

and brane actions for “visible” and “hidden” branes respectively,

$$S_{vis} = \int d^4x \sqrt{-g_{vis}} (\mathcal{L}_{vis} - V_{vis}) \quad (1.5)$$

$$S_{hid} = \int d^4x \sqrt{-g_{hid}} (\mathcal{L}_{hid} - V_{hid}) \quad (1.6)$$

the fundamental Planck scale is realised on a (hidden) 3-brane at one end of a 5 dimensional spacetime ($y = 0$) with a metric given by

$$ds^2 = g_{MN} dx^M dx^N = e^{-2A(y)} \eta_{\mu\nu} dx^\mu dx^\nu - dy^2 \quad (1.7)$$

where $\eta = \text{diag}(1, -1, -1, -1, -1)$ and M, N range over $0, 1, 2, 3, 5$ ¹. Equivalently in “conformally flat” coordinates with $dz \equiv e^A dy$,

$$ds^2 = e^{-2A(z)} (\eta_{\mu\nu} dx^\mu dx^\nu - dz^2) \quad (1.8)$$

$$= e^{-2A(z)} \eta_{MN} dx^M dx^N \quad (1.9)$$

such that the metric is related to 5D Minkowski via an overall rescaling. A flat, static, Poincaré invariant 4D theory is realised on another (visible) brane separated by a finite proper distance in the extra dimension at a point $y = L$. In the original construction, the two branes bound the extra dimension, which has an orbifold compactification S_1/Z_2 . The energy density on the branes or “brane tension” back-reacts on the geometry to produce a warping which defines the function $A(y)$. In other words, a bulk cosmological constant offsets the tension of the branes giving a stable 5D geometry. Explicitly, the

¹These conventions are assumed for the remainder of this thesis

5D Einstein equations for the system can be solved to find [56]

$$A(y) = |y| \sqrt{\frac{-\Lambda_{cc}}{24M^3}} = k|y| \quad (1.10)$$

which is real only in the case that the bulk cosmological constant Λ_{cc} is negative. The space is thus anti-deSitter, namely a slice of AdS_5 . The square-root of the metric determinant following from (1.7) and (1.10) is $\sqrt{-|g|} = e^{-4A(y)} = e^{-4ky}$. We now consider the action for the Higgs localised on the brane at $y = L$, having a metric $g_{\mu\nu}^{vis} = g_{\mu\nu}(x^\mu, y = L)$,

$$S_{Higgs} = \int dx^4 \sqrt{-|g|} (g_{vis}^{\mu\nu} D_\mu H^\dagger D_\nu H - \lambda(|H|^2 - v_0^2)^2) \quad (1.11)$$

$$= \int dx^4 e^{-4kL} (e^{-2kL} \eta^{\mu\nu} D_\mu H^\dagger D_\nu H - \lambda(|H|^2 - v_0^2)^2) \quad (1.12)$$

where v_0 sets the fundamental scale. One can write a canonical kinetic term by taking the normalisation $\tilde{H} = e^{-kL} H$,

$$S_{Higgs} = \int dx^4 (\eta^{\mu\nu} D_\mu \tilde{H}^\dagger D_\nu \tilde{H} - \lambda(|\tilde{H}|^2 - e^{-kL} v_0^2)^2) \quad (1.13)$$

which gives rise to an effective vev

$$v_{eff} = v_0 e^{-kL} \quad (1.14)$$

i.e. the effective mass scale of the 4D theory at $y = L$ is warped down with respect to $y = 0$. For this reason, the branes at each point are usually referred to as infra-red (IR) and ultraviolet (UV) respectively. The tuning problem now concerns simply the ratio

v_0/M_{Pl} which should be close to unity, while simultaneously requiring $v_{eff} \sim M_{EW}$.

The hierarchy is therefore naturally stabilised (fine-tuning is small) if

$$kL \sim \log(10^{16}) \quad (1.15)$$

which determines the required ratio of the fundamental and observed scales in the theory. Choosing a coordinate $-\pi < \phi < \pi$, such that $y = r_c \phi$, one explicitly factors out the “radius” r_c of the compact extra dimension and the metric is then given by

$$ds^2 = e^{-2kr_c|\phi|} \eta_{\mu\nu} r_c dx^\mu dx^\nu - r_c d\phi^2. \quad (1.16)$$

Clearly, the value of r_c here is a free parameter and not fixed dynamically. However, it was shown in [36] that if one introduces a bulk scalar field, acquiring a vacuum expectation value via interactions on the brane, there exists a potential with a stable minimum from which r_c can be determined. Such a configuration can produce the required hierarchy of scales. This is known as the Goldberger-Wise mechanism. Consider a bulk action

$$S_{bulk} = \frac{1}{2} \int d^4x \int_{-\pi}^{\pi} d\phi \sqrt{g} (g^{MN} \partial_M \Phi \partial_N \Phi - m^2 \Phi^2) \quad (1.17)$$

and actions on the hidden and visible branes

$$S_{hid} = - \int d^4x \sqrt{-g_{hid}} \lambda_{hid} (\Phi^2 - v_{hid}^2)^2 \quad (1.18)$$

$$S_{vis} = - \int d^4x \sqrt{-g_{vis}} \lambda_{vis} (\Phi^2 - v_{vis}^2)^2 \quad (1.19)$$

where g_{hid} and g_{vis} are the determinants of the induced metrics on the respective branes. Minimising the combined action yields

$$\begin{aligned}
0 = & -\frac{1}{r_c^2} \partial_\phi (e^{-4\sigma} \partial_\phi \Phi) + m^2 e^{-4\sigma} \Phi + 4e^{-4\sigma} \lambda_{vis} \Phi (\Phi^2 - v_{vis}^2) \frac{\delta(\phi - \pi)}{r_c} \\
& + 4e^{-4\sigma} \lambda_{hid} \Phi (\Phi^2 - v_{hid}^2) \frac{\delta(\phi)}{r_c}
\end{aligned} \tag{1.20}$$

where $\sigma(\phi) = kr_c |\phi|$ and the solution in the bulk is then

$$\Phi(\phi) = e^{2\sigma} [Ae^{\gamma\sigma} + Be^{-\gamma\sigma}] \tag{1.21}$$

with $\gamma = \sqrt{4 + m^2/k^2}$. Substituting back into the action for the scalar field and integrating out the ϕ coordinate yields a potential

$$\begin{aligned}
V_\Phi(r_c) = & k(\gamma + 2)A^2(e^{2\gamma kr_c\pi} - 1) + k(\gamma - 2)B^2(1 - e^{-2\gamma kr_c\pi}) \\
& + \lambda_{vis} e^{-4kr_c\pi} (\Phi(\pi)^2 - v_{vis}^2)^2 + \lambda_{hid} (\Phi(0)^2 - v_{hid}^2)^2.
\end{aligned} \tag{1.22}$$

One can now fix the constants A and B by applying boundary conditions (see [36]) and one eventually obtains

$$kr_c = \left(\frac{4}{\pi}\right) \frac{k^2}{m^2} \ln \left[\frac{v_{hid}}{v_{vis}} \right] \tag{1.23}$$

provided λ_{vis} , λ_{hid} and kr_c are assumed to be large. With v_{hid} and v_{vis} having the same order of magnitude, it is clear the value of $kr_c\pi = kL$ can “naturally” satisfy (1.15). In Chapter 2, we will see in the context of soft-wall models, that a scalar dilaton field can in fact define the warped geometry while simultaneously playing the role of a Goldberger-Wise stabilising field.

1.2 Historical Developments in WEDs

Shortly after the discovery by Randall and Sundrum that a warped extra dimension bounded by two three-branes could be used to explain the $M_{Pl} \gg M_{TeV}$ hierarchy [56] (RS1), it was also shown that such a mechanism could be realised in a setup with only one brane [57] (RS2). By localising fermions in the bulk, the geometry can also account for the fermion mass structure of the standard model (SM) without requiring a hierarchy in the Yukawas [39, 38, 34]. However, such a scenario is seen to yield a continuum of Kaluza-Klein (KK) states, since one end of the extra dimension is unconstrained. It was subsequently noted that a *soft-wall* (SW), due to a smoothly decaying non-dynamical scalar dilaton field Φ , could serve as an alternative to the hard cutoff provided by the IR brane in RS1[31]. The original motivation of this idea was to obtain the correct meson mass spectrum in the context of the AdS/QCD correspondence, as confinement behaviour is determined by the precise power law dependence of the dilaton on the fifth dimension [42]. Specifically, linear confinement is obtained for $\Phi(z) \sim z^2$ with KK resonances obeying Regge-like behaviour, whereas in a slice of pure AdS_5 the mass scales as $m_n^2 \sim n$. It was later demonstrated, however, that electroweak symmetry breaking could be realised in such a scenario with a bulk scalar [31]. The SM can be constructed as an effective 4D theory with flavour hierarchies practicable as in the hard-wall case [48]. However, since SW models had been considered as bottom-up constructions with a non-dynamical dilaton (essentially modifications of RS1), the question of the gravitational stability of such models ought to be addressed. This has been done in [11, 18, 58] in which effective 4D scalar dilaton models can be seen to arise from a dynamical setup in 5D, taking into account the geometrical back-reaction of the dilaton.

Although the mechanism of warped extra dimensions is successful in addressing the naturalness problem and generating fermion mass hierarchies, it has been important to consider the potential problem of excessive flavour violation in such models [59, 50, 38, 2, 13, 29, 12, 3, 22]. The origins and underlying physics of this issue will be explained in Chapter 4 and this topic is a central concern of this thesis. It turns out that there exists a natural suppression mechanism, often referred to as RS-GIM (see Section 4.4). It was found in RS models however, that although this mechanism has a significant impact in suppressing flavour violation, one still need set the length of the extra dimension small enough to produce masses of the lightest Kaluza-Klein particles no less than around 10-20 TeV, depending on how much fine-tuning one allows [59]. Generally, the most stringent constraints come from $K - \bar{K}$ mixing, namely from the indirect CP violation parameter ϵ_K [59, 38, 5, 29, 12] (see Section 4.5). In order to ameliorate such constraints, one approach that has been followed is to modify the geometry of the extra dimension, specifically by considering SW models [9, 8, 38, 20]. It was found that such an approach can indeed lead to additional suppression of flavour violating effects in the K meson mixing system. In [8], it was demonstrated that the SW with quadratic dilaton can satisfy flavour constraints more easily than RS, but the question arises as to what effect further modifications can have, specifically variations in the power law behaviour of the dilaton. Analogously, the power of the fifth dimensional dependence of the fermion masses in the theory (see Section 3.1) is also a free parameter. This thesis explores the two-dimensional theory space spanned by these two parameters and extends this analysis of the flavour physics - geometry relationship to a much wider class than has been done previously, with the results for $\Delta F = 2$ effects in both K and B mixing systems presented in Section 6.2.

1.3 Synopsis

In the following section, the possible landscape of warped 5D geometries is examined. A working framework and parameterisation of the theory space we wish to explore is established. The co-ordinate systems and frames of reference used in the literature are explained, along with the transformations between them. Although these are initially established from a bottom-up perspective, in Section 2.2 it is seen that stable soft-wall models exist, which are consistent with Einstein's equations and produce the required hierarchy $R/R' \sim 10^{15}$.

A specific model is chosen, for the purpose of phenomenology, in Section 3 and is seen to be a particular realisation of the gravitationally viable soft-wall setup analysed in Section 2.2. Having established that this is a sensible model to work with, the field content of the model is defined and studied. This begins with the Kaluza-Klein expansions of the 5D fermion and gauge boson fields, determining and solving the equations of motion of the wavefunction profiles in the 5th dimension. Then, in Section 3.5, the essential steps of defining the gauge boson propagators and determining equations of motion for the two-point correlation functions in warped 5D spacetime with a scalar dilaton are worked through. The methods used previously in the literature for evaluating the correlators in a soft-wall model with quadratic dilaton are reviewed.

The required background on flavour physics in the standard model and WED scenarios is discussed in Chapter 4, including quark mixing and neutral meson mixing. The origin of FCNCs at tree-level in WEDs is then explained along with the significance for phenomenology. It is seen that there are various sources of suppression of FCNCs that will come into play in the phenomenological study presented in Chapter 6.

In Chapter 5, the application of effective field theory techniques in calculating observables in the neutral meson mixing systems is discussed and explained. A methodology for the perturbative analysis of these systems is defined. A derivation of the precise formulas required for calculating the effects on neutral meson mixing due to KK modes of the gauge bosons is given and results concisely stated. Chapter 5 concludes with a perturbative treatment of the two-point correlation functions found in Section 3.5.2, yielding a novel approach to their evaluation, which is straightforwardly applicable to the two-parameter family of soft-wall theories defined in Chapter 3.

The remaining chapters of the thesis constitute a phenomenological analysis of the K and B meson mixing systems across the two-parameter family. In Chapter 6, the numerical methodology is presented, with a detailed description of the steps taken in the computer calculations and the associated technical challenges. Precise formulas are stated for the observables under study. In Chapter 6.2, the numerical results are presented and analysed. Finally, in Chapter 7 the results and conclusions are summarised, with comments on the significance of the findings for future probes of flavour physics in collider experiments.

Chapter 2

The Class of Viable Warped Geometries

2.1 Frames and Formulations In The Bottom-Up Perspective

Although the mechanism of generating a large hierarchy from a small, warped extra dimension was originally proposed for a pure AdS metric, there is no a priori reason why such a mechanism could not be realised in similar but modified warped backgrounds. Indeed, various gravitationally viable alterations of the RS1 model exist, in which one can still establish a large hierarchy with small fine-tuning[18, 58]. The essence of soft-wall models is that the IR dynamics are cut off by a smoothly decaying scalar field instead of the hard cutoff provided by a brane. From a bottom up perspective, one can construct such a model in pure AdS using a single UV brane at $z = R = 1/k$ and introduce a “dilaton” Φ into the action

$$S = \int d^4x \int_R^\infty dz \sqrt{g} e^{-\Phi(z)} \mathcal{L} \tag{2.1}$$

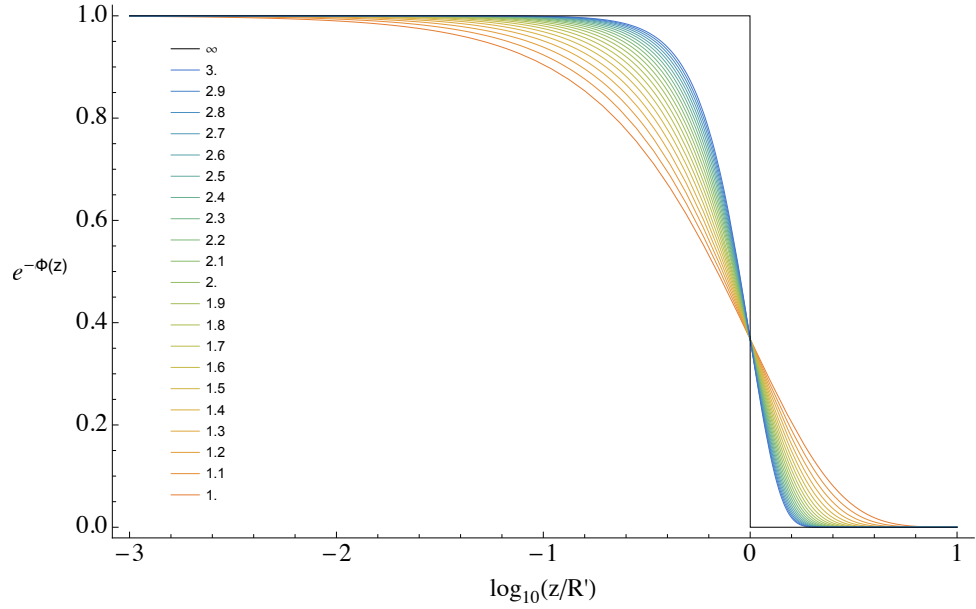


Figure 2.1: The shape of the soft wall, with the hard wall as the limit $\nu \rightarrow \infty$. The legend labels the value of ν .

where $\Phi(z) = \left(\frac{z}{R'}\right)^\nu$ and R' is the inverse KK scale $R' = 1/M_{KK}$. Since the role of the dilaton is simply to constrain the dynamics in the IR of the extra dimension, it is taken to be a pure function z . The value of ν clearly sets the “shape” of the soft-wall as shown in Fig.2.1 with the hard-wall case recovered as $\nu \rightarrow \infty$. It was noted in [42] that the mass spectrum of the KK modes is consequently set by the power of the dilaton. In particular, for the case of a quadratic dependence, one obtains Regge behaviour $m_n^2 \sim n$ in the context of a strongly coupled 4D dual theory.

Proceeding as (2.1), one is working in what is referred to as the “Jordan” frame [32]. Alternatively, one can in fact interpret the scalar dilaton as simply a deformation of the AdS background in which case it is absorbed into the metric, yielding an action

$$S = \int d^4x \int_R^\infty dz \sqrt{g} \tilde{\mathcal{L}} \quad (2.2)$$

where $\tilde{\mathcal{L}}$ again has canonical kinetic terms. This construction is traditionally referred to as the “Einstein” frame. The two schemes are related by field redefinitions and as such they are physically equivalent. In looking at this in more detail we will draw on [40]. Assume an action of the form

$$S = S_{\text{ferm}} + S_{\text{gauge}} \quad (2.3)$$

$$S_{\text{ferm}} = \int d^5x \sqrt{g} e^{-\Phi} \left[\frac{i}{2} (\bar{\psi} \Gamma^M \nabla_M \psi - \overline{\nabla_M \psi} \Gamma^M \psi) - M(x) \bar{\psi} \psi \right] \quad (2.4)$$

$$S_{\text{gauge}} = - \int d^5x \sqrt{g} e^{-\Phi} \frac{1}{4} F_{MN}^a F^{aMN}. \quad (2.5)$$

Here $\nabla_M = D_M + \omega_M$ is the 5-dimensional gravitationally and gauge-covariant derivative where ω_M is the spin connection, ψ is a Dirac spinor, and F_{MN}^a denotes the gauge field strength (a labeling the generator). The massless fermionic part is invariant under the local Weyl rescaling

$$\psi \rightarrow K^{-2} \psi, g_{MN} \rightarrow K^2 g_{MN}, A_M \rightarrow A_M \quad (2.6)$$

while under the same transformation (which implies $F_{MN} \rightarrow F_{MN}$), the fermion mass term transforms as $M \rightarrow KM$ and the gauge part transforms as

$$S_{\text{gauge}} \rightarrow - \int d^Dx \sqrt{g} e^{-\Phi} K \frac{1}{4} F_{MN}^a F^{aMN}. \quad (2.7)$$

On the other hand, under a local rescaling of only the fermion field,

$$\psi \rightarrow K_\psi^{1/2} \psi, g_{MN} \rightarrow g_{MN}, A_M \rightarrow A_M \quad (2.8)$$

the fermionic action transforms as

$$S_{\text{ferm}} \rightarrow \int d^5x K_\psi e^{-\Phi} \frac{i}{2} \left[(\bar{\psi} \Gamma^M \nabla_M \psi - \overline{\nabla_M \psi} \Gamma^M \psi) - M(x) \bar{\psi} \psi \right]$$

while the bosonic action is evidently invariant. Note that the rescaling factors K are arbitrary functions on the 5-dimensional space.

The upshot of this is that in order to eliminate the dilaton factor from the action, one needs to simply combine a Weyl transformation with $K = e^\Phi$ followed by a fermion rescaling with $K_\psi = e^{\Phi/2}$. Conceptually, this formulation lends itself to the idea of a deformed AdS background with an automatic physical cutoff at finite proper distance in the IR, in the absence of a bounding brane or explicit conformal coupling of the dilaton to the other fields in the theory. Formally, in this picture one must work with an Einstein frame action with a modified mass $M \rightarrow e^\Phi M$ and a metric rescaled according to

$$A(z) \rightarrow \tilde{A}(z) = A(z) + \Phi(z) \tag{2.9}$$

$$g_{MN} \rightarrow \tilde{g}_{MN} = e^{-2\Phi} g_{MN}. \tag{2.10}$$

2.2 Scalar-Gravity System

Note that we have so far not considered kinetic terms for the dilaton, that is to say it has been taken to be non-dynamical. The question therefore arises as to whether the construction makes sense gravitationally, i.e. whether it is consistent with Einstein's equations for a setup with a dynamical scalar field, which back-reacts on the metric

to produce a naturally stabilised hierarchy. This matter is explicitly addressed in [19] and further analysed in [58]. The key findings are reviewed below¹. Working with the 4D Poincaré invariant metric (1.7) and a single (flat) brane at $y = 0$ one can write an action for the entire system, including both bulk and brane terms and a scalar field,

$$S = \int d^5x \sqrt{-g} [M^3 R - 3(\partial\Phi)^2 - V(\Phi)] - \int d^4x \sqrt{-g_{ind}} \lambda(\Phi) \quad (2.11)$$

where $V(\Phi)$ and $\lambda(\Phi)$ are the bulk and brane potentials respectively and g_{ind} is the induced metric on the brane and M is the 5D Planck Mass which we set to unity. The equations of motion in the bulk are

$$6\Phi'' - 24A'\Phi' - \partial_\Phi V(\Phi) = 0 \quad (2.12)$$

$$A'' - \Phi'^2 = 0 \quad (2.13)$$

$$12A'^2 - 3\Phi'^2 + V = 0 \quad (2.14)$$

with the boundary conditions

$$A'(0_+) = \frac{1}{6} \lambda(\Phi_0) \quad (2.15)$$

$$\Phi'(0_+) = \frac{1}{6} \partial_\Phi \lambda(\Phi_0) \quad (2.16)$$

where $\Phi_0 = \Phi(0)$. Differentiating (2.14) and substituting for A'' from (2.13) one obtains (2.12) which may therefore be discarded. The system of equations can then be re-written

¹note that the convention for the metric signature differs from the aforementioned literature

as first order differential equations,

$$A' = W(\Phi) \tag{2.17}$$

$$\Phi' = \partial_\Phi W(\Phi) \tag{2.18}$$

by introducing the “superpotential” $W(\Phi)$, defined such that

$$3(\partial_\Phi W(\Phi))^2 - 12W(\Phi)^2 = V(\Phi) \tag{2.19}$$

which has a solution provided that V satisfies

$$\frac{1}{12}[\partial_\Phi \lambda(\Phi_0)]^2 - \frac{1}{3}\lambda(\Phi_0)^2 = V(\Phi_0) \tag{2.20}$$

which follows from applying the boundary conditions in (2.14). The complete potential on the brane is then

$$V_{4D}(\Phi) = \lambda(\Phi) - 6W(\Phi) \tag{2.21}$$

Since we require the brane to be flat, the potential must vanish at the boundary at Φ_0 .

One can now write down a superpotential satifying (2.17) and (2.18)

$$W(\Phi) = k(1 + e^{\zeta\Phi}) \tag{2.22}$$

where ζ is a new free parameter of order unity. This implies that the bulk scalar potential following from (2.19) is

$$V(\Phi) = (3k^2\zeta^2 - 12k^2)e^{2\zeta\Phi} - 12k^2(2k^2e^{\zeta\Phi} - 1) \tag{2.23}$$

and yields explicit solutions for $\tilde{A}(y)$ and $\Phi(y)$

$$\tilde{A}(y) = ky - \frac{1}{\zeta^2} \log(1 - y/y_s) \quad (2.24)$$

$$\Phi(y) = -\frac{1}{\zeta} \log(k\zeta^2(y_s - y)) . \quad (2.25)$$

In the Einstein frame, one therefore finds a 5D metric satisfying

$$ds^2 = e^{-2ky} \left(1 - \frac{y}{y_s}\right)^{\frac{1}{\zeta^2}} \eta_{\mu\nu} dx^\mu dx^\nu - dy^2. \quad (2.26)$$

Still in the Einstein frame, but now in conformal coordinates $dy = e^{-A} dz$, our bottom-up construction (2.1), with $1 < \nu < \infty$, corresponds to a choice

$$\tilde{A}(z) = \log(kz) + \Phi(z) \quad (2.27)$$

$$\Phi(z) = (\rho z)^\nu . \quad (2.28)$$

The function $\tilde{A}(z)$ here has the asymptotic behaviour of a solution to the EOMs arising from setting $\zeta = 1$ with a superpotential now growing as $W(\Phi) \sim e^\Phi \Phi^{\frac{1}{2} - \frac{1}{2\nu}}$, i.e. one must now take account of the subleading behaviour [18]. In such a case, the backreaction of the scalar field becomes important at $z \approx 1/\rho \equiv R'$ which we can think of as the position of the soft-wall. Such models are referred to as SW2 type models by the authors of [58]. The required hierarchy $R/R' \sim 10^{15}$ can be stabilised without the need

for significant fine tuning, namely, the dominant contribution is given by

$$\log\left(\frac{R'}{R}\right) \sim \frac{e^{-\zeta\Phi_0}}{\zeta^2} \quad (2.29)$$

where $\Phi_0 = \Phi(0)$ is again the value of the scalar field on the UV brane. We thus have a well-defined construction according to (2.27) and (2.28) for a class of models parametrised by ν . This class forms the basis of the framework investigated in the following sections.

Chapter 3

The Model

We will work in a setup very similar to that of [8] which we will outline here. In the conformally flat frame, the background is described by a line element

$$ds^2 = e^{-2A(z)} \eta_{MN} dx^M dx^N. \quad (3.1)$$

Here we are also working in the Jordan frame such that the metric is independent of the dilaton. The action

$$S = \int d^4x \int_R^\infty dz e^{-\Phi(z)} \mathcal{L} \quad (3.2)$$

is then automatically cut off as $z \rightarrow \infty$, since the dilaton scales as a positive power of the fifth coordinate. Specifically, in this frame we have a pure AdS metric and dilaton such that

$$A(z) = \log \left(\frac{R}{z} \right) \quad (3.3)$$

$$\Phi(z) = \left(\frac{z}{R'} \right)^\nu \quad (3.4)$$

The parameter R' gives the inverse “KK scale” as $M_{KK} = 1/R'$. In the absence of an IR brane, the Higgs propagates in the full 5D bulk, although we assume it is predominantly localised near to the SW at $z = R'$, specifically we choose a form

$$h(z) = h_0 R^{-3/2} \left(\frac{z}{R'} \right)^\alpha \quad (3.5)$$

Note that the h_0 is not simply the SM Higgs vev, but rather a generically $\mathcal{O}(1)$ dimensionless quantity that will depend on the length of the extra dimension. We will look at this dependence in more detail in Section 6.1.4.

For a single generation of fermions the action is given by

$$\begin{aligned} S = \int d^5x \sqrt{g} e^{-\Phi} & \left[\frac{1}{2} (i \bar{\Psi} \Gamma^M \nabla_M \Psi - i \bar{\nabla}_M \bar{\Psi} \Gamma^M \Psi) + \frac{1}{2} (i \bar{\Upsilon} \Gamma^M \nabla_M \Upsilon - i \bar{\nabla}_M \bar{\Upsilon} \Gamma^M \Upsilon) \right. \\ & \left. - M_\Psi(z) \bar{\Psi} \Psi - M_\Upsilon(z) \bar{\Upsilon} \Upsilon \right] \end{aligned} \quad (3.6)$$

where $\nabla_M = D_M + \omega_M$ and D_M is a component of the covariant derivative, ω_M is a component of the spin connection and Ψ and Υ are SU(2) doublets and singlets respectively. In the effective 4D theory, these give rise to left and right chiral components of Dirac fermions respectively. The Γ matrix carries a spacetime index since $\Gamma^M = E_A^M \gamma^A$ where E_A^M is a Fünfbein component.

We will assume generation diagonal mass matrices in the 5D bulk and the general form of the z -dependent mass term to be

$$M(z) = \frac{c_0}{R} + \frac{c_1 z^\alpha}{R R'^\alpha}. \quad (3.7)$$

As explained in [48, 8], the fermions, unlike the gauge fields, do not feel the dilaton aside

from a z -dependence in the mass (see (3.10) and (3.23)). Therefore, the second term in (3.7) serves to ensure a discrete spectrum for the fermions. An advantage of this is that we avoid introducing Yukawa terms directly into (3.6) which would induce mixing of the generations and yield analytically unsolvable coupled differential equations. Instead we can then treat the coupling to the Higgs as an additional perturbation after solving the equations of motion with the z -dependent bulk mass as stated. One may wish to speculate about a relationship between the profile of the Higgs and the fermion mass but suffice to say that here we will restrict ourselves to studying models where the exponent α is equal to that of (3.5).

3.1 Fermions

Writing the action for a fermion

$$S_{matter} = \int d^5x \sqrt{g} e^{-\Phi} \bar{\Psi} (i \Gamma^M \nabla_M - M(z)) \Psi \quad (3.8)$$

the 5D fields can be decomposed into 4D fields and 1D profiles via the Kaluza Klein expansions

$$\Psi(x, z) = \sum_{n=0}^{\infty} e^{2A+\Phi/2} \psi(x)^n f^n(z). \quad (3.9)$$

Substituting into (3.8), varying with respect to $\bar{\Psi}$ and applying the 4D Dirac equation $i\gamma^\mu D_\mu \Psi_{L,R}^{(n)} = m_n \Psi_{R,L}^{(n)}$, one then obtains the equations of motion for the fermion profiles

$$(\partial_z \pm e^A M(z)) f_{L,R}^n = \pm m_n f_{R,L}^n. \quad (3.10)$$

The wavefunctions obey the orthonormality relation

$$\int_R^\infty dz f_n f_m = \delta_{nm} \quad (3.11)$$

and one finds a fermion zero mode given by

$$f_{L,R}^{(0)} = N(c_0, c_1, \alpha) z^{\mp c_0} \exp\left(\mp \frac{c_1}{\alpha} \frac{z^\alpha}{R'^\alpha}\right) \quad (3.12)$$

where

$$N(c_0, c_1, \alpha) = \sqrt{\frac{\frac{\pm 2c_1}{(R')^{1 \mp 2c_0}} \left(\frac{\alpha}{\pm 2c_1}\right)^{1 - \frac{1 \mp 2c_0}{\alpha}}}{\Gamma\left(\frac{1 \mp 2c_0}{\alpha}, \pm \frac{2c_1}{\alpha} \Omega^{-\alpha}\right)}} \quad (3.13)$$

and $\Omega \equiv R'/R$. Parameters c_0 and c_1 therefore set the localisation of the zero mode, although it was shown in [8] that the flavour physics effects we consider in later sections of this thesis are fairly insensitive to changes in the c_1 parameter. For this reason, we will generally be assuming $c_1 = 1$. Although by definition the zero modes have vanishing mass eigenvalues, they gain a mass from a 4D coupling to the Higgs, treated as a perturbation

$$M_{ij} = \int_R^\infty dz \frac{R}{z} Y_{ij} h(z) f_{iL}^{(0)}(z) f_{jR}^{(0)}(z) \quad (3.14)$$

where i, j label generation and $Y_{ij} = \lambda_{ij} \sqrt{R}$ are the components of a complex 3×3 matrix.

3.2 Gauge Bosons

The 5D kinetic term for the simple case of a massless U(1) gauge field is simply

$$\mathcal{L}_{gauge} = -\frac{1}{4}F_{MN}F^{MN}. \quad (3.15)$$

Substituting into (3.2) one obtains a 5D equation of motion of the form

$$0 = \partial_M(e^{-\Phi}\sqrt{g}g^{MN}g^{PQ}F_{NQ}) \quad (3.16)$$

$$= \eta^{\mu\nu}\eta^{PQ}\partial_\mu(e^{-\Phi-A}F_{\nu Q}) - \eta^{RS}\partial_z(e^{-\Phi-A}F_{5Q}). \quad (3.17)$$

The first four components of the gauge field A_μ are expanded according to

$$A_\mu(x, z) = \sum_{n=0}^{\infty} A_\mu^n(x) f_A^n(z) \quad (3.18)$$

and obey the orthonormality condition

$$\int_R^\infty dz e^{-\Phi} \frac{R}{z} f_n^A f_m^A = \delta_{nm}. \quad (3.19)$$

Note that the completeness relation

$$\sum_{n=0}^{\infty} e^{-\Phi} \frac{R}{z} f_n(z) f_n(z') = \delta(z - z') \quad (3.20)$$

follows straightforwardly by multiplying (3.19) by $f_n(z')$ and taking the sum over the entire set of modes.

As we move to the 4D effective theory, gauge invariance is broken for all the KK excitations above the zero-mode. The A_5 component of each 5-vector becomes a Goldstone scalar mode in 4D, eaten by the respective KK 4-vectors which gain a mass in what is referred to as the unitary gauge [55]. Thus setting $A_5 = 0$, applying (3.18) and the 4D Klein-Gordon equation $\partial^\nu \partial_\nu A^{(n)} + m_n^2 A^{(n)} = 0$, the profiles are seen to obey

$$((-\Phi' - A')\partial_z + \partial_z^2 + m_n^2) f_n^A = 0. \quad (3.21)$$

For massive bosons coupling to the Higgs, one simply need include a mass term

$$\Delta\mathcal{L} = \frac{1}{4}g^2 h(z)^2 A_\mu A^\mu \quad (3.22)$$

in the Lagrangian. The general equation for the bosonic profiles, for the pure AdS metric defined by (3.3) with $A' = \frac{1}{z}$, is therefore

$$\left(\partial_z^2 - \left(\frac{1}{z} + \Phi' \right) \partial_z + m_n^2 + \mu(z) \right) f_n^A = 0 \quad (3.23)$$

where $\mu(z) = \frac{1}{2} \frac{R^2}{z^2} g^2 h(z)^2$. Clearly, the massless case is then given by setting $g \rightarrow 0$. Note that the solutions to (3.23), normalised according to (3.19) have an explicit dependence on the dilaton, in contrast to (3.10), whose solutions are normalised according to (3.11), i.e. with the dilaton factor absorbed. In case of the bosons, the equation of motion has both first and second order derivatives and one cannot completely eliminate the dependence on Φ' .

3.3 Gauge Fixing and the 5D Action

For the sake of doing quantum field theory in this model, we would like to find the propagator for the first four components of the gauge fields. For this we need to look at the quadratic part of the action, read off a differential operator and find its Green's function. First we can compute the fully expanded action. As above take

$$S_1 = \int d^5x \left(\frac{R}{z} \right)^5 e^{-\Phi} \left(-\frac{1}{4} F_{MN} F^{MN} \right) \quad (3.24)$$

where

$$F_{MN} F^{MN} = g_{MR} g_{NS} F^{MN} F^{RS} = \left(\frac{z}{R} \right)^4 \eta_{MR} \eta_{NS} F^{MN} F^{RS} \quad (3.25)$$

$$= \left(\frac{z}{R} \right)^4 (F_{\mu\nu} F^{\mu\nu} + F_{\mu 5} F^{\mu 5} + F_{5\nu} F^{5\nu} + F_{55} F^{55}) \quad (3.26)$$

$$= \left(\frac{z}{R} \right)^4 (F_{\mu\nu} F^{\mu\nu} + 2F_{\mu 5} F^{\mu 5}) \quad (3.27)$$

since F_{MN} is antisymmetric. Substituting (3.27) into (3.24) gives three terms

$$S_1 = \int d^5x \frac{R}{z} e^{-\Phi} \left(-\frac{1}{4} (\partial_\mu A_\nu - \partial_\nu A_\mu) (\partial^\mu A^\nu - \partial^\nu A^\mu) - \frac{1}{2} (\partial_5 A_\nu - \partial_\nu A_5) (\partial^5 A^\nu - \partial^\nu A^5) \right) \quad (3.28)$$

$$= \int d^5x \frac{R}{z} e^{-\Phi} \left(-\frac{1}{4} (\partial_\mu A_\nu \partial^\mu A^\nu - \partial_\mu A_\nu \partial^\nu A^\mu - \partial_\nu A_\mu \partial^\mu A^\nu + \partial_\nu A_\mu \partial^\nu A^\mu) \right. \\ \left. - \frac{1}{2} (\partial_5 A_\nu \partial^5 A^\nu - \partial_5 A_\nu \partial^\nu A^5 - \partial_\nu A_5 \partial^5 A^\nu + \partial_\nu A_5 \partial^\nu A^5) \right) \quad (3.29)$$

Then integrating by parts and picking up a factor of 2 from $\mu \leftrightarrow \nu$ symmetry,

$$\begin{aligned}
&= \int d^5x \frac{R}{z} e^{-\Phi} \left(-\frac{1}{2} A^\nu \partial_\mu \partial^\mu A_\nu - A^\mu \partial^\nu \partial_\mu A_\nu - A^\nu \partial^\mu \partial_\nu A_\mu + A^\mu \partial_\nu \partial_\nu A_\mu \right) \\
&\quad - (\Phi' + \frac{1}{z}) (2A_\nu \partial^2 A^5) + 2A^\mu \partial_5 \partial^\mu \partial^5 - A_5 \partial^\nu \partial_\nu A_5 \\
&\quad - A^\nu \partial^5 \partial_5 A_\nu + (\Phi' + \frac{1}{z}) \partial_5 A_\nu \Big) \tag{3.30}
\end{aligned}$$

$$\begin{aligned}
&= \int d^5x \frac{e^{-\Phi}}{2} \frac{R}{z} \left(A_\mu (\eta^{\mu\nu} \partial^2 - \partial^\mu \partial^\nu - \eta^{\mu\nu} (\partial_5 \partial_5 - \Phi' \partial_5 - \frac{1}{z} \partial_5)) A_\nu \right. \\
&\quad \left. + 2A_\mu \partial_5 \partial^\mu A^5 - (\Phi' + \frac{1}{2}) (2A_\nu \partial^2 A^5) - A_5 \partial^2 A_5 \right). \tag{3.31}
\end{aligned}$$

As noted in [7] there is an apparent problem of the A_5 mode mixing with the first four components once we go to the 4D theory. However, this can be rectified by introducing a gauge fixing term $\mathcal{L}_{GF} = -\frac{1}{2\xi} \frac{R}{z} e^{-\Phi} \left(\partial_\mu A^\mu - \xi e^\Phi \frac{z}{R} \partial_5 \left(\frac{R}{z} e^{-\Phi} A^5 \right) \right)^2$, which gives three terms:

$$S_{GF1} = \int d^5x \frac{e^{-\Phi}}{2\xi} \frac{R}{z} (A_\mu \partial^\mu \partial^\nu A_\mu) \tag{3.32}$$

$$S_{GF2} = \int d^5x -\frac{\xi}{2} \frac{e^\Phi}{2} \frac{z}{R} \left(\partial_5 (e^{-\Phi} \frac{R}{z}) A_5 \partial_5 (e^{-\Phi} \frac{R}{z}) A_5 \right) \tag{3.33}$$

$$= \int d^5x -\frac{\xi}{2} (-\Phi' - \frac{1}{z} + \partial_5) A^5 \partial_5 (e^{-\Phi} \frac{R}{z}) A_5 \tag{3.34}$$

$$= \int d^5x -\frac{\xi}{2} A^5 (-\Phi' - \frac{1}{z} - \partial_5) \partial_5 (e^{-\Phi} \frac{R}{z}) A_5 \tag{3.35}$$

$$= \int d^5x \frac{\xi}{2} e^{-\Phi} \frac{R}{z} \partial_5 \left(\frac{e^\Phi}{2} \frac{z}{R} \partial_5 (e^{-\Phi} \frac{R}{z}) A_5 \right) \tag{3.36}$$

$$S_{GF3} = \int d^5x \partial_\mu A^\mu \partial_5 \left(e^{-\Phi} \frac{R}{z} A_5 \right) \quad (3.37)$$

$$= \int d^5x \left(-A^\mu \partial_\mu \partial_5 \left(e^{-\Phi} \frac{R}{z} A_5 \right) \right) \quad (3.38)$$

$$= \int d^5x e^{-\Phi} \frac{R}{z} A^\mu \left(-\Phi' - \frac{1}{z} + \partial_5 \right) \partial^\mu A_5. \quad (3.39)$$

Combining with the rest of the action we have

$$S = S_1 + S_{GF1} + S_{GF2} + S_{GF3} \quad (3.40)$$

$$\begin{aligned} &= \int d^5x \left[\frac{e^{-\Phi}}{2} \frac{R}{z} A_\mu \left(\eta^{\mu\nu} \partial^2 - \left(1 - \frac{1}{\xi} \right) \partial^\mu \partial^\nu - \frac{e^\Phi z}{R} \eta^{\mu\nu} \partial_5 \left(e^{-\Phi} \frac{R}{z} \partial_5 \right) \right) A_\nu \right. \\ &\quad \left. - \frac{e^{-\Phi}}{2} \frac{R}{z} A_5 \partial^2 A_5 + \frac{\xi e^{-\Phi}}{2} \frac{R}{z} A_5 \partial_5 \left(e^\Phi \frac{z}{R} \partial_5 \left(e^{-\Phi} \frac{R}{z} A_5 \right) \right) \right]. \end{aligned} \quad (3.41)$$

One can now see that taking $\xi \rightarrow \infty$, the last term in would imply that the A_5 fields are infinitely heavy and therefore decouple from the theory. We can ignore the terms in A_5 and simply read off a differential operator for the first four components:

$$\Delta^{\mu\nu} = \left(\eta^{\mu\nu} \partial^2 - \left(1 - \frac{1}{\xi} \right) \partial^\mu \partial^\nu - \eta^{\mu\nu} \frac{e^\Phi z}{R} \partial_5 \left(e^{-\Phi} \frac{R}{z} \partial_5 \right) \right) \quad (3.42)$$

which may be thought of as a warped 5D analog of the d'Alembertian for fields in 4D Minkowski spacetime. In line with that analogy, we can use this to define the bosonic two point correlation function for the model, via a Green's equation. In order to derive this equation, we first must establish a quantisation procedure for a generic boson in the theory.

3.4 Canonical Quantisation of Gauge Fields

The second quantisation of the theory will proceed in much the same way as the 4D case, although we must take care to include appropriate geometrical factors in our definitions. We will follow closely the treatment of the 4D case found in [41] in both establishing commutation rules for the gauge fields and the application of these rules in deriving the propagator. Writing the action in its compact form

$$S = \int d^4x \int_R^\infty dz \sqrt{g} e^{-\Phi} \left(-\frac{1}{4} F_{MN} F^{MN} \right) + \mathcal{L}_{GF} \quad (3.43)$$

$$\mathcal{L}_{GF} = -\frac{1}{2\xi} e^{-\Phi} \frac{R}{z} \left(\partial_\sigma A^\sigma - \xi e^\Phi \frac{z}{R} \partial_5 \left(e^{-\Phi} \frac{R}{z} A_5 \right) \right)^2 \quad (3.44)$$

and inserting (3.27) we find the conjugate momentum

$$\pi^\mu \equiv \frac{\delta S}{\delta(\partial_0 A_\mu)} = e^{-\Phi} \frac{R}{z} \left(F^{\mu 0} - \frac{1}{\xi} (A_\sigma A^\sigma) + e^\Phi \frac{z}{R} \partial_5 \left(e^{-\Phi} \frac{R}{z} A_5 \right) \right). \quad (3.45)$$

Now writing $F^{\mu 0} = -\dot{A} + \partial^\mu A^0$,

$$[A_\nu, \pi_\mu] = e^{-\Phi} \frac{R}{z} \left(-[A_\nu, \dot{A}_\mu] + [A_\nu, \partial^\mu A^0] \right. \quad (3.46)$$

$$\begin{aligned} & -\frac{1}{\xi} \eta_{ij} [A_\nu, \partial^i A^j] - \frac{1}{\xi} \eta_{00} [A_\nu, \dot{A}_\mu] \\ & \quad \left. + [A_\nu, \frac{1}{2} \partial_5 \left(e^{-\Phi} \frac{R}{z} \right)] \right) \\ & = e^{-\Phi} \frac{R}{z} \left([\dot{A}_\mu, A_\nu] - \frac{1}{\xi} [\dot{A}_0, A_\nu] \eta_{\mu 0} \right) \end{aligned} \quad (3.47)$$

since equal time commutators of fields and spatial derivatives vanish from the definition of the derivative and the explicit commutation relations, but commutators of fields and time derivatives contain contributions from commutators of fields at unequal times and do not trivially vanish (this can be seen by writing the explicit definition for the first derivative). Now assuming, as a trivial extension of the 4D scenario,

$$[A_\mu, \pi_\nu] = i g_{\mu\nu} \delta^{(3)}(\vec{x} - \vec{y}) \delta(z - z') \quad (3.48)$$

we have for $\mu = 0$

$$[\dot{A}_0, \pi_\nu] = [\dot{A}_0, A_\nu] - \frac{1}{\xi} [\dot{A}_0, A_\nu] = i e^\Phi \frac{z}{R} g_{\nu 0} \delta^{(4)}(x - y) \left(1 - \frac{1}{\xi}\right)^{-1} \quad (3.49)$$

$$= i e^\Phi \frac{z}{r} g_{\nu 0} \delta^{(4)}(x - y) \left(\frac{\xi}{\xi - 1}\right) \quad (3.50)$$

and for $\mu = i$

$$[\dot{A}_i, \pi_\nu] = [\dot{A}_i, A_\nu] = i e^\Phi \frac{z}{R} g_{\nu i} \delta^{(4)}(x - y). \quad (3.51)$$

We will apply these relations in determining the form of the two-point correlation function.

3.5 Gauge Boson Propagators

3.5.1 The Hybrid Approach

The treatment of boson propagators in warped 5D backgrounds requires some care, specifically because translational invariance in the extra dimension is broken by the dependence of the metric on the fifth coordinate (and indeed the presence of one or

more branes lying at a fixed position). Nevertheless, an adequate treatment has existed for some time [55] and has since seen multiple applications to flavour physics in WEDs [8, 20, 23, 12]. Although the precise results derived below are not new, the pedagogical presentation here is original. The approach is to work with a “hybrid” object defined in momentum space for the first four coordinates and position space for the fifth. We have the equation of motion

$$\Delta^\mu{}_\rho A^\rho = 0. \quad (3.52)$$

We are also now ready to consider $\Delta_x^\mu \langle 0 | T A^\rho(x, z) A_\nu(y, z') | 0 \rangle$. Bearing in mind that

$$T A^\rho(x, z) A_\nu(y, z') = \theta(x^0 - y^0) A^\rho(x, z) A^\nu(y, z') + \theta(y^0 - x^0) A^\nu(x, z) A^\rho(y, z') \quad (3.53)$$

so

$$\partial_x T A^\rho(x, z) A_\nu(y, z') = \delta(x^0 - y^0) [A^\rho(x, z), A^\nu(y, z')] + T \partial_x A^\rho(x, z) A^\nu(y, z'), \quad (3.54)$$

then

$$\begin{aligned} \Delta_x^\mu \langle 0 | T A^\rho(x, z) A_\nu(y, z') | 0 \rangle &= \langle 0 | T \Delta_x^\mu A^\rho(x, z) A_\nu(y, z') | 0 \rangle \\ &+ \langle 0 | \eta^\mu{}_\rho \partial_0 [A^\rho(x, z), A_\nu(y, z')] \delta(x^0 - y^0) | 0 \rangle \\ &- \langle 0 | (1 - \frac{1}{\xi}) \eta^{\mu 0} \partial_\rho [A^\rho(x, z), A_\nu(y, z')] \delta(x^0 - y^0) | 0 \rangle \\ &- \langle 0 | \eta^\mu{}_\rho e^\Phi \frac{z}{R} \partial_5 (e^{-\Phi} \frac{R}{z} \partial_5) [A^\rho(x, z), A_\nu(y, z')] \delta(x^0 - y^0) | 0 \rangle. \end{aligned} \quad (3.55)$$

The first line of the RHS will vanish due to (3.52) and all commutators of fields with spatial derivatives will also vanish as explained above. This leaves

$$\langle 0 | \eta^\mu_\rho [\dot{A}^\rho(x, z), A_\nu(y, z')] \delta(x^0 - y^0) | 0 \rangle - \langle 0 | \eta^\mu_0 (1 - \frac{1}{\xi}) [\dot{A}^0(x, z), A_\nu(y, z')] \delta(x^0 - y^0) | 0 \rangle \quad (3.56)$$

$$= \langle 0 | \left(\eta^\mu_0 - \eta^\mu_0 (1 - \frac{1}{\xi}) \right) [\dot{A}^0(x, z), A_\nu(y, z')] \delta(x^0 - y^0) | 0 \rangle \\ + \langle 0 | \eta^\mu_i [\dot{A}^i(x, z), A_\nu(y, z')] \delta(x^0 - y^0) | 0 \rangle. \quad (3.57)$$

Now substituting for the commutators and writing $\delta^{(5)}(X - Y) \equiv \delta^{(4)}(x - y) \delta(z - z')$ we have

$$\langle 0 | 0 \rangle \eta^\mu_0 g^0_\nu i e^\Phi \frac{z}{R} \delta^{(5)}(X - Y) + \langle 0 | 0 \rangle \eta^\mu_i g^i_\nu i e^\Phi \frac{z}{R} \delta^{(5)}(X - Y) = i e^\Phi \frac{z}{R} \delta^\mu_\nu \delta^{(5)}(X - Y) \quad (3.58)$$

since $\eta^\mu_0 g^0_\nu + \eta^\mu_i g^i_\nu = \eta^\mu_\lambda g^\lambda_\nu = \eta^\mu_\nu$. The result is therefore

$$\Delta_x^\mu \langle 0 | T A^\rho(x, z) A_\nu(y, z') | 0 \rangle = i e^\Phi \frac{z}{R} \delta^\mu_\nu \delta^{(5)}(X - Y) \quad (3.59)$$

which will serve as our analogue of the familiar 4D Green's equation. Now, Fourier transforming all but the fifth coordinate of the propagator yields

$$\langle 0 | T A^\rho(x, z) A_\nu(y, z') | 0 \rangle = \int \frac{d^4 p}{(2\pi)^4} e^{-ip \cdot (x - y)} \langle 0 | T \tilde{A}^\rho(p, z) \tilde{A}_\nu(p, z') | 0 \rangle. \quad (3.60)$$

We thus define an object existing in a hybrid momentum-position space. With a little work, we will see in Section 5.3 that this form is indeed practical for the purposes of calculating quantum amplitudes in perturbation theory in the full 5D background. We

first need to write and solve a differential equation for the hybrid two-point correlation function. To do this, let us consider the Lorentz structure of the propagator.

3.5.2 General form of the Bosonic Propagator

Employing the simplified notation $\langle 0|T\tilde{A}^\mu(p, z)\tilde{A}^\nu(p, z')|0\rangle \equiv \langle A^\mu A^\nu \rangle$, the most general form of the propagator, for want of any other Lorentz tensors to provide contributions, is

$$\langle A^\mu A^\nu \rangle = A(p^2, z, z')\eta^{\mu\nu} + B(p^2, z, z')\frac{p^\mu p^\nu}{p^2} \quad (3.61)$$

i.e. it can be constructed entirely from the 4D Minkowski metric and four-momenta. Then making the redefinition $\tilde{B} = A + B$ one can write

$$\langle A^\mu A^\nu \rangle = A(p^2, z, z')\left(\eta^{\mu\nu} - \frac{p^\mu p^\nu}{p^2}\right) + \tilde{B}(p^2, z, z')\frac{p^\mu p^\nu}{p^2}. \quad (3.62)$$

Notice that the first term is transverse since $p_\mu(\eta^{\mu\nu} - \frac{p^\mu p^\nu}{p^2}) = 0$. Inserting (3.60) into (3.59) one finds

$$\left(-p^2\eta^\mu{}_\rho + \left(1 - \frac{1}{\xi}\right)p^\mu p_\rho - \eta^\mu{}_\rho e^\Phi \frac{z}{R}\partial_5\left(e^{-\Phi}\frac{R}{z}\partial_5\right)\right)\langle A^\rho A_\nu \rangle = ie^\Phi \frac{z}{R}\delta^\mu{}_\nu \delta(z - z'). \quad (3.63)$$

Then substituting from (3.62),

$$\begin{aligned} & -p^2\left[\delta^\mu{}_\nu - \frac{p^\mu p_\nu}{p^2}\right]A - p^2\frac{p^\mu p_\nu}{p^2}\tilde{B} + \left(1 - \frac{1}{\xi}\right)p^\mu p_\nu\tilde{B} - \left[\delta^\mu{}_\nu - \frac{p^\mu p_\nu}{p^2}\right]\frac{e^\Phi z}{R}\partial_5\left(e^{-\Phi}\frac{R}{z}\partial_5\right)A \\ & - \frac{p^\mu p_\nu}{p^2}\frac{e^\Phi z}{R}\partial_5\left(e^{-\Phi}\frac{R}{z}\partial_5\right)\tilde{B} = ie^\Phi \frac{z}{R}\delta^\mu{}_\nu \delta(z - z'). \end{aligned} \quad (3.64)$$

Then contracting with p_μ one finds

$$-p^2 \tilde{B} + \left(1 - \frac{1}{\xi}\right) p^2 \tilde{B} - \frac{e^\Phi z}{R} \partial_5 \left(e^{-\Phi} \frac{R}{z} \partial_5 \right) \tilde{B} = i e^\Phi \frac{z}{R} \delta(z - z') \quad (3.65)$$

$$\left(\frac{-p^2}{\xi} - \frac{e^\Phi z}{R} \partial_5 \left(e^{-\Phi} \frac{R}{z} \partial_5 \right) \right) \tilde{B} = i e^\Phi \frac{z}{R} \delta(z - z'). \quad (3.66)$$

Contracting instead with δ^ν_μ yields

$$-3p^2 A - p^2 \tilde{B} + \left(1 - \frac{1}{\xi}\right) p^2 \tilde{B} - 3 \frac{e^\Phi z}{R} \partial_5 \left(e^{-\Phi} \frac{R}{z} \partial_5 \right) A - \frac{e^\Phi z}{R} \partial_5 \left(e^{-\Phi} \frac{R}{z} \partial_5 \right) \tilde{B} = 4i e^\Phi \frac{z}{R} \delta(z - z') \quad (3.67)$$

and substituting from (3.65) we find,

$$\left(-p^2 + \frac{e^\Phi z}{R} \partial_5 \left(e^{-\Phi} \frac{R}{z} \partial_5 \right) \right) A = e^\Phi \frac{z}{R} \delta(z - z'). \quad (3.68)$$

So defining $A \equiv -iG_p(z, z')$ and $\tilde{B} \equiv -iG_{\frac{p}{\sqrt{\xi}}}(z, z')$ the full form of the propagator is therefore

$$\langle A^\mu A^\nu \rangle = -iG_p(z, z') \left(\eta^{\mu\nu} - \frac{p^\mu p^\nu}{p^2} \right) - iG_{\frac{p}{\sqrt{\xi}}}(z, z') \left(\frac{p^\mu p^\nu}{p^2} \right). \quad (3.69)$$

For all calculations in future sections, we will work in Lorenz gauge with $\xi = 0$ and $\partial_\mu A^\mu = 0$, in which case the propagator is purely transverse,

$$\langle A^\mu A^\nu \rangle = -iG_p(z, z') \left(\eta^{\mu\nu} - \frac{p^\mu p^\nu}{p^2} \right) \quad (3.70)$$

with the two point correlation function obeying (3.68), namely

$$\boxed{\left(e^{\Phi} \frac{z}{R} \partial_5 \left(e^{-\Phi} \frac{R}{z} \partial_5\right) + p^2\right) G_p(z, z') = e^{\Phi} \frac{z}{R} \delta(z - z')} \quad (3.71)$$

Note that this derivation is trivially extended to the case of a boson field with a non-zero bulk mass, simply by including a mass term in the differential operator,

$$\boxed{\left(e^{\Phi} \frac{z}{R} \partial_5 \left(e^{-\Phi} \frac{R}{z} \partial_5\right) + p^2 - \mu(z)\right) G_p(z, z') = e^{\Phi} \frac{z}{R} \delta(z - z')} \quad (3.72)$$

Equations (3.71) and (3.72) match those found in [8, 7].

3.5.3 The Correlation Functions

There are in fact a number of approaches one can take to the evaluation of the two-point correlator $G_p(z, z')$ for a given boson. One can either calculate each mode individually, or one can solve (3.71) or (3.72). Applying the Kaluza Klein expansions for the gauge fields (3.18) and substituting the usual flat 4D Klein-Gordon Green's function yields

$$\langle A^\mu(x, z) A^\nu(x', z') \rangle = \sum_{n=0}^{\infty} f^n(z) f^n(z') \langle A_n^\mu(x) A_n^\nu(x') \rangle \quad (3.73)$$

$$= \int \frac{d^4 p}{(2\pi)^4} \sum_{n=0}^{\infty} \frac{f^n(z) f^n(z')}{p^2 - m_n^2} e^{-ip(x-x')} \Pi^{\mu\nu} \quad (3.74)$$

where Π is a gauge dependent Lorentz structure. Combining (3.60), (3.62) and (3.74) in Lorenz gauge one then infers

$$G_p(z, z') = \sum_{n=0}^{\infty} \frac{f^n(z) f^n(z')}{p^2 - m_n^2}. \quad (3.75)$$

Multiplying (3.23) with $f_n(z')$ and applying the completeness relation (3.20), one sees that (3.75) indeed satisfies (3.72).

3.5.4 Determining the Correlation Function for Quadratic Dilaton

We are now in a position to find $G_p(z, z')$. Let us do this by massaging (3.71) into the form:

$$x \frac{d^2 w}{dx^2} + (b - x) \frac{dw}{dx} - aw = 0 \quad (3.76)$$

which is Kummer's differential equation. One immediately sees that (3.71) is homogeneous for $z \neq z'$. Expanding the LHS in this region gives

$$\left(\partial_5^2 - \Phi' \partial_5 - \frac{1}{z} \partial_5 + p^2 \right) G_p(z, z') = 0. \quad (3.77)$$

We can switch to dilaton space by making the associations:

$$\partial_5 = \frac{\partial}{\partial z} = \frac{\partial \Phi}{\partial z} \frac{\partial}{\partial \Phi} \quad (3.78)$$

$$= \Phi' \partial_\Phi \quad (3.79)$$

and

$$\partial_5^2 = \frac{\partial^2}{\partial z^2} = \frac{\partial}{\partial z} \left(\frac{\partial \Phi}{\partial z} \frac{\partial}{\partial \Phi} \right) = \left(\frac{\partial}{\partial z} \frac{\partial \Phi}{\partial z} \right) \frac{\partial}{\partial \Phi} + \frac{\partial \Phi}{\partial z} \left(\frac{\partial}{\partial z} \frac{\partial}{\partial \Phi} \right) \quad (3.80)$$

$$= \Phi'' \partial_\Phi + \Phi'^2 \partial_\Phi^2. \quad (3.81)$$

Then (3.77) becomes

$$\left(\Phi'^2 \partial_\Phi^2 + \Phi'' \partial_\Phi - \Phi'^2 \partial_\Phi - \frac{\Phi'}{z} \partial_\Phi + p^2 \right) G_p(z, z') = 0. \quad (3.82)$$

In [8] the dilaton was fixed by $\nu = 2$ with $\Phi = \frac{z^\nu}{R'^\nu}$. This gives

$$0 = \left(\frac{2}{R'^2} \partial_\Phi^2 + \frac{4z^2}{R'^4} \partial_\Phi - \left(\frac{2z}{R'^2} \right)^2 \partial_\Phi - \frac{2}{R'^2} \partial_\Phi + p^2 \right) G_p(z, z') \quad (3.83)$$

$$= \left(\frac{4z^2}{R'^4} \partial_\Phi^2 - \frac{4z^2}{R'^4} \partial_\Phi + p^2 \right) G_p(z, z') \quad (3.84)$$

$$= \left(\frac{z^\nu}{R'^\nu} \partial_\Phi^2 - \frac{z^\nu}{R'^\nu} \partial_\Phi + \frac{R'^2 p^2}{4} \right) G_p(z, z') \quad (3.85)$$

which is Kummer's equation (3.76) with $a = -\frac{R'^2 p^2}{4}$, $b = 0$ and $x = \frac{z^2}{R'^2}$. We have linearly independent solutions $\frac{z^2}{R'^2} M\left(1 - a, 2, \frac{z^2}{R'^2}\right)$ and $\frac{z^2}{R'^2} U\left(1 - a, 2, \frac{z^2}{R'^2}\right)$. It follows that we can describe the homogeneous scenario by writing:

$$G_p(z, z') = \begin{cases} Az^2 M\left(1 - a, 2, \frac{z^2}{R'^2}\right) + Bz^2 U\left(1 - a, 2, \frac{z^2}{R'^2}\right) & \text{if } z < z' \\ Cz^2 M\left(1 - a, 2, \frac{z^2}{R'^2}\right) + Dz^2 U\left(1 - a, 2, \frac{z^2}{R'^2}\right) & \text{if } z > z' \end{cases} \quad (3.86)$$

Introducing $u = \min(z, z')$ and $v = \max(z, z')$ and requiring that $G_p(u, u) = G_p(v, v)$

(since $u(z, z') = v(z, z')$ if $z = z'$), one can make the general ansatz:

$$G_p(u, v) = Nu^2 v^2 \left(AM\left(1 - a, 2, \frac{u^2}{R'^2}\right) + BU\left(1 - a, 2, \frac{u^2}{R'^2}\right) \right) \\ \times \left(CM\left(1 - a, 2, \frac{v^2}{R'^2}\right) + DM\left(1 - a, 2, \frac{v^2}{R'^2}\right) \right) \quad (3.87)$$

where N is a normalisation constant to be found. The result found in [8] was

$$N = \frac{\Gamma(1-a)}{2(BC-AD)RR^2}. \quad (3.88)$$

One can determine the constants A, B, C and D using the Neumann boundary condition on the UV brane, and the condition that the propagator is comprised of KK modes normalisable according to $\int_R^\infty dz e^{-\Phi \frac{R}{z}} f_n^2 = 1$, by considering the way the Kummer functions scale in their arguments. Again, a similar calculation is possible for the bosons with a non-zero bulk mass. The upshot is that for $\nu = 2$, one can find a closed form for the entire (including all KK modes) correlation function, in terms of Kummer functions.

Had we taken $\nu \rightarrow \infty$ in (3.71), then in the region $R < z < R'$, $\Phi \rightarrow 0$ and so we would have recovered the equivalent hard-wall equation, i.e. (4.5) of [55]. In that case, the solution is in terms of Bessel functions. However, it turns out that the complete solution for $\nu = 2$ is not practical for numerical purposes, since for large warp factors one encounters integrals which are difficult to evaluate [8]. Furthermore, in order to explore a range of backgrounds corresponding to different values of ν , one would have to re-solve (3.71) every time. Worse still is that while for $\nu \rightarrow \infty$ and $\nu = 2$ one has Bessel and Kummer equations respectively, the resulting forms of (3.71) for arbitrary values of ν are not well studied equations with well known solutions. While for the sake of numerics, the first issue can be overcome by working with an approximation via a finite truncation of the sum of KK modes, one still has the problem of finding explicit forms of the gauge profiles in arbitrary backgrounds. For this reason, we present in Section 5.3 an alternative methodology, which is applicable to numerical evaluation of $G_p(z, z')$ for

a general dilaton, without the need to solve any further differential equations. It should be noted that a similar approach has been applied previously [19] in the non-conformal frame, so although the precise formulas differ due to the use of alternative coordinates, the methodology is comparable.

Chapter 4

Flavour Physics Overview

4.1 Quark Mixing and the CKM Matrix

In order to elucidate the full significance of FCNCs arising in the WED scenarios, it will be instructive to first consider how these processes occur in the standard model. The following discussion is informed by [26]. Post spontaneous symmetry breaking, the Yukawa terms for the three generations of quarks, left-handed SU(2) doublets and right-handed singlets have the form

$$\mathcal{L}_{Yuk} = \frac{v}{\sqrt{2}} \lambda_{ij}^u \bar{Q}_{iL}^u q_{jR}^u + \frac{v}{\sqrt{2}} \lambda_{ij}^d \bar{Q}_{iL}^d q_{jR}^d + h.c. \quad (4.1)$$

where u, d denote up-like and down-like quarks respectively. In general, the resulting mass matrices $M_{ij}^{u,d} = v/\sqrt{2} \lambda_{ij}^{u,d}$ need not be diagonal. Thus the “interaction-basis” or “gauge-basis” fields Q and q are not manifestly physical states. However, one can

always find a bi-unitary transformation to diagonalise the mass matrix as

$$M_{diag} = U^\dagger M V \quad (4.2)$$

The matrices U and V affect a basis rotation between the gauge-basis fields and eigenstates of the diagonal mass matrix, i.e. “mass-basis” fields. To see this one can simply write

$$Q_{iL}^{u,d} = U_{ia}^{u,d} Q'_{aL}{}^{u,d} \quad q_{iR}^{u,d} = V_{ia}^{u,d} q'_{aR}{}^{u,d} \quad (4.3)$$

where primes indicate mass-basis fields, and a and i, j are generation indices for mass-basis and gauge-basis fields respectively. Thus the physical mass-basis fields are in fact admixtures of the different generations in the gauge-basis. Then (4.1) becomes

$$\mathcal{L}_{Yuk} = \frac{v}{\sqrt{2}} U_{ai}^{\dagger u} \lambda_{ij}^u V_{jb}^u \bar{Q}'_{aL}{}^u q'_{bR}{}^u + \frac{v}{\sqrt{2}} U_{ai}^{\dagger d} \lambda_{ij}^d V_{jb}^d \bar{Q}'_{aL}{}^d q'_{bR}{}^d + h.c. \quad (4.4)$$

$$= (M_{diag}^u)_{ab} \bar{Q}'_{aL}{}^u q'_{bR}{}^u + (M_{diag}^d)_{ab} \bar{Q}'_{aL}{}^d q'_{bR}{}^d + h.c. \quad (4.5)$$

as required. The mixing of the quark flavours may be parametrised in terms of angles of rotation relating the different bases. For the simple example of two generations, the weak charged-current interaction is described by

$$J^\mu W_\mu^+ = (\bar{u}, \bar{c})_L \gamma^\mu \begin{pmatrix} \cos \theta_c & \sin \theta_c \\ -\sin \theta_c & \cos \theta_c \end{pmatrix} \begin{pmatrix} d \\ s \end{pmatrix}_L W^+ \quad (4.6)$$

where θ_c is the Cabibbo angle. Generalising to three generations, one has

$$(\bar{u}_L^{bulk} \bar{c}_L^{bulk} \bar{t}_L^{bulk}) \gamma^\mu W_\mu^+ \begin{pmatrix} d_L^{bulk} \\ s_L^{bulk} \\ b_L^{bulk} \end{pmatrix} = (\bar{u}_L^{std} \bar{c}_L^{std} \bar{t}_L^{std}) \gamma^\mu W_\mu^+ U^{u\dagger} U^d \begin{pmatrix} d_L^{std} \\ s_L^{std} \\ b_L^{std} \end{pmatrix} \quad (4.7)$$

(4.8)

$$= (\bar{u}_L^{std} \bar{c}_L^{std} \bar{t}_L^{std}) \gamma^\mu W_\mu^+ V_{CKM} \begin{pmatrix} d_L^{std} \\ s_L^{std} \\ b_L^{std} \end{pmatrix} \quad (4.9)$$

(4.10)

where “std” denotes the “standard” basis and the CKM matrix is the 3x3 unitary matrix

$$V_{CKM} \equiv \hat{U}^{u\dagger} \hat{U}^d = \begin{pmatrix} V_{ud} & V_{us} & V_{ub} \\ V_{cd} & V_{cs} & V_{cb} \\ V_{td} & V_{ts} & V_{tb} \end{pmatrix} \quad (4.11)$$

which can be expressed just in terms of three mixing angles $\theta_{12}, \theta_{23}, \theta_{13}$ and single phase δ . In the “standard parametrisation” it is given by

$$V_{CKM} = \begin{pmatrix} c_{12}c_{13} & s_{12}c_{13} & s_{13}e^{-i\delta} \\ -s_{12}c_{23} - c_{12}s_{23}s_{13}e^{i\delta} & c_{12}c_{23} - s_{12}s_{23}s_{13}e^{i\delta} & s_{23}c_{13} \\ s_{12}s_{23} - c_{12}c_{23}s_{13}e^{i\delta} & -c_{12}s_{23} - s_{12}c_{23}s_{13}e^{i\delta} & c_{23}c_{13} \end{pmatrix} \quad (4.12)$$

where $s_{ij} \equiv \sin(\theta_{ij})$ and $c_{ij} \equiv \cos(\theta_{ij})$. This form can be found in [52] and is stated there with observed numerical values.

4.2 Suppression of FCNCs in the SM

We are now in a position to consider the effect of (4.3) on the other terms in the Lagrangian. In particular, we are interested in the gauge terms of the covariant derivatives, since these define fermion interactions with the standard model gauge bosons, namely γ, W^\pm, Z^0 and g . One finds there is a significant difference in the behaviour of charged versus neutral current interactions under the basis transformations. Explicitly, a charged left-handed quark current becomes

$$J^\mu = \bar{Q}_{iL}^{u,d} \gamma^\mu Q_{iL}^{d,u} = \bar{Q}'_{aL}{}^{u,d} \gamma^\mu U_{ai}^{\dagger u,d} U_{ib}^{d,u} Q'_{bL}{}^{d,u} \quad (4.13)$$

and likewise a right-handed charged current,

$$J^\mu = \bar{q}_{iR}^{u,d} \gamma^\mu q_{iR}^{d,u} = \bar{q}'_{aR}{}^{u,d} \gamma^\mu V_{ai}^{\dagger u,d} V_{ib}^{d,u} q'_{bR}{}^{d,u} \quad (4.14)$$

but in contrast, a left-handed neutral current is invariant:

$$J_0^\mu = \bar{Q}_{iL}^{u,d} \gamma^\mu Q_{iL}^{u,d} = \bar{Q}'_{aL}{}^{u,d} \gamma^\mu \underbrace{U_{ai}^{\dagger u,d} U_{ib}^{u,d}}_{\mathbb{1}} Q'_{bL}{}^{u,d} \quad (4.15)$$

$$= \bar{Q}'_{aL}{}^{u,d} \gamma^\mu Q'_{aL}{}^{u,d} \quad (4.16)$$

as is a right-handed neutral current:

$$J_0^\mu = \bar{q}_{iR}^{u,d} \gamma^\mu q_{iR}^{u,d} = \bar{q}_{aR}'^{u,d} \gamma^\mu \underbrace{V_{ai}^{\dagger u,d} V_{ib}^{u,d}}_{\mathbb{1}} q_{bR}'^{u,d} \quad (4.17)$$

$$= \bar{q}_{aR}'^{u,d} \gamma^\mu q_{aR}'^{u,d}. \quad (4.18)$$

So for charged currents, our gauge-fermion interactions for an arbitrary charged boson, quark and coupling g are generally of the form

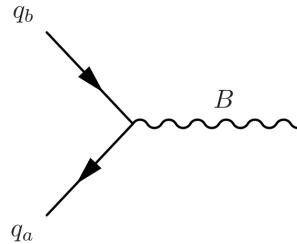
$$i\bar{\psi}_L \not{D} \psi_L \supset -ig J_L^\mu W_\mu^\pm \sim g U_{ai}^{\dagger u,d} U_{jb}^{d,u} \quad (4.19)$$

$$i\bar{\psi}_R \not{D} \psi_R \supset -ig J_R^\mu W_\mu^\pm \sim g V_{ia}^{\dagger u,d} V_{aj}^{d,u} \quad (4.20)$$

whereas for neutral currents coupling to an arbitrary neutral boson, interactions are necessarily still flavour-diagonal in the mass-basis:

$$i\bar{\psi}_{L,R} \not{D} \psi_{L,R} \supset -ig J_{0L,R}^\mu A_\mu \sim g \delta_{ab}. \quad (4.21)$$

Thus we see there are no couplings of neutral bosons to currents consisting of quarks of different generations in the SM, i.e. no FCNCs. Diagrammatically, the consequences are such that any neutral vertex always conserves flavour:



$$B = \begin{cases} \gamma, Z^0, g & a = b \\ W^\pm & a \neq b \end{cases}$$

This is of course, not the end of the story, since so far we have neglected to consider the effect of loops in flavour changing processes. In fact, at one-loop level, one already sees the possibility of both $\Delta F = 2$ and $\Delta F = 1$ processes in the quark sector. In the former case, the original mechanism was proposed by Glashow, Iliopoulos and Maiani, who, in the process, predicted the existence of the charm quark [35]. One achieves an overall charge neutrality via both a W^+ and W^- running in a box diagram. The details of this are explained in the following section in the context of neutral meson mixing. Here however, the crucial point that should be noted is simply that processes which change flavour with no overall charge difference between in and out states have a leading contribution from one-loop diagrams, that is to say their amplitudes are suppressed by the mass of the W boson, namely by a factor $1/M_W^2$. As such, one would expect any new physics theory with tree-level FCNCs to show up fairly easily amongst the low SM background. Conversely, given that experimental constraints on flavour violation are typically very stringent[59, 38, 5, 29, 12], these processes are dangerous for such NP theories, in the absence of some additional suppression mechanism. Indeed, in Section 4.4 we will see how this is the case in models with warped extra dimensions, and explain the importance of what has been dubbed the “RS-GIM” mechanism [4] for suppressing tree-level contributions to flavour changing neutral processes.

4.3 Neutral Meson Mixing in the SM

In Section 6.1, we will look in some detail at the precise numerical calculations of physical observables in both the $K - \bar{K}$ and $B_{d,s} - \bar{B}_{d,s}$ meson mixing systems. For now, we shall concern ourselves primarily with elucidating the basic physics underlying

the origin of CP violation in these systems. For this purpose, let us focus on the kaons, although much of the physics naturally also applies to the B mesons. The following draws on discussions from [15, 51]. In the gauge eigenbasis, one can define QCD bound states $K^0 = \bar{s}d$ and $\bar{K}^0 = s\bar{d}$. These can be chosen to satisfy a behaviour under charge C and parity P transformations according to

$$\begin{aligned} C|K^0\rangle &= |\bar{K}^0\rangle & C|\bar{K}^0\rangle &= |K^0\rangle \\ P|K^0\rangle &= -|K^0\rangle & P|\bar{K}^0\rangle &= -|\bar{K}^0\rangle \\ CP|K^0\rangle &= -|\bar{K}^0\rangle & CP|\bar{K}^0\rangle &= -|K^0\rangle \end{aligned} \tag{4.22}$$

which fixes our choice of complex phases. One can form normalised CP eigenstates as linear combinations,

$$|K_1\rangle = \frac{1}{\sqrt{2}} (|K^0\rangle - |\bar{K}^0\rangle) \tag{4.23}$$

$$|K_2\rangle = \frac{1}{\sqrt{2}} (|K^0\rangle + |\bar{K}^0\rangle) \tag{4.24}$$

satisfying

$$CP|K_{1,2}\rangle = \pm |K_{1,2}\rangle. \tag{4.25}$$

The Schrödinger evolution from $t = 0$ for a stable particle state $|\psi(t)\rangle$ of energy M is given simply by

$$|\psi(t)\rangle = e^{-iH(t)}|\psi(0)\rangle = e^{-iMt}|\psi(0)\rangle. \tag{4.26}$$

For Kaons in the SM however, there are possible decay routes provided by the one-loop box diagrams. In particular, $K^0 - \bar{K}^0$ oscillations can occur as shown in Figure 4.1. As

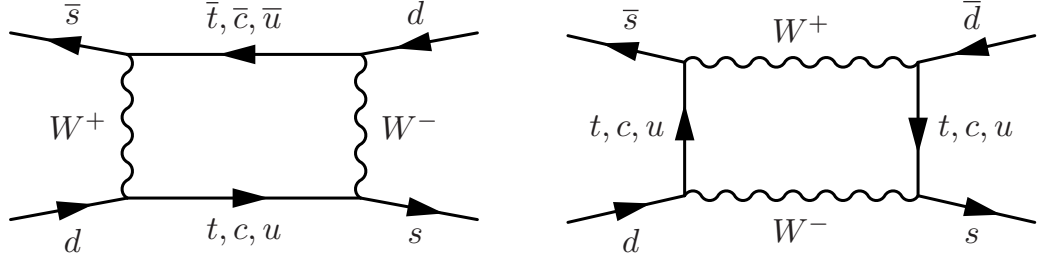


Figure 4.1: W -mediated box diagrams providing the leading contributions to $K - \bar{K}$ mixing in the standard model [44].

such the amplitude for a Kaon to survive attenuates over time according to

$$|\langle K^0(0) | K^0(t) \rangle|^2 = \sum_i e^{-\Gamma_i t} \quad (4.27)$$

where the index i runs over all possible decay modes. We thus write a Hamiltonian of the simple form

$$H = M - i\Gamma/2 \quad (4.28)$$

satisfying (4.26) and (4.27), writing the total decay width $\Gamma = \sum_i \Gamma_i$. For K mixing, the Hamiltonian can then be promoted to a two by two matrix,

$$\hat{H} = \begin{pmatrix} \hat{M}_{11} - \frac{i}{2}\hat{\Gamma}_{11} & \hat{M}_{12} - \frac{i}{2}\hat{\Gamma}_{12} \\ \hat{M}_{21} - \frac{i}{2}\hat{\Gamma}_{21} & \hat{M}_{22} - \frac{i}{2}\hat{\Gamma}_{22} \end{pmatrix} \quad (4.29)$$

$$i\frac{d}{dt}|\chi(t)\rangle = \hat{H}|\chi(t)\rangle \quad |\chi(t)\rangle = \begin{pmatrix} |K^0\rangle \\ |\bar{K}^0\rangle \end{pmatrix} \quad (4.30)$$

We require that \hat{M} and $\hat{\Gamma}$ have real eigenvalues, namely that they are hermitian:

$$\hat{M} = \hat{M}^\dagger \quad \hat{\Gamma} = \hat{\Gamma}^\dagger \quad (4.31)$$

which implies

$$M_{12} = M_{21}^* \quad \Gamma_{12} = \Gamma_{21}^* \quad (4.32)$$

whereas CPT symmetry implies that the decay rate and mass of K^0 must be precisely that of \bar{K}^0

$$M_{11} = M_{22} \equiv M \quad \Gamma_{11} = \Gamma_{22} \equiv \Gamma. \quad (4.33)$$

With these associations, the Hamiltonian matrix takes the simplified form

$$\hat{H} = \begin{pmatrix} \hat{M} - \frac{i}{2}\hat{\Gamma} & \hat{M}_{12} - \frac{i}{2}\hat{\Gamma}_{12} \\ \hat{M}_{12}^* - \frac{i}{2}\hat{\Gamma}_{12}^* & \hat{M} - \frac{i}{2}\hat{\Gamma} \end{pmatrix}. \quad (4.34)$$

The diagonal elements here are the flavour conserving parts. These therefore capture the physics of the strong interactions. Weak interactions can change flavour, these being responsible for the off-diagonal elements. The CP-violating phase arises of course from the weak interactions, defined as $\phi = \arg(-M_{12}/\Gamma_{12})$. The physical eigenstates are obtained in a basis in which the mass matrix is diagonal. As such, they are simple linear combinations of the gauge eigenstates K^0 and \bar{K}^0 . The matrix in (4.34) can be straightforwardly diagonalised according to $\hat{H}_{diag} = S^{-1}\hat{H}S$. Explicitly, the eigenvalues follow from

$$\det(\hat{H} - \lambda \mathbb{1}) = 0 \quad (4.35)$$

$$\lambda^2 - 2\lambda \left(M - \frac{i}{2}\Gamma \right) + \left(M - \frac{i}{2}\Gamma \right)^2 - \left(M_{12} - \frac{i}{2}\Gamma_{12} \right) \left(M_{12}^* - \frac{i}{2}\Gamma_{12}^* \right) = 0 \quad (4.36)$$

with solutions

$$\lambda = \left(M - \frac{i}{2}\Gamma \right) \pm \sqrt{\left(M_{12} - \frac{i}{2}\Gamma_{12} \right) \left(M_{12}^* - \frac{i}{2}\Gamma_{12}^* \right)}. \quad (4.37)$$

The corresponding eigenstates, expressed in terms of a small complex parameter $\bar{\epsilon}$, defined via

$$\frac{1 - \bar{\epsilon}}{1 + \bar{\epsilon}} = \sqrt{\frac{M_{12}^* - \frac{i}{2}\Gamma_{12}^*}{M_{12} - \frac{i}{2}\Gamma_{12}}} \quad (4.38)$$

are

$$|K_{L,S}\rangle = \frac{(1 + \bar{\epsilon})|K^0\rangle \pm (1 - \bar{\epsilon})|\bar{K}^0\rangle}{\sqrt{2(1 + |\bar{\epsilon}|^2)}} \quad (4.39)$$

which, in terms of the CP eigenstates, take the form

$$|K_S\rangle = \frac{|K_1\rangle + \bar{\epsilon}|K_2\rangle}{\sqrt{1 + |\bar{\epsilon}|^2}} \quad |K_L\rangle = \frac{|K_2\rangle + \bar{\epsilon}|K_1\rangle}{\sqrt{1 + |\bar{\epsilon}|^2}}. \quad (4.40)$$

We thus see that the physical states are not quite CP eigenstates, namely CP violation is parameterised by $\bar{\epsilon}$, albeit in a manner depending on the phase convention determined by (4.22). The effect of this is most easily understood in terms of the decay of K_L and K_S into pion states. In the absence of CP violation, naïvely one would expect the CP even $K_L \rightarrow \pi\pi\pi$ and CP odd $K_S \rightarrow \pi\pi$ decay channels to be pure and entirely definitive of the decays of each initial state into final pion states. The original discovery by Cronin and Fitch in 1964 [27] that K_L can in fact be seen to decay to two pions was the first evidence of CP violation in standard model. One can quantify the (indirect)¹ CP violation in kaon mixing as

$$\epsilon_K = \frac{A(K_L \rightarrow (\pi\pi)_{I=0})}{A(K_S \rightarrow (\pi\pi)_{I=0})} \quad (4.41)$$

¹Violation in this case occurs via the mixing of CP eigenstates. Here we are focussing only on physics relevant to the phenomenological results in later sections of this thesis. For a discussion of direct CP violation in the kaon system, the reader is referred to [15]

which is phase invariant. ϵ_K will, however, depend on the precise choice of parametrisation of the CKM matrix. In the standard parameterisation [52] we work with the formula [12]

$$\epsilon_K = \frac{\kappa_\epsilon e^{i\Phi_\epsilon}}{\sqrt{2}(\Delta m_K)_{exp}} \text{Im}[\langle K^0 | H^{\Delta S=2} | \bar{K}^0 \rangle] \quad (4.42)$$

where $\Delta m_K = (3.484 \pm 0.006) \times 10^{-15} \text{GeV}$ and $\Phi_\epsilon = 43.51^\circ$. [52] Here, $\kappa_\epsilon = 0.92$ is the suppression factor discussed in [16]. The Hamiltonian $H^{\Delta S=2}$ describes the evolution of $\bar{K} \rightarrow K$ and can be treated in terms of local operators in an effective field theory. The details of this are left to Chapter 5 in which a tree-level analysis is given, neglecting loop contributions and therefore ignoring any possible modifications to the QCD contributions via $\eta_{cc}, \eta_{ct}, \eta_{tt}$. The ϵ_K observable has been shown to provide stringent constraints on the parameter space of warped models, both in hard-wall RS [12] and with a soft-wall with $\nu = 2$ [8]. In Section 6.2 we will extend this analysis to soft-walls with a range of values for both ν and α .

4.4 Tree-Level FCNCs in WEDs

When we looked at FCNCs in the context of the standard model in Section 4.1, we in fact glossed over a subtlety which turns out to be crucial once we consider flavour physics in the warped extra dimension. Since all quark flavours couple with identical strength to a given gauge boson in the SM, the convention is simply to write the couplings as scalar constants in the action. To be precise however, one could write a coupling as a matrix in generation space

$$g_{ij} = \text{diag}(g1, g2, g3)_{ij} \quad (4.43)$$

Clearly in the case of the SM, one simply has $g_{ij} \sim \delta_{ij}$ since $g_1 = g_2 = g_3$, but this is not necessarily the case in general. Under the transformations (4.3), the result stated in (4.21) no longer holds if the fermion flavours couple non-universally. In general one must write expressions of the form

$$g_{ab} = U_{ai}^\dagger g_{ij} U_{jb} \quad (4.44)$$

where for simplicity we are ignoring chirality. Although the coupling matrix in the gauge basis is still diagonal (by definition), it is not directly proportional to the identity, and as such it no longer remains diagonal in the mass basis. Tree-level FCNCs arise in warped scenarios due to non-universality of couplings between fermions and KK modes of the gauge bosons [38]. In the gauge basis, this non-universality comes in the form of multiplicative corrections to the effective couplings, which appear in the 4D theory after performing the Kaluza Klein decompositions in the 5D action and integrating out the extra dimension. Explicitly, an arbitrary 5D gauge-fermion interaction arises in the (conformal) Jordan frame as,

$$S_{5D} \supset \int d^4x \int_R^\infty dz \sqrt{g} e^{-\Phi} (-ig \Psi \bar{\Gamma}^M A_M \Psi) \quad (4.45)$$

and noting that $\sqrt{g} \Gamma^\mu = e^{-4A} \gamma^\mu$, one obtains, after applying (3.9) and (3.18), a 4D interaction for two fermion zero modes and the n -th bosonic KK mode

$$S_{4D} \supset \int d^4x -ig g_{ii}^n \bar{\psi}^0(x) A^n(x) \psi^0(x) \quad (4.46)$$

$$g_{ii}^n = \int_R^\infty dz f_i^0(z) f^n(z) f_i^0(z). \quad (4.47)$$

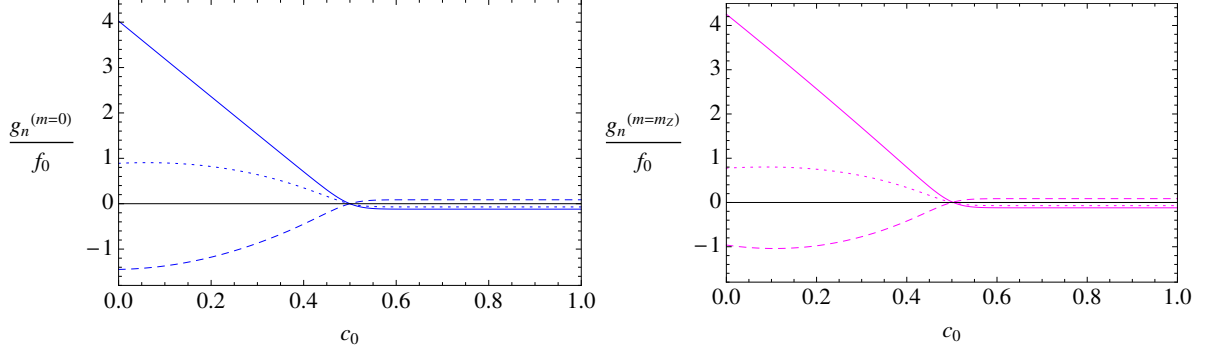


Figure 4.2: The overlap integral factors appearing in the effective 4D couplings of fermions localised at c_0 with the gauge profiles. On the left in blue, the solid, dashed and dotted lines correspond to first, second and third KK modes for a massless zero-mode gauge field and likewise on the right in pink for a massive zero-mode gauge field, with $\nu = 2$, $\alpha = 2$, $c_1 = 1$. Similar plots are found in [48, 8, 9]

The correct expression for the 4D coupling in the mass basis is therefore given by substituting (4.47) into (4.44). In the case of the zero-modes of the massless gauge fields, i.e. the gluon and photon, the bosonic profiles are completely flat. Thus (4.47) becomes simply

$$g_{ii}^n = f_A^0 \int_R^\infty dz f_i^0(z) f_i^0(z) \propto \delta_{ij} \quad (4.48)$$

which follows from the orthonormality of the fermion profiles, specifically the zero-modes of (3.11). In this case, the coupling matrix is still diagonal in the mass basis. However, for all other (non-flat) fields, fermions localised at different points in the fifth dimension have different overlap integrals given by (4.47), as depicted in Figure 4.2. Since zero-mode fermions get their mass from coupling to the Higgs as in (3.14), localising the fermions in different points in the extra dimension is necessary to establish the fermion mass structure without a hierarchy in the 5D Yukawas. Thus, flavour non-universality arises in the coupling to neutral gauge bosons, and one obtains off-diagonal entries after rotating to the mass-basis.

In WEDs the dominant contributions to flavour changing neutral processes are typ-

ically given by tree-level 2-2 diagrams. One must evaluate an effective coupling at each vertex and for each KK mode, so the full series of diagrams for a given boson has an amplitude proportional to

$$\mathcal{I}_{abcd} = \sum_{i,j=1}^3 (U_\psi^\dagger)^{ai} (U_\chi)^{ib} \sum_{n=0}^{\infty} \frac{g_{ii}^{nL,R}(z) g_{jj}^{nL,R}(z')}{p^2 - m_n^2} (U_\xi^\dagger)^{cj} (U_\sigma)^{jd} \quad (4.49)$$

where ψ, χ, ξ and σ label chiralities. The denominator clearly just comes from the familiar 4D propagator. In practice, we can evaluate such expressions using a perturbative treatment of the bosonic correlation functions (Section 5.3), but the form of (4.49) gives a good theoretical picture of the physics at play. We see in this form, that flavour violation at each vertex is explicitly decoupled. One could simply set $c=d$, with q_b, q_c, q_d having outgoing momenta, to get flavour violation at only one vertex, i.e. $\Delta F = 1$. Alternatively, $\Delta F = 2$ processes such as K and B mixing correspond to $a = c, b = d$. It will be shown explicitly in Chapter 5 that such identifications give rise to effective Hamiltonians, expressed as linear combinations of local operators.

The point here is simply to note that, since FCNCs are no longer loop-suppressed, one expects potentially very sizeable NP effects. One immediately notices from 4.2, however, that the extent of this seems to be highly dependant on where the fermion profiles are localised in the extra dimension. The remarkable fact is that the profiles of all the KK modes flatten off towards the IR. If two different flavours both fall towards the IR, namely they have $c_{L,R}$ parameters greater(less) than approximately ± 0.5 , their couplings to neutral gauge fields will be approximately universal. As such, tree-level contributions to flavour changing processes will be suppressed. This is known as the RS-GIM mechanism [34] and contrasts with the case of flat extra dimensions [30]. In

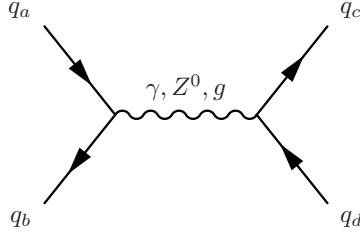


Figure 4.3: Tree-level FCNCs are possible in warped extra dimensions, i.e. $a \neq b$, $c \neq d$. The mediating bosons are resonant KK modes of the standard model neutral bosons. The flat zero-modes couple universally to all flavours, so can only produce flavour conserving vertices, i.e. require $a = b$ and $c = d$.

the flat case, the suppression is not present, since the gauge profiles are sinusoidal and therefore not flattening off in the UV. So in light of the RS-GIM mechanism, the game to be played now is how to localise the fields such that one obtains the correct mass hierarchy, without generating unacceptably large FCNC contributions. The details of this form the subject of the following sections.

4.5 Neutral Meson Mixing In WEDs

Effects from warped extra dimensions on $\Delta F = 2$ processes have been well understood for some time [38, 4, 34, 29]. With the Higgs localised sufficiently far in the IR that one can reproduce the required hierarchy of M_{Pl}/TeV , the heavy quark doublet $(t, b)_L$ must also be localised towards the IR. This places it outside the region in which couplings to gauge bosons are approximately universal, i.e. outside the viable range of the RS-GIM suppression mechanism. In the presence of the warping, one can establish the correct SM Fermion mass hierarchy with the other two generations localised in the UV, without any significant hierarchies in the 5D Yukawa couplings. Generally, FCNCs depend on the extent of the non-universality of effective couplings of the different generations to each gauge boson, as well the relevant mixing parameters. In the

setup described, non-universality in the left handed sector is dominated by the third generation, thus we expect that the size of effective flavour changing neutral couplings is roughly proportional to just the coupling of the third generation in the gauge basis,

$$g_{ab}^{nL} \sim U_{a3}^{\dagger L} g_{33}^L U_{3b}^L \quad (4.50)$$

where the indices a, b label generations of the initial and final states for the physical, mass-basis 4D quarks. The left handed rotation matrices inherit the hierarchy of the CKM matrix since $U_L^{\dagger(u)} U_L^{(d)} \equiv V_{CKM}$, so for $K(a=1, b=2)$ and $B_{d/s}(a=1/a=2, b=3)$ mesons respectively one finds approximate dependences [4]

$$g_{12}^{nL} \sim |V_{td}| |V_{ts}| g_{33}^L, \quad g_{13}^{nL} \sim |V_{td}| g_{33}^L, \quad g_{23}^{nL} \sim |V_{ts}| g_{33}^L. \quad (4.51)$$

For the right-handed sector, the fact that the 5D Yukawas (which lack any significant hierarchy) relate left and right-handed fields to the effective 4D quark masses implies relations $U_{ab}^R \sim \frac{m_a}{m_b} |V_{ab}|^{-1}$. However, in the numerical procedures in Section 6.1, the left-handed localisations are fixed as input parameters, and the c_0^R values are fitted to the observed quark masses. This typically gives right-handed fields localised such that non-universality of the couplings is not solely attributable to large 3rd generation coupling as in the left-handed sector. Thus the game is more subtle than writing relations such as those in (4.50) and (4.51). In general for neutral meson mixing, with $a = b, c = d$ one has

$$\mathcal{I}_{abab}^{LLLL} \sim \sum_{i,j} g_{ii}^{nL} g_{jj}^{nL} |V_{ia}^*| |V_{jb}| \quad (4.52)$$

$$\mathcal{I}_{abab}^{RRLl} \sim \sum_{i,j} g_{ii}^{nR} g_{jj}^{nL} \frac{m_a}{m_b} \quad (4.53)$$

$$\mathcal{I}_{abab}^{RRRR} \sim \sum_{i,j} \frac{g_{ii}^{nR} g_{jj}^{nR}}{|V_{ab}|^2} \frac{m_a^2}{m_b^2}. \quad (4.54)$$

One should bear in mind that such results are typically valid in RS models, specifically those in which one has the Higgs or even fermions confined to the TeV brane. In such a scenario the mixing matrices are approximately proportional to ratios of the fermion profiles evaluated on the brane [38]. Here we assume that the overlap integrals with the Higgs are sufficiently dominated by the peak values defined by the c_0 localisation parameters, such that one retains the same approximate hierarchies for the class of models under study.

Chapter 5

Effective Field Theory Methodology

A thorough discussion of the theoretical background of Effective Field Theory (EFT) can be found in [53], we will focus here on the specific application of such methods relevant to our purposes. In general, for quantitative predictions involving FCNC processes, one must compute the amplitudes of the relevant diagrams as shown in Fig 5.1. EFT allows to absorb the short distance physics into Wilson coefficients, the renormalisable effective couplings of local operators. At energies below the mass of the mediating bosons, real production of a physical particle is not possible. Since in order to make contact with experiment, we need only consider a scenario in which the COM energy is much less than the mass scale of the KK boson modes, we can collapse the diagram to a single effective vertex, with a corresponding effective coupling. The effects of the heavy mediating particles can be entirely factorised into the Wilson coefficients, giving an effective description of the entire infinite series of KK mediated diagrams. Expanding the boson propagators in inverse powers of the square of the large scale in the theory, one systematically suppresses effects of higher dimensional operators. In our case, we have the large mass scale M_{KK} .

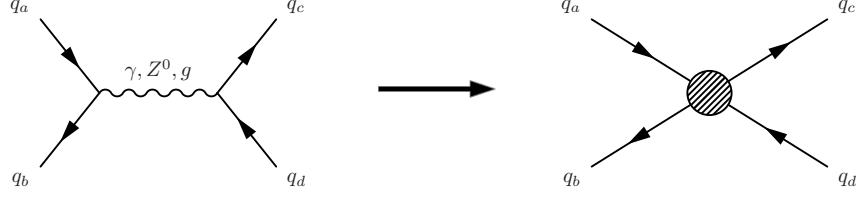


Figure 5.1: The general, approximate description of an FCNC process with a single, local effective vertex.

We can write the effective Hamiltonian in a complete basis for all interactions of interest as

$$H_{\text{eff}}^{\Delta S=2} = \sum_{i=1}^5 C_i Q_i^{ab} + \sum_{i=1}^3 \tilde{C}_i \tilde{Q}_i^{ab} \quad (5.1)$$

where a and b are generation indices of mass-basis 4D quark fields, in the "SUSY" basis of dimension 6 operators defined by

$$\begin{aligned} Q_1^{ab} &= (\bar{q}_{aL} \gamma^\mu q_{bL})(\bar{q}_{aL} \gamma_\mu q_{bL}) & \tilde{Q}_1^{ab} &= (\bar{q}_{aR} \gamma^\mu q_{bR})(\bar{q}_{aR} \gamma_\mu q_{bR}) \\ Q_2^{ab} &= (\bar{q}_{aR} q_{bL})(\bar{q}_{aR} q_{bL}) & \tilde{Q}_2^{ab} &= (\bar{q}_{aL} q_{bR})(\bar{q}_{aL} q_{bR}) \\ Q_3^{ab} &= (\bar{q}_{aR}^\alpha q_{bL}^\beta)(\bar{q}_{aR}^\beta q_{bL}^\alpha) & \tilde{Q}_3^{ab} &= (\bar{q}_{aL}^\alpha q_{bR}^\beta)(\bar{q}_{aL}^\beta q_{bR}^\alpha) \\ Q_4^{ab} &= (\bar{q}_{aR} q_{bL})(\bar{q}_{aL} q_{bR}) \\ Q_5^{ab} &= (\bar{q}_{aR}^\alpha q_{bL}^\beta)(\bar{q}_{aL}^\beta q_{bR}^\alpha) \end{aligned}$$

The operators for $B_{d,s}$ mixing are obtained by setting $a = c = 1, 2$ and $b = d = 3$ and those for K mixing by setting $a = c = 1$ and $b = d = 2$. The EFT allows to factorise the 5D physics from the non-perturbative QCD effects in the matrix elements of the local operators, acting between hadronic in and out states. The matrix operators are parameterised by scale-dependent Bag factors $P_i^M(\mu)$ for $i = 1, 4, 5$ and a meson M according to

$$\langle M|Q_i^{ab}(\mu)|\bar{M}\rangle \equiv \frac{m_M f_M^2}{3} P_i^M(\mu). \quad (5.2)$$

For B and K physics, EFT thus allows to resum large logarithms $\log(M_{KK}^2/M_{B,K}^2)$ from loop corrections into the renormalisable Bag factors, where they appear as $\log(M_{KK}^2/\mu^2)$. We can then evaluate these at a matching scale $\mu \sim M_{KK}$. For numerical computations, we take values for low μ from lattice calculations [6, 21, 43] and perform the RG-evolution to the required scale. A more complete explanation with further details on the Bag Factors, including precise numerical values can be found in Sections 6.1.12 and 6.1.13.

In this formalism, the task is now to evaluate the hadronic matrix elements and Wilson coefficients. The details of these calculations are the subject of the following sections. We will find a complete description of the full interaction Hamiltonian in terms of the local operator expansion, for each of the three neutral gauge bosons of the standard model and their KK modes. It is worth noting that this methodology is also applicable to the SM box diagrams discussed in section 4.3, as these simply yield different values of the Wilson coefficients for the same basis of operators [44].

5.1 Operator Product Expansion for Tree-Level FCNCs

In calculating the amplitude of a 2-2 process in the 5D theory, one needs to compute, at second order, the S matrix element of the form

$$S - 1 = \frac{g_B^2 (-i)^2}{2!} \int_{t'}^t dt'' \int_{t''}^{t'} dt''' T \left\{ \int d^3x \int dz \int d^3x' \int dz' J_\mu A^\mu J_\nu A^\nu \right\}. \quad (5.3)$$

Where g_B is the coupling to the relevant boson.

5.1.1 Gluon Mediated

In the case of the gluon, $g_B = g_s$ and $J_M = \bar{\Psi} \tau^a \Gamma_M \Psi$, then writing $\mathcal{A} = \Gamma_M A^M$

$$S-1 = \frac{-g_s^2}{2} \int_{t'}^t dt'' \int_{t''}^{t'} dt''' T \left\{ \int d^3x \int dz \int d^3x' \int dz' \bar{\Psi}(x_1, z_1) \tau^a \mathcal{A}(x_1, z_1) \Psi(x_1, z_1) \bar{\Psi}(x_2, z_2) \tau^a \mathcal{A}(x_2, z_2) \Psi(x_2, z_2) \right\}. \quad (5.4)$$

After Wick expanding, we find a term

$$\langle f | : \int d^3x \int dz \int d^3x' \int dz' \bar{\Psi}(x, z) \tau^a \overbrace{\mathcal{A}(x, z) \Psi(x, z) \bar{\Psi}(x', z') \tau^a \mathcal{A}(x', z') \Psi(x', z')} : | i \rangle. \quad (5.5)$$

We expand the 5D fields according to $\Psi(x, z) = \sum_{n=0}^{\infty} e^{\Phi/2} \frac{z^2}{R^2} \psi^n(x) f^n(z)$ and we will work in the zero-mode approximation [28] such that we truncate the sum and neglect mixing with higher fermionic modes after basis rotation since these contributions are suppressed by powers of $1/M_{KK}^2$. Noting also that $\mathcal{A} = \Gamma_M A^M = \frac{z}{R} \gamma^\mu A_\mu$ since $g_{\mu\nu} = \frac{R^2}{z^2} \eta_{\mu\nu}$, we

have

$$\sum_{\substack{\omega, \xi \\ i, j}} \int dx \int dx' \int dz \int dz' \left[f_{\omega}^i(z) f_{\omega}^i(z) f_{\xi}^j(z') f_{\xi}^j(z') \right. \quad (5.6)$$

$$\left. \times \langle f | : \frac{-g_s}{2} \bar{\psi}_{\omega}^i(x) \tau^a \gamma^{\mu} \psi_{\omega}^i(x) \bar{\psi}_{\xi}^j(x') \tau^a \gamma^{\nu} \psi_{\xi}^j(x') : | i \rangle \langle A_{\mu}(x, z) A_{\nu}(x', z') \rangle \right] \quad (5.7)$$

where $|i\rangle, |f\rangle$ have total momenta p_i, p_f respectively (two particle fermion states). The two point function is given by

$$\langle A_{\mu}(x, z) A_{\nu}(x', z') \rangle = \int \frac{d^4 p}{(2\pi)^4} i G_p^{(\gamma/g)}(z, z') e^{-ip \cdot (x-x')} \Pi_{\mu\nu} \quad (5.8)$$

and writing $\psi(x) = \int \frac{d^4 k}{(2\pi)^4} \tilde{\psi}(k) e^{ik \cdot x}$, (5.6) becomes

$$\sum_{\substack{\omega, \xi \\ i, j}} \int dx \int dx' \int dz \int dz' \int \frac{d^4 k_{1, \dots, 4}}{(2\pi)^{16}} \int \frac{d^4 p}{(2\pi)^4} \left[f_{\omega}^i(z) f_{\omega}^i(z) f_{\xi}^j(z') f_{\xi}^j(z') \frac{-g_s^2}{2} \right. \quad (5.9)$$

$$\left. \times \langle f | : \bar{\psi}_{\omega}^i(k_1) \tau^a \gamma^{\mu} \tilde{\psi}_{\omega}^i(k_2) \bar{\psi}_{\xi}^j(k_3) \tau^a \gamma^{\nu} \tilde{\psi}_{\xi}^j(k_4) : | i \rangle \right.$$

$$\left. \times i G_p^{(\gamma/g)}(z, z') \Pi_{\mu\nu} e^{-ip \cdot (x-x')} e^{i(k_1+k_2) \cdot x + i(k_3+k_4) \cdot x'} \right]. \quad (5.10)$$

Performing the x and x' integrals, we get

$$= \sum_{\substack{\omega, \xi \\ i, j}} \int dz \int dz' \int \frac{d^4 k_{1, \dots, 4}}{(2\pi)^{16}} \int \frac{d^4 p}{(2\pi)^4} \left[f_{\omega}^i(z) f_{\omega}^i(z) f_{\xi}^j(z') f_{\xi}^j(z') \frac{-g_s^2}{2} \right. \quad (5.11)$$

$$\left. \times \langle f | : \bar{\psi}_{\omega}^i(k_1) \tau^a \gamma^{\mu} \tilde{\psi}_{\omega}^i(k_2) \bar{\psi}_{\xi}^j(k_3) \tau^a \gamma^{\nu} \tilde{\psi}_{\xi}^j(k_4) : | i \rangle \right.$$

$$\left. \times i G_p^{(\gamma/g)}(z, z') \Pi_{\mu\nu} (2\pi)^8 \delta^{(4)}(p + k_1 + k_2) \delta^{(4)}(-p + k_3 + k_4) \right] \quad (5.12)$$

then the p integral gives:

$$= \sum_{\substack{\omega, \xi \\ i, j}} \int dz \int dz' \int \frac{d^4 k_{1, \dots, 4}}{(2\pi)^{12}} \left[f_{\omega}^i(z) f_{\omega}^i(z) f_{\xi}^j(z') f_{\xi}^j(z') \frac{-g_s^2}{2} \right. \quad (5.13)$$

$$\times \langle f | : \bar{\psi}_{\omega}^i(k_1) \tau^a \gamma^{\mu} \tilde{\psi}_{\omega}^i(k_2) \bar{\psi}_{\xi}^j(k_3) \tau^a \gamma^{\nu} \tilde{\psi}_{\xi}^j(k_4) : | i \rangle \\ \times i G_{-(k_1+k_2)}^{(\gamma/g)}(z, z') \Pi_{\mu\nu} \delta(k_1 + k_2 + k_3 + k_4) \left. \right] \quad (5.14)$$

$$= \sum_{\substack{\omega, \xi \\ i, j}} \int dz \int dz' \int \frac{d^4 k_{1, \dots, 4}}{(2\pi)^{12}} \left[f_{\omega}^i(z) f_{\omega}^i(z) f_{\xi}^j(z') f_{\xi}^j(z') \frac{-g_s^2}{2} \right. \quad (5.15)$$

$$\times \langle f | : \bar{\psi}_{\omega}^i(k_1) \tau^a \gamma^{\mu} \tilde{\psi}_{\omega}^i(k_2) \bar{\psi}_{\xi}^j(k_3) \tau^a \gamma^{\nu} \tilde{\psi}_{\xi}^j(k_4) : | i \rangle \\ \times i G_{-(k_1+k_2)}^{(\gamma/g)}(z, z') \Pi_{\mu\nu} \int \frac{d^4 x}{(2\pi)^4} e^{ix \cdot (k_1 + k_2 + k_3 + k_4)} \left. \right] \quad (5.16)$$

then inverse fourier transforming, we find in terms of operators localised at x :

$$= \sum_{\substack{\omega, \xi \\ i, j}} \int d^4 x \int dz \int dz' \left[f_{\omega}^i(z) f_{\omega}^i(z) f_{\xi}^j(z') f_{\xi}^j(z') \frac{-g_s^2}{2} \right. \quad (5.17) \\ \times \langle f | : \bar{\psi}_{\omega}^i(x) \tau^a \gamma^{\mu} \psi_{\omega}^i(x) \bar{\psi}_{\xi}^j(x) \tau^a \gamma^{\nu} \psi_{\xi}^j(x) : | i \rangle i G_{-(k_1+k_2)}^{(\gamma/g)}(z, z') \Pi_{\mu\nu} \left. \right].$$

5.1.2 Photon Mediated

For the case of photon mediated interactions, a similar calculation with $g_B = e$, and

$J_M = \bar{\Psi}\Gamma_M\Psi$ gives

$$\sum_{\substack{\omega,\xi \\ i,j}} \int d^4x \int dz \int dz' \left[f_\omega^i(z) f_\omega^i(z) f_\xi^j(z') f_\xi^j(z') \frac{-e^2}{2Q_i q_j} \right. \quad (5.18)$$

$$\left. \times \langle f | : \bar{\psi}_\omega^i(x) \gamma^\mu \psi_\omega^i(x) \bar{\psi}_\xi^j(x) \gamma^\nu \psi_\xi^j(x) : | i \rangle i G_{-(k_1+k_2)}^{(\gamma/g)}(z, z') \Pi_{\mu\nu} \right].$$

5.1.3 Z Mediated

For the Z boson, $g_B = g/c_w$ and including chirality dependant factors the result is

$$\sum_{\substack{\omega,\xi \\ i,j}} \int d^4x \int dz \int dz' \left[f_\omega^i(z) f_\omega^i(z) f_\xi^j(z') f_\xi^j(z') \frac{-g^2}{2c_w^2} \right. \quad (5.19)$$

$$\times \left(\delta_{L\omega} \delta_{L\xi} (t_i - q_i s_w^2) (t_j - q_j s_w^2) + \delta_{R\omega} \delta_{R\xi} (q_i q_j s_w^4) \right.$$

$$\left. + \delta_{R\omega} \delta_{L\xi} q_i s_w^2 (t_j - q_j s_w^2) + \delta_{L\omega} \delta_{R\xi} (t_i - q_i s_w^2) (q_j s_w^2) \right)$$

$$\times \langle f | : \bar{\psi}_\omega^i(x) \gamma^\mu \psi_\omega^i(x) \bar{\psi}_\xi^j(x) \tau^a \gamma^\nu \psi_\xi^j(x) : | i \rangle i G_{-(k_1+k_2)}^{(Z)}(z, z') \Pi_{\mu\nu} \right].$$

5.2 Effective Operators

5.2.1 Gluon Contribution

From (5.17), the mass basis flavour-violating effective Hamiltonian for gluon mediated two to two processes is found to be:

$$\begin{aligned}
\mathcal{H}_{eff}^g = & \int dz \int dz' \sum_{\substack{i,j \\ \omega, \xi}} U_{ai}^\dagger U_{ib} f_\omega^i(z) f_\omega^i(z') \frac{g_s^2}{2} G_p^{(\gamma/g)}(z, z') f_\xi^j(z') f_\xi^j(z') U_{cj}^\dagger U_{jd} \\
& \times \left[\frac{1}{2} (\bar{\psi}_{La}'^\alpha \gamma^\mu \psi_{Lb}'^\beta \bar{\psi}_{Lc}'^\beta \gamma_\mu \psi_{Ld}'^\alpha + \bar{\psi}_{Ra}'^\alpha \gamma^\mu \psi_{Rb}'^\beta \bar{\psi}_{Rc}'^\beta \gamma_\mu \psi_{Rd}'^\alpha \right. \\
& + \bar{\psi}_{Ra}'^\alpha \gamma^\mu \psi_{Rb}'^\beta \bar{\psi}_{Lc}'^\beta \gamma_\mu \psi_{Ld}'^\alpha + \bar{\psi}_{La}'^\alpha \gamma^\mu \psi_{Lb}'^\beta \bar{\psi}_{Rc}'^\beta \gamma_\mu \psi_{Rd}'^\alpha) \\
& - \frac{1}{2N_c} (\bar{\psi}_{La}'^\alpha \gamma^\mu \psi_{Lb}'^\alpha \bar{\psi}_{Lc}'^\beta \gamma_\mu \psi_{Ld}'^\beta + \bar{\psi}_{Ra}'^\alpha \gamma^\mu \psi_{Rb}'^\alpha \bar{\psi}_{Rc}'^\beta \gamma_\mu \psi_{Rd}'^\beta \\
& \left. + \bar{\psi}_{Ra}'^\alpha \gamma^\mu \psi_{Rb}'^\alpha \bar{\psi}_{Lc}'^\beta \gamma_\mu \psi_{Ld}'^\beta + \bar{\psi}_{La}'^\alpha \gamma^\mu \psi_{Lb}'^\alpha \bar{\psi}_{Rc}'^\beta \gamma_\mu \psi_{Rd}'^\beta) \right] \quad (5.20)
\end{aligned}$$

where a,b,c,d are generation indices for mass basis fields. For $\Delta F = 2$, set $c = a$, $d = b$ and, after applying the Fierz relations

$$\bar{\psi}_R \gamma^\mu \psi_R \bar{\chi}_L \gamma_\mu \chi_L = -2 \bar{\psi}_R \chi_L \bar{\chi}_L \psi_R \quad (5.21)$$

$$\bar{\psi}_{R,L} \gamma^\mu \psi_{R,L} \bar{\chi}_{R,L} \gamma_\mu \chi_{R,L} = \bar{\psi}_{R,L} \gamma^\mu \chi_{R,L} \bar{\chi}_{R,L} \gamma_\mu \psi_{R,L} \quad (5.22)$$

we have the operator

$$\mathcal{O}_G^{\Delta F=2} = \left[\left(\frac{1}{2} - \frac{1}{2N_c} \right) (\bar{\psi}_{La}'^\alpha \gamma^\mu \psi_{Lb}'^\alpha \bar{\psi}_{La}'^\beta \gamma_\mu \psi_{Lb}'^\beta + \bar{\psi}_{Ra}'^\alpha \gamma^\mu \psi_{Rb}'^\alpha \bar{\psi}_{Ra}'^\beta \gamma_\mu \psi_{Rb}'^\beta) \right. \quad (5.23)$$

$$\left. - 2 \bar{\psi}_{Ra}'^\alpha \gamma^\mu \psi_{Lb}'^\alpha \bar{\psi}_{La}'^\beta \gamma_\mu \psi_{Rb}'^\beta + \frac{2}{N_c} \bar{\psi}_{Ra}'^\alpha \gamma^\mu \psi_{Lb}'^\beta \bar{\psi}_{La}'^\beta \gamma_\mu \psi_{Rd}'^\alpha \right] \quad (5.24)$$

which is just ($N_c = 3$):

$$\boxed{= \frac{1}{3}(Q_1^{ab} + \tilde{Q}_1^{ab}) - 2Q_4^{ab} + \frac{2}{3}Q_5^{ab}}. \quad (5.25)$$

5.2.2 Photon Contribution

For the photon, we read off from (5.18):

$$\begin{aligned} \mathcal{H}_{eff}^\gamma = & \int dz \int dz' \sum_{\substack{i,j \\ \omega, \xi}} U_{ai}^\dagger U_{ib} f_\omega^i(z) f_\omega^i(z) \frac{e^2}{2q_i q_j} G_p(z, z') f_\xi^j(z') f_\xi^j(z') U_{cj}^\dagger U_{jd} \\ & \times \left[\bar{\psi}_{La}'^{\alpha} \gamma^\mu \psi_{Lb}'^{\alpha} \bar{\psi}_{Lc}'^{\beta} \gamma_\mu \psi_{Ld}'^{\beta} + \bar{\psi}_{Ra}'^{\alpha} \gamma^\mu \psi_{Rb}'^{\alpha} \bar{\psi}_{Rc}'^{\beta} \gamma_\mu \psi_{Rd}'^{\beta} \right. \\ & \left. + \bar{\psi}_{Ra}'^{\alpha} \gamma^\mu \psi_{Rb}'^{\alpha} \bar{\psi}_{Lc}'^{\beta} \gamma_\mu \psi_{Ld}'^{\beta} + \bar{\psi}_{La}'^{\alpha} \gamma^\mu \psi_{Lb}'^{\alpha} \bar{\psi}_{Rc}'^{\beta} \gamma_\mu \psi_{Rd}'^{\beta} \right]. \end{aligned} \quad (5.26)$$

Applying (5.21) and (5.22) and setting $a = c$, $b = d$ we have the operator

$$\mathcal{O}_\gamma^{\Delta F=2} = \left[(\bar{\psi}_{La}'^{\alpha} \gamma^\mu \psi_{Lb}'^{\alpha} \bar{\psi}_{La}'^{\beta} \gamma_\mu \psi_{Lb}'^{\beta} + \bar{\psi}_{Ra}'^{\alpha} \gamma^\mu \psi_{Rb}'^{\alpha} \bar{\psi}_{Ra}'^{\beta} \gamma_\mu \psi_{Rb}'^{\beta}) - 4\bar{\psi}_{Ra}'^{\alpha} \psi_{Lb}'^{\beta} \bar{\psi}_{La}'^{\beta} \psi_{Rb}'^{\alpha} \right] \quad (5.27)$$

$$\boxed{= Q_1 + \tilde{Q}_1 - 4Q_5} \quad (5.28)$$

5.2.3 Z Contribution

In the case of the Z one finds:

$$\begin{aligned}
\mathcal{H}_{eff}^Z = & \int dz \int dz' \sum_{\substack{i,j \\ \omega, \xi}} U_{ai}^\dagger U_{ib} f_\omega^i(z) f_\omega^i(z) \frac{g^2}{2} G_p^{(Z)}(z, z') f_\xi^j(z') f_\xi^j(z') U_{cj}^\dagger U_{jd} \\
& \times \left[(t_i - q_i s_w^2)(t_j - q_j s_w^2) \bar{\psi}_{La}'^{\alpha} \gamma^\mu \psi_{Lb}'^{\alpha} \bar{\psi}_{Lc}'^{\beta} \gamma_\mu \psi_{Ld}'^{\beta} + (q_i q_j s_w^4) \bar{\psi}_{Ra}'^{\alpha} \gamma^\mu \psi_{Rb}'^{\alpha} \bar{\psi}_{Rc}'^{\beta} \gamma_\mu \psi_{Rd}'^{\beta} \right. \\
& \left. + q_i s_w^2 (t_j - q_j s_w^2) \bar{\psi}_{Ra}'^{\alpha} \gamma^\mu \psi_{Rb}'^{\alpha} \bar{\psi}_{Lc}'^{\beta} \gamma_\mu \psi_{Ld}'^{\beta} + (t_i - q_i s_w^2) (q_j s_w^2) \bar{\psi}_{La}'^{\alpha} \gamma^\mu \psi_{Lb}'^{\alpha} \bar{\psi}_{Rc}'^{\beta} \gamma_\mu \psi_{Rd}'^{\beta} \right].
\end{aligned} \tag{5.29}$$

Applying, as above, (5.21) and (5.22) and setting $a = c$, $b = d$

$$\mathcal{O}_Z^{\Delta F=2} = \left[(t_i - q_i s_w^2)(t_j - q_j s_w^2) \bar{\psi}_{La}'^{\alpha} \gamma^\mu \psi_{Lb}'^{\alpha} \bar{\psi}_{La}'^{\beta} \gamma_\mu \psi_{Lb}'^{\beta} + (q_i q_j s_w^4) \bar{\psi}_{Ra}'^{\alpha} \gamma^\mu \psi_{Rb}'^{\alpha} \bar{\psi}_{Ra}'^{\beta} \gamma_\mu \psi_{Rb}'^{\beta} \right. \tag{5.30}$$

$$\left. - 2q_i s_w^2 (t_j - q_j s_w^2) \bar{\psi}_{Ra}'^{\alpha} \psi_{Lb}'^{\beta} \bar{\psi}_{La}'^{\beta} \psi_{Rb}'^{\alpha} - 2(t_i - q_i s_w^2) (q_j s_w^2) \bar{\psi}_{La}'^{\alpha} \psi_{Rb}'^{\beta} \bar{\psi}_{Ra}'^{\beta} \psi_{Lb}'^{\alpha} \right] \tag{5.31}$$

which is

$$= (t_i - q_i s_w^2)(t_j - q_j s_w^2) Q_1 + (q_i q_j s_w^4) \tilde{Q}_1 - 2(q_i s_w^2(t_j - q_j s_w^2) + (t_i - q_i s_w^2)(q_j s_w^2)) Q_5. \tag{5.32}$$

For down type in and out states, bearing in mind $q_i = q_j = \frac{1}{3}$ and we have

$$\boxed{= \left(\frac{1}{2} - \frac{s_w^2}{3} \right)^2 Q_1 + \frac{s_w^4}{9} \tilde{Q}_1 - \frac{4s_w^2}{3} \left(\frac{1}{2} - \frac{s_w^2}{3} \right) Q_5}. \tag{5.33}$$

5.2.4 Wilson Coefficients for Hadronic Processes

Combining (5.20),(5.26),(5.29),(5.25),(5.28), and (5.33), we can summarise the results for the $\Delta F = 2$ Wilson coefficients as follows:

$$C_1 = \frac{g_s^2}{6} \mathcal{I}_{L_a L_b L_a L_b}^{(g)} + \frac{e^2}{18} \mathcal{I}_{L_a L_b L_a L_b}^{(\gamma)} + \frac{g^2}{2c_w^2} \left(\frac{1}{2} - \frac{s_w^2}{3} \right)^2 \mathcal{I}_{L_a L_b L_a L_b}^{(Z)} \quad (5.34)$$

$$\tilde{C}_1 = \frac{g_s^2}{6} \mathcal{I}_{R_a R_b R_a R_b}^{(g)} + \frac{e^2}{18} \mathcal{I}_{R_a R_b R_a R_b}^{(\gamma)} + \frac{g^2 s_w^4}{18 c_w^2} \mathcal{I}_{R_a R_b R_a R_b}^{(Z)} \quad (5.35)$$

$$C_4 = -g_s^2 \mathcal{I}_{R_a R_b L_a L_b}^{(g)} \quad (5.36)$$

$$C_5 = \frac{g_s^2}{3} \mathcal{I}_{R_a R_b L_a L_b}^{(g)} + \frac{g^2}{2c_w^2} \left(\frac{1}{2} - \frac{s_w^2}{3} \right) \mathcal{I}_{R_a R_b L_a L_b}^{(g)} - \frac{2e^2}{9} \mathcal{I}_{R_a R_b L_a L_b}^{(\gamma)} \quad (5.37)$$

where in general, there is a dependence on factors

$$\mathcal{I}_{\psi_a \chi_b \xi_c \sigma_d}^{(B)} = \sum_{i,j=1}^3 (U_\psi^\dagger)^{ai} (U_\chi)^{ib} \left[\int_R^\infty dz \int_R^\infty dz' f_\psi^i(z) f_\chi^i(z) G_p^{(B)}(z, z') f_\xi^j(z') f_\sigma^j(z') \right] (U_\xi^\dagger)^{cj} (U_\sigma)^{jd} \quad (5.38)$$

given as convolutions of the kernels defined in Section 3.5 with chiral zero modes (ψ, χ labelling chiralities) of the fermions, with the U -matrices providing the translation between the flavour basis and the bulk mass eigenstate fields. Similar results were presented in [8].

5.3 Bosonic Correlation Function for General Dilaton

We now return to computation of the Bosonic propagators. With an arbitrary dilaton, let us proceed by first making a power series expansion and working in an appropriate

order for dimension 6 operators in the EFT. For the gluonic/photon propagator, we will carry out an expansion in p^2 since there is flat massless zero-mode profile for these bosons. For the Z/W propagator, we can make the expansion in powers of $\left(\frac{h_0^2}{M_{KK}^2}\right)$ which is very small since $h_0 \ll M_{KK}$.

5.3.1 Photon/Gluon (Massless Case)

In terms of the KK tower of bosonic modes,

$$G_p^{(\gamma/G)}(z, z') = \sum_{n=0}^{\infty} \frac{f_A^n(z) f_A^n(z')}{p^2 - m_n^2}, \quad (5.39)$$

which we may expand as (since $m_0 = 0$)

$$G_p^{(\gamma/G)}(z, z') = \frac{f_A^0(z) f_A^0(z')}{p^2} + \sum_{n=1}^{\infty} \frac{f_A^n(z) f_A^n(z')}{p^2 - m_n^2} \quad (5.40)$$

$$= \frac{A_0}{p^2} + G_0^{(\gamma/G)}(z, z') + p^2 G_1^{(\gamma/G)}(z, z') + \mathcal{O}(p^4) \quad (5.41)$$

with $A_0 = \text{const.}$ Then to zeroth order, we have from (3.71)

$$\partial_z \left(e^{-\Phi(z)} \frac{R}{z} \partial_z \right) G_0^{(\gamma/G)}(z, z') + A_0 e^{-\Phi(z)} \frac{R}{z} = \delta(z - z') \quad (5.42)$$

which we can solve for G_0 in integral form as follows. Consider first the integral of
(5.42)

$$\left[e^{-\Phi(z_0)} \frac{R}{z_0} \partial_{z_0} G_0^{(\gamma/G)}(z_0, z') \right]_R^z + A_0 \int_R^z e^{-\Phi(z_0)} \frac{R}{z_0} dz_0 = k. \quad (5.43)$$

For the homogenous case,

$$\partial_{z_0} G_0^{(\gamma/G)}(z_0, z') = A e^{\Phi(z)} \frac{z}{R} \quad (5.44)$$

i.e.

$$G_0^{(\gamma/G)}(z, z') = A \int_R^{z'} e^{\Phi(z_1)} \frac{z}{R} dz_1 + B. \quad (5.45)$$

We can make a general ansatz for the inhomogenous case with $u = \min(z, z')$ and $v = \max(z, z')$,

$$G_0^{(\gamma/G)}(u, v) = \left(A \int_R^u e^{\Phi(t)} \frac{t}{R} dt + B \right) \left(C \int_R^v e^{\Phi(t)} \frac{t}{R} dt + D \right) + g(u) + g(v) \quad (5.46)$$

with $g(z) = -A_0 \int_R^z dz_1 \left(e^{\Phi(z_1)} \int_R^{z_1} e^{-\Phi(z_0)} \frac{R}{z_0} dz_0 \right)$, since the first term will vanish under action of the differential operator in (5.42) at either $z = u$ or $z = v$. So

$$\partial_u G_0^{(\gamma/G)}(u, v) = A e^{\Phi(u)} \frac{u}{R} \left(C \int_R^v e^{\Phi(t)} \frac{t}{R} dt + D \right) + g'(u) \quad (5.47)$$

and

$$\partial_v G_0^{(\gamma/G)}(u, v) = C e^{\Phi(v)} \frac{v}{R} \left(A \int_R^u e^{\Phi(t)} \frac{t}{R} dt + B \right) + g'(v) \quad (5.48)$$

and subsequently

$$\begin{aligned} & \left(\lim_{\epsilon \rightarrow 0} \partial_v G_p^{(\gamma/G)}(u, v)|_{z'+\epsilon} - \lim_{\epsilon \rightarrow 0} \partial_u G_p^{(\gamma/G)}(u, v)|_{z'+\epsilon} \right) \\ &= -A e^{\Phi(z')} \frac{z'}{R} \left(C \int_R^{z'} e^{\Phi(t)} \frac{t}{R} dt + D \right) \end{aligned} \quad (5.49)$$

$$+ C e^{\Phi(z')} \frac{z'}{R} \left(A \int_R^{z'} e^{\Phi(t)} \frac{t}{R} dt + B \right). \quad (5.50)$$

Applying the jump condition [8],

$$\lim_{\epsilon \rightarrow 0} \partial_z G_p^{(\gamma/G)}(u, v)|_{z' - \epsilon}^{z' + \epsilon} = e^{\Phi(z')} \frac{z'}{R}, \quad (5.51)$$

we then find

$$AC \int_R^{z'} e^{\Phi(t)} + BC - AC \int_R^{z'} e^{\Phi(t)} - AD = 1 \quad (5.52)$$

$$BC - AD = 1. \quad (5.53)$$

There is a particular solution for $A = B = C = D = 0$

$$G_0^{part}(u, v) = g(u) + g(v) \quad (5.54)$$

and applying the Neumann boundary condition on the UV brane

$$\partial_u G_0(u, v)|_{u=R} = 0 = A e^{\Phi(R)} \left(C \int_R^v e^{\Phi(t)} \frac{t}{R} dt + D \right). \quad (5.55)$$

To be consistent with (5.53), C and D cannot simultaneously equal zero, so $A = 0$ and thus $BC = 1$. Using these facts, (5.46) becomes

$$\boxed{G_0(u, v) = \int_R^v e^{\Phi(t)} \frac{t}{R} dt + BD + g(u) + g(v)} \quad (5.56)$$

We thus have an integral solution which is straightforwardly numerically computable for any choice of ν .

5.3.2 W/Z (Massive Case)

For the massive case, the propagator has no pole for zero momentum, so we can set $p = 0$ and write:

$$e^\Phi \frac{z}{R} \left(\partial z \left(e^{-\Phi} \frac{R}{z} \partial z \right) - \mu(z) \right) G_{v,p=0}^{(W/Z)} = e^\Phi \frac{z}{R} \delta(z - z') \quad (5.57)$$

where $\mu(z) = \frac{h_0^2 g^2}{2Rz^2} \left(\frac{z}{R} \right)^{2\alpha}$. Expanding the solution to (5.57) in powers of $\left(\frac{h_0^2}{M_{KK}} \right)^2$ we have

$$\begin{aligned} G_{v,p}^{(W/Z)}(z, z') &= \sum_{n=1}^{\infty} \frac{f_Z^n(z) f_Z^n(z')}{-m_n^2} \quad (5.58) \\ &= \frac{1}{h_0^2} \left[G_{-1,p=0}^{(W/Z)}(z, z') + \frac{G_{0,p=0}^{(W/Z)}(z, z')}{M_{KK}^2} + \left(\frac{h_0^2}{M_{KK}} \right)^2 G_{1,p=0}^{(W/Z)}(z, z') + \mathcal{O} \left(\frac{h_0^2}{M_{KK}} \right)^4 \right] \end{aligned} \quad (5.59)$$

so at zeroth order,

$$e^\Phi \frac{z}{R} \partial z \left(e^{-\Phi} \frac{R}{z} \partial z \right) \frac{G_{0,p=0}^{(W/Z)}(z, z')}{M_{KK}^2} - e^{-\Phi} \frac{R}{z} \tilde{\mu}(z) = e^\Phi \frac{z}{R} \delta(z - z') \quad (5.60)$$

where $\tilde{\mu}(z) = \mu(z)/h_0^2$. Choosing the ansatz

$$G_{0,p=0}^{(W/Z)}(u, v)/M_{KK}^2 = \left(A \int_R^u e^{\Phi(t)} \frac{t}{R} dt + B \right) \left(C \int_R^v e^{\Phi(t)} \frac{t}{R} dt + D \right) + g^{(W/Z)}(u) + g^{(W/Z)}(v) \quad (5.61)$$

one can show that (5.57) is satisfied provided

$$g^{(W/Z)}(z) = \int_R^z dz_1 e^{\Phi(z_1)} \frac{z_1}{R} \int_R^{z_1} e^{-\Phi(z_0)} \frac{R}{z_0} G_{-1,p=0}^{(W/Z)}(z_0, z') dz_0. \quad (5.62)$$

Then we have

$$\boxed{G_{0,p=0}^{(W/Z)}(u, v)/M_{KK}^2 = \int_R^v e^{\Phi(t)} \frac{t}{R} dt + BD + g^{(W/Z)}(u) + g^{(W/Z)}(v)} \quad (5.63)$$

similar to (5.56) above.

5.3.3 Calculation of $G_{-1,p=0}^{(W/Z)}(z_0, z')$

We require to calculate the innermost integral in (5.62). We can first find $G_{-1,p=0}^{(W/Z)}(z_0, z')$ by considering the perturbative solution to the equation of motion for the massive gauge profiles. We have for the zero-mode mass and profile,

$$m_0^{2(Z)} = ah_0^2 + b \frac{(h_0^2)^2}{M_{KK}^2} + \mathcal{O}((h_0^2)^3) \quad (5.64)$$

and

$$f_0(z)^{(Z)} = f_A^{(0)} + \frac{f^{(1)}(z)h_0^2}{M_{KK}^2} + \mathcal{O}((h_0^2)^3). \quad (5.65)$$

Substituting in (5.58) we have

$$G^{(W/Z)}(z, z') = \sum_{n=0}^{\infty} \frac{f_0^A f_0^A + \mathcal{O}(h_0^2)}{-m_n^2} \quad (5.66)$$

then

$$G_{(W/Z)}^{(-1)}(z, z') = \lim_{h_0^2 \rightarrow 0} h_0^2 G_{p=0}^{(W/Z)}(z, z') = -\frac{f_0^A f_0^A}{a}. \quad (5.67)$$

Now writing $\mathcal{D} = (\partial_z^2 - (\frac{1}{z} + \Phi') \partial_z)$ and setting $n = 0$ in (3.23),

$$\left(\mathcal{D} - h_0^2 \tilde{\mu}(z) + m_0^{2(Z)} \right) f_0^{(Z)} = 0. \quad (5.68)$$

Multiplying from the left by a factor $e^{-\Phi} \frac{R}{z} f_0^{(Z)}(z)$, one finds

$$\int_R^\infty dz e^{-\Phi} \frac{R}{z} f_0^{(Z)}(z) (\mathcal{D} - h_0^2 \tilde{\mu}(z)) f_0^{(Z)}(z) = -m_0^{2(Z)} \quad (5.69)$$

after applying the normalisation condition

$$\int_R^\infty dz e^{-\Phi} \frac{R}{z} f_0^{(Z)}(z) f_0^{(Z)}(z) = 1 \quad (5.70)$$

on the RHS. Dividing by h_0^2 and taking the limit $h_0^2 \rightarrow 0$ one obtains

$$\int_R^\infty dz e^{-\Phi} \frac{R}{z} f_0^{(Z)}(z) \left(\frac{1}{h_0^2} \mathcal{D} - \tilde{\mu}(z) \right) f_0^{(Z)}(z) = a \quad (5.71)$$

$$\frac{1}{M_{KK}^2} \int_R^\infty dz e^{-\Phi} \frac{R}{z} f^{(1)}(z) \mathcal{D} f^{(1)}(z) - \int_R^\infty dz e^{-\Phi} \frac{R}{z} f_0^{(A)}(z) \tilde{\mu} f_0^{(A)}(z) = a. \quad (5.72)$$

Now since one can write $\mathcal{D} = e^{\Phi} \frac{z}{R} \partial_z (e^{-\Phi} \frac{R}{z} \partial_z)$, the first term in (5.72) is

$$\frac{1}{M_{KK}^2} \int_R^\infty dz f^{(A)} \partial_z \left(e^{-\Phi} \frac{R}{z} \partial_z \right) f^{(1)}(z) = \frac{1}{M_{KK}^2} \left[e^{-\Phi} \frac{R}{z} \partial_z f^{(1)}(z) \right]_R^\infty = 0. \quad (5.73)$$

So from (5.67) and (5.72) we find

$$G_{(W/Z)}^{(-1)} = -\frac{1}{e^{-\Phi} \frac{R}{z} \tilde{\mu}(z)} \quad (5.74)$$

which allows for the evaluation of (5.62). Note also that

$$m_0^2 \approx a h_0^2 = A_0 \int_R^\infty e^{-\Phi} \frac{R}{z} \tilde{\mu}(z) \quad (5.75)$$

follows directly from (5.72) and gives a ν -independent means of approximating the Z or W mass. This can be used for evaluating the electroweak parameter h_0 at an arbitrary KK scale, details of which will be discussed in Section 6.1.4.

5.3.4 Comparison: KK expansion vs $1/M^2$ expansion.

As a consistency check, for a test sample, the completely left-handed 3×3 matrix defined by the double integrals in (5.38) (in the gauge interaction basis), is compared to the equivalent matrix calculated using the first 20KK modes of the neutral bosons 5.1. By taking the differences of non-diagonal elements, one eliminates any flavour conserving constant parts such the integration constants appearing in (5.56) and (5.63). We find a close agreement, with errors $\sim 6\%$ in each case for both massless and massive bosons.

Propagator	$I(0.72, 0.64) - I(0.72, 0.52)$	$I(0.72, 0.64) - I(0.64, 0.52)$	$I(0.72, 0.52) - I(0.64, 0.52)$
Massless, 20-modes	2.73664×10^{-9}	2.73886×10^{-9}	2.21824×10^{-12}
Massless, $G_0^{(\gamma/g)}$	2.84039×10^{-9}	2.84272×10^{-9}	2.32976×10^{-12}
Massive, 20-modes	-1.0907×10^{-7}	-1.0922×10^{-7}	-1.5428×10^{-10}
Massive, $G_0^{(Z)}$	-1.16566×10^{-7}	-1.16729×10^{-7}	-1.63647×10^{-10}

Table 5.1: Values are in units of GeV^{-2} . $M_{KK} = 1000\text{GeV}$. In the top row, $I(c_i^0, c_j^0)$ is the double integral in square brackets in (6.28), with c_i^0, c_j^0 the localisations of each respective same-generation pair of left-handed gauge basis fields at each vertex. $\nu = 2, \alpha = 2$.

Similar evaluations were carried out in [8] with 5, 10 and 20 KK modes in the sum and the result compared with the same computation using the analytic solution for the correlation function with quadratic dilaton. It was suggested there that the with the inclusion of more KK modes, the value seems to steadily converge to the value obtained using analytical solutions for the full tower, i.e. that the size of contributions diminish with increasing KK number. While this could be a reasonable assumption, we satisfy ourselves here that there is a good agreement with 20 modes and need not worry about

the behaviour of individual higher modes since we will be computing the full tower exactly at zero momentum for massless fields, and to the appropriate perturbative order in $(h_0/M_{KK})^2$ for the massive fields.

With regards to the question of convergence for different values of ν and α , one must simultaneously consider the behaviour of both the fermion profiles (changing with α) and the gauge profiles (changing with ν) since both appear as factors in the double convolutions. This is done below in 6.1.11, where a convergence condition is derived.

Chapter 6

Flavour Phenomenology of WEDs

With the theoretical background above, we now have a good understanding of the physics of flavour violation in SW models, and we are in a position to carry out a phenomenological analysis. We have a complete set of analytic expressions required for numerical evaluation of $\Delta F = 2$ observables in a well-defined EFT, with the exception of the hadronic matrix elements which are discussed below. Presented here is a detailed description of the numerical methods employed and the precise nature of the scans conducted. Following this, we look at the results obtained in both K and B mixing systems.

6.1 Numerical Methodology

6.1.1 Boson Propagators: Coordinate Transformations

The first order solutions for the expanded fifth dimension position space Green's functions are:

$$G_0(u, v) = \int_R^v e^{\Phi(t)} \frac{t}{R} dt + BD + g(u) + g(v) \quad (6.1)$$

where

$$g(z) = -A_0 \int_R^z dz_1 \left(e^{\Phi(z_1)} \int_R^{z_1} e^{-\Phi(z_0)} \frac{R}{z_0} dz_0 \right), \quad (6.2)$$

and

$$G_{0,p=0}^{(W/Z)}(u, v)/M_{KK}^2 = \int_R^v e^{\Phi(t)} \frac{t}{R} dt + BD + g^{(W/Z)}(u) + g^{(W/Z)}(v) \quad (6.3)$$

where

$$g^{(W/Z)}(z) = \int_R^z dz_1 e^{\Phi(z_1)} \frac{z_1}{R} \int_R^{z_1} e^{-\Phi(z_0)} \frac{R}{z_0} G_{-1,p=0}^{(W/Z)}(z_0, z') dz_0 \quad (6.4)$$

for the massless and massive bosons respectively. For the entirety of the numerical evaluations, we set $R = 10^{-18} GeV^{-1}$. Let us refer to the first term in (6.1) as the “homogeneous” term, and the functions “ $g(z)$ ” as the “inhomogeneous” terms (and likewise for the massive case). For numerical purposes, we would like to work with expressions for the inhomogeneous terms which do not contain nested integrals. This is done by choosing mappings from $[R, \infty)$ to a finite interval $[0, 1]$ via $z_0 = t_0(z_1 - R) + R$

and $z_1 = t(z - R) + R$. We then make additional transformations of the form $z = e^{\tilde{y}}$,

$$\begin{aligned}
g(z) = & -A_0 \int_0^1 dt_1 \int_0^1 dt_0 (\tilde{y} - \log(R))^2 t_1 \exp\{2(t_1(\tilde{y} - \log(R)) + \log(R)) \\
& + \Phi(e^{t_1(\tilde{y} - \log(R)) + \log(R)}) \\
& - \Phi(e^{t_0 t_1(\tilde{y} - \log(R)) + \log(R)})\} \quad (6.5)
\end{aligned}$$

and

$$\begin{aligned}
g^{(W/Z)}(z) = & Z_0 \int_0^1 dt_1 \int_0^1 dt_0 (\tilde{y} - \log(R))^2 t_1 \exp\{2(t_1(\tilde{y} - \log(R)) + \log(R)) \\
& + \Phi(e^{t_1(\tilde{y} - \log(R)) + \log(R)}) \\
& - \Phi(e^{t_0 t_1(\tilde{y} - \log(R)) + \log(R)}) \\
& + (2\alpha - 2)(t_0 t_1(\tilde{y} - \log(R)) + \log(R))\}. \quad (6.6)
\end{aligned}$$

Since the homogeneous term does not contain a nested integral, it is already computationally practical as it appears in (6.1) and (6.3).

6.1.2 Boson Propagators: Convergence

Numerically the task was quite involved to evaluate these formulas in a way that was robust and stable in all parts of the ν -space. In order to maintain a good integration behaviour in computing the terms in $G_0(z, z')$, we factor out the precise asymptotic behaviour of the integrand including all constants and z -dependence. L'Hôpital's rule implies

$$\lim_{v \rightarrow \infty} \frac{\frac{v}{R} e^{\Phi(v)} / \Phi'(v)}{\int_R^v e^{\Phi(t)} \frac{t}{R} dt} = 1 \quad (6.7)$$

so the asymptotic behaviour of the denominator is simply given by the numerator. We therefore divide this out of the integrands in the homogeneous terms in (6.1) and (6.3) and the integrands of (6.5) and (6.6). The graphs in Figure 6.1 show each of the resulting terms separately for a range of values for ν . In this way we ensure $\mathcal{O}(1)$ integrands which can be practically calculated over a finite domain, since they level off as they enter the region where the soft-wall comes into play. The code interpolates up to $\tilde{y} = 100R'$, i.e. deep into the flat region, and the integrals are performed up to $10R'$.

6.1.3 Boson Propagators: Interpolation

Having defined expressions in the variable $\tilde{y} = \log(z)$ for the terms in (6.1) and (6.3), one should now construct interpolations, so as to avoid numerically re-computing the rather complicated integrals which will appear within an additional, encasing double convolution. We simply construct interpolating functions once per KK scale and then perform all subsequent calculations with those functions. This is done by first sampling the expressions for a given KK scale ($1/R'$) in the region $\log(10^{-18}) \leq \tilde{y} \leq \log(5R')$ at intervals of 0.05. The factor of 5 in the argument of the upper-bounding logarithm corresponds to half an order of magnitude in the coordinate z , with R' marking approximately the start of the soft wall. For a randomly selected sample of 20 KK scales for both the massive and massless cases and the homogeneous term, this gave, with stability, a set of points that ends comfortably in the region where the function becomes constant in the IR (i.e. deep in the soft wall region). Clearly for our purposes, we only require that the approximating function extends as far as this flat region, since the integrals will vanish any further in to the IR, all the way to infinity. The interval

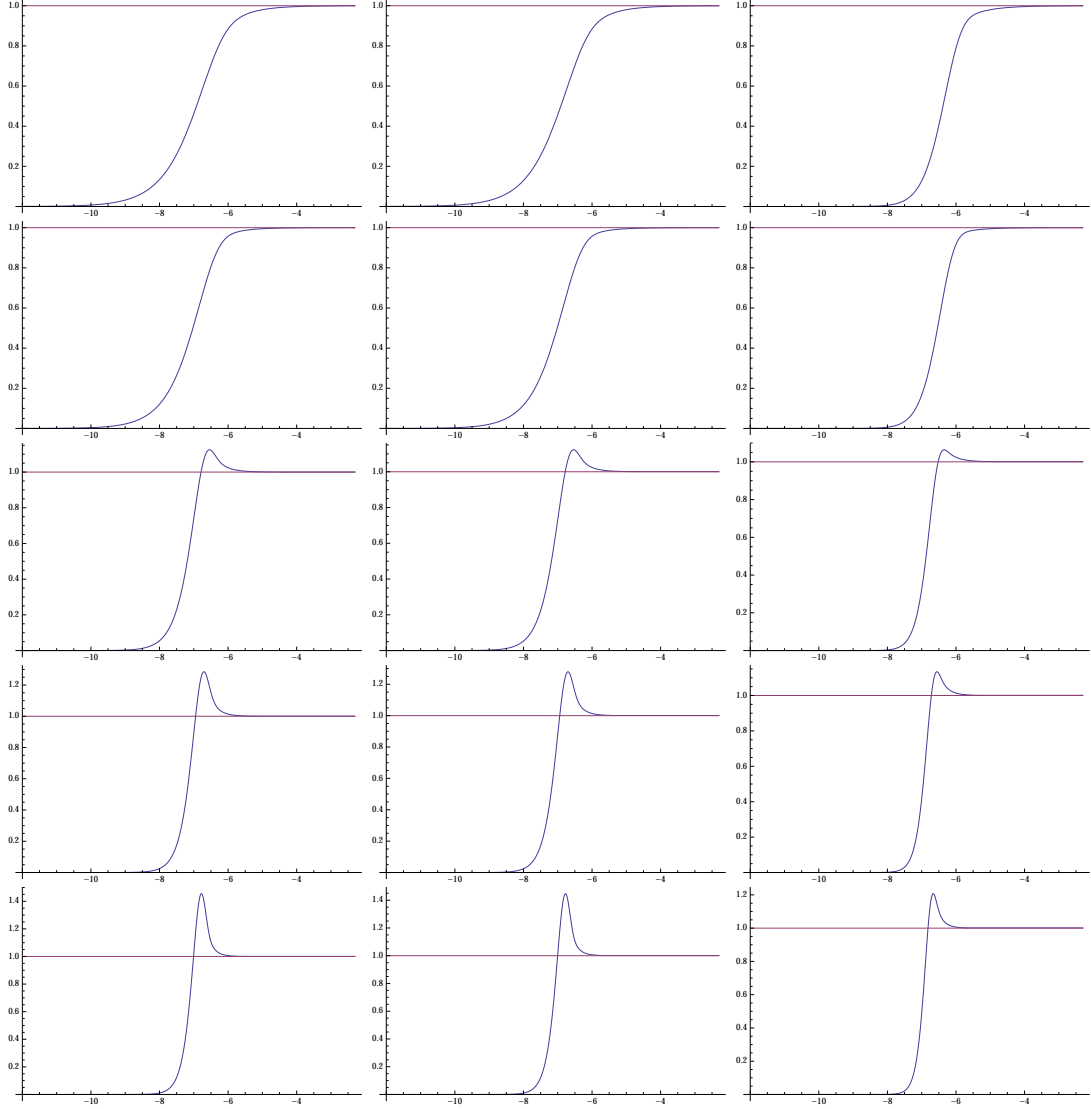


Figure 6.1: From left to right, the ratios of the homogeneous, massless inhomogeneous and massive inhomogeneous terms to their asymptotic forms, for $\nu = 1.5, 1.75, 3, 4, 5$ from top to bottom, all as function of $\tilde{y} = \log(z)$ on the horizontal axis

was chosen via some trial and error, to find a relatively accurate interpolation which also takes a reasonable time to construct (one can determine the accuracy by plotting the difference of the function and interpolation).

6.1.4 Calculation of h_0

When fitting to the quark masses during the numerical procedure, it is necessary to know the value of the parameter h_0 for given values of M_{KK} , ν and α . For this we fit to the mass of the SM Z-boson. One method is to impose a Neumann boundary condition on the massive gauge profile and solve for the lowest mass eigenvalue. Clearly for $\nu \neq 2$ one cannot do this since explicit forms for the gauge profiles are not known in this case. Instead we make use of the arguments in Section 5.3.3. We saw from (5.75) that

$$a = (f_0^A)^2 \int_R^\infty e^{-\Phi} \frac{R}{z} \tilde{\mu}(z) \quad (6.8)$$

which, for $h_0^2 \ll M_{KK}^2$ allows to find a good approximation of the predicted SM Z mass for a given soft wall via,

$$h_0^2 = m_Z^2/a = \frac{m_Z^2}{(f_0^A)^2 \frac{g_5^2}{2} \int_R^\infty e^{-\Phi} \frac{1}{z} \left(\frac{z}{R'}\right)^{2\alpha}} \quad (6.9)$$

noting that

$$\mu(z) = \frac{1}{2} \frac{R^2}{z^2} g^2 h(z) \quad (6.10)$$

Since $g_5^2 (f_0^A)^2 = 4\pi/128s_w^2$, the precise formula for fitting h_0 to the experimental value of the Z mass is

$$h_0 = \frac{m_Z}{\sqrt{\frac{2\pi}{128s_w^2} \int_R^\infty e^{-\Phi} \frac{1}{z} \left(\frac{z}{R'}\right)^{2\alpha}}} \quad (6.11)$$

6.1.5 Fit to Quark Masses

We ultimately need to find, for a given set of left-handed localisations, the localisations of the up-like and down-like right-handed particles, which, together with appropriate Yukawa couplings, give the correct quark masses, mixing angles and phase-invariant quantity (we will use the Jarlskog invariant). However, we first find “natural” right-handed localisations which fit to the quark masses, by generating random Yukawas $|\lambda_{ij}| \in [1, 3]$, feeding into the expression for the zero-mode fermion mass matrix (after running the quark masses to $2 M_{KK}$), and then scanning through each of the three c_0^R values from -0.9 to -0.2 at intervals of 0.01 , with the exception of the largest value of the up-like values for which the scan is between -0.6 to 0.6 . The loop starts by finding a point in the three-dimensional parameter space which has a total relative error squared of less than 1.5 , which is quite large, but then proceeds to update the parameters for any point which gives a smaller error. In this way the point giving the smallest sum of squares of the relative errors is found with a scanning resolution of 0.01 .

6.1.6 Naturalness

For the sake of ensuring that the right-handed localisations found using the above process are actually a fair representation of typical values, the process is performed in parallel for nine separate, randomly chosen Yukawa matrices, for both the up and the down cases. The median of the resulting c_0^R values is then taken. The procedure in the following section is then used to find the Yukawa couplings for the down-like quarks, starting with the full set of localisation parameters which have now been found.

6.1.7 Yukawa Couplings

The current procedure involves randomly scanning over 10million points in the space of possible Yukawas with modulus in $[1, 3]$. For each randomly chosen parameter point:

- the up-like and down-like fermion mass matrices are generated using the localisation parameters already obtained and the randomly chosen up and down Yukawas.
- This is then diagonalised, with the resulting quark masses and rotation matrices stored in memory.
- The CKM matrix is calculated, the mixing angles V_{us} , V_{ub} and V_{cb} are then extracted, and the Jarlskog invariant is calculated using $Im[V_{ij}V_{kl}V_{il}^*V_{kj}^*] = J\sum_{m,n}\epsilon_{ikm}\epsilon_{jln}$ (specifically $i=1, j=1, k=2, l=2$ is used).
- The six quark masses, three mixing angles and Jarlskog invariant are subtracted from the target values from [52] and [24] respectively, the results individually squared and expressed as a fraction of the squared target value and the sum of all 10 taken.
- A small sample of 100 points are then chosen which give the smallest value for the sum.
- The rotation matrices associated with these these 100 points are recorded in arrays, written to text file and used later to calculate mass differences and CP violation parameters, over which the mean of the 100 values will be taken, giving one result per KK scale.

6.1.8 Input Configurations

Since we will fit to the quark masses and mixing angles to fix the right-handed quark localisations and Yukawa couplings, we will take as input parameters the localisations of the left-handed quark generations. The values are chosen so as to give approximately the right mixing angles. These are the same values used in [8, 7], which permits a comparison with the study of flavour in the $\nu = 2$ soft-wall model therein. Since the investigation presented here may well be thought of as an extension of that work, this is logical choice. The five configurations of left-handed fermions are:

A	B	C	D	E
0.72, 0.64, 0.52	0.69, 0.63, 0.49	0.66, 0.60, 0.42	0.63, 0.57, 0.34	0.60, 0.52, 0.25

where the second row shows the respective c_0^L values.

6.1.9 Computation of Gauge Basis Double Integrals

The effective operators have the possible chiralities $LLLL, RRLL, RRRR$. Double convolutions must be computed for each possibility. For each of the configurations listed above, c_0^R values are calculated as explained, enabling the calculation of convolutions involving right-handed fermions. These calculations are all, of course, in the gauge basis. The double convolutions are calculated for possible pair of in and out generations, giving a 3×3 matrix (with each entry calculated in parallel) for each chiral possibility for the fermions, and for both massless and massive boson propagators (calculated as explained). This makes 6 matrices in total, with the total number of double integral

computations equaling 54. These are written to file, which completes the calculation for a specific KK scale and a specific configuration. 50 KK scales are randomly generated for each configuration and the calculations are run in full.

6.1.10 Basis Rotations

Having obtained values for the double convolutions in the gauge basis, one must now affect the correct unitary transformations to ultimately find Wilson coefficients in the mass basis. For each 3x3 matrix of double convolutions, the rotations are affected by U and V matrices. Note that this involves sums over generation number. The indices of the rotated matrix must be chosen to match the generations of the in and out states in the mass basis.

Since we want to calculate physical observables, one must be careful to use the correct phase conventions for the physical fields. The formula (6.40) is valid only in the standard CKM parameterisation, whereas we in fact encounter a phase redundancy in fitting to the quark masses [52]. To see the details of this, let us define up and down quark fields in different bases

$$u_{a(L,R)}^{std} = e^{i\alpha^a} u_{a(L,R)}^{int} \quad (6.12)$$

$$d_{a(L,R)}^{std} = e^{i\beta^a} d_{a(L,R)}^{int} \quad (6.13)$$

$$u_{iL}^{bulk} = \sum_a \hat{U}_{ia}^u u_{aL}^{int} \quad u_{aR}^{bulk} = \sum_a \hat{V}_{ia}^u u_{aR}^{int} \quad (6.14)$$

$$d_{iL}^{bulk} = \sum_a \hat{U}_{ia}^d d_{aL}^{int} \quad d_{aR}^{bulk} = \sum_a \hat{V}_{ia}^d d_{aR}^{int} \quad (6.15)$$

$$u_{iL}^{bulk} = \sum_a e^{-i\alpha^a} \hat{U}_{ia}^u u_{aL}^{std} \quad u_{aR}^{bulk} = \sum_a e^{-i\alpha^a} \hat{V}_{ia}^u u_{aR}^{std} \quad (6.16)$$

$$d_{iL}^{bulk} = \sum_a e^{-i\beta^a} \hat{U}_{ia}^d d_{aL}^{std} \quad d_{aR}^{bulk} = \sum_a e^{-i\beta^a} \hat{V}_{ia}^d d_{aR}^{std}. \quad (6.17)$$

Let us also define $U^{u,d}$ and $V^{u,d}$ s.t.

$$u_{iL}^{bulk} = \sum_a U_{ia}^u u_{aL}^{std} \quad u_{iR}^{bulk} = \sum_a V_{ia}^u u_{aR}^{std} \quad (6.18)$$

$$d_{iL}^{bulk} = \sum_a U_{ia}^d d_{aL}^{std} \quad d_{iR}^{bulk} = \sum_a V_{ia}^d d_{aR}^{std} \quad (6.19)$$

and so

$$U_{ia}^u = e^{-i\alpha^a} \hat{U}_{ia}^u \quad V_{ia}^u = e^{-i\alpha^a} \hat{V}_{ia}^u \quad (6.20)$$

$$U_{ia}^d = e^{-i\beta^a} \hat{U}_{ia}^d \quad V_{ia}^d = e^{-i\beta^a} \hat{V}_{ia}^d. \quad (6.21)$$

To make sense of the labels, after KK expanding to find an effective 4D theory, we are still in the “bulk mass basis” i.e. the basis in which the 5D mass matrix is diagonal. This is what we call the 4D gauge basis (4D mass matrix non-diagonal). In the above numerical procedure, rotation matrices are found which diagonalise the 4D mass matrix. In general, since there is a phase redundancy in (4.2) these might not be in the standard CKM parameterisation, so we can call them “intermediate”. With a Yukawa term

$$\mathcal{L} \supset \frac{v}{\sqrt{2}} \lambda_{ij} \bar{Q}_{iL}^{bulk} q_{jR}^{bulk} + h.c. \quad (6.22)$$

the mass matrix is diagonalised via

$$M_{diag}^{int} = \hat{U}^\dagger M^{bulk} \hat{V}. \quad (6.23)$$

The CKM matrix is defined by

$$(\bar{u}_L^{bulk} \bar{c}_L^{bulk} \bar{t}_L^{bulk}) \gamma^\mu W_\mu^+ \begin{pmatrix} d_L^{bulk} \\ s_L^{bulk} \\ b_L^{bulk} \end{pmatrix} = (\bar{u}_L^{std} \bar{c}_L^{std} \bar{t}_L^{std}) \gamma^\mu W_\mu^+ U^{u\dagger} U^d \begin{pmatrix} d_L^{std} \\ s_L^{std} \\ b_L^{std} \end{pmatrix} \quad (6.24)$$

$$= (\bar{u}_L^{std} \bar{c}_L^{std} \bar{t}_L^{std}) \gamma^\mu W_\mu^+ V_{CKM} \begin{pmatrix} d_L^{std} \\ s_L^{std} \\ b_L^{std} \end{pmatrix} \quad (6.25)$$

$$= \sum_i (\bar{u}_L^{std} \bar{c}_L^{std} \bar{t}_L^{std}) \gamma^\mu W_\mu^+ e^{i\alpha^a} \hat{U}_{ai}^{u\dagger} e^{-i\beta^b} \hat{U}_{ib}^d \begin{pmatrix} d_L^{std} \\ s_L^{std} \\ b_L^{std} \end{pmatrix} \quad (6.26)$$

with no sum in place over i and j . Then defining $\hat{V}_{CKM} \equiv \hat{U}^{u\dagger} \hat{U}^d$ we find a relation,

$$V_{CKM} = e^{i(\alpha^a - \beta^b)} \hat{V}_{CKM} \quad (6.27)$$

and so we can find the phases by taking $\arg(V_{CKM}^{ab}/\hat{V}_{CKM}^{ab})$. One must then ensure that the phases are correctly taken into account before calculating Wilson coefficients.

Explicitly,

$$\mathcal{I}_{\psi_a \chi_b \xi_c \sigma_d}^{(B)} = \sum_{i,j=1}^3 (U_\psi^\dagger)^{ai} (U_\chi)^{ib} \left[\int_R^\infty dz \int_R^\infty dz' f_\psi^i(z) f_\chi^i(z) G_p^{(B)}(u, v) f_\xi^j(z') f_\sigma^j(z') \right] (U_\xi^\dagger)^{cj} (U_\sigma)^{jd} \quad (6.28)$$

$$= \sum_{i,j=1}^3 (\hat{U}_\psi^\dagger)^{ai} e^{i\beta^a} (\hat{U}_\chi)^{ib} e^{-i\beta^b} \left[\int_R^\infty dz \int_R^\infty dz' f_\psi^i(z) f_\chi^i(z) G_p^{(B)}(u, v) f_\xi^j(z') f_\sigma^j(z') \right] \quad (6.29)$$

$$\times (\hat{U}_\xi^\dagger)^{cj} e^{i\beta^a} (\hat{U}_\sigma)^{jd} e^{-i\beta^b} \quad (6.30)$$

so

$$\mathcal{I}_{\psi_a \chi_b \xi_c \sigma_d}^{(B)} = e^{2i(\beta^a - \beta^b)} \hat{\mathcal{I}}_{\psi_a \chi_b \xi_c \sigma_d}^{(B)}. \quad (6.31)$$

6.1.11 The Range of α and ν

Although α and ν are independent free variables, there exist some automatic constraints on the range of values we can sensibly explore numerically. First, for $\alpha < 1.5$ or $\alpha > 4$ it becomes difficult to fit to zero-mode quark masses without reintroducing a hierarchy in the Yukawas. It therefore makes sense to restrict our study to $1.5 \leq \alpha \leq 4$, if we wish to maintain the geometrical mechanism of generating the fermion masses in warped extra dimensions, one of the attractive features of such models.

An additional restriction comes from the requirement that the double convolutions converge. The asymptotic behaviour of the first term in (5.56) and (5.63) is given by

$$\lim_{v \rightarrow \infty} \frac{\frac{v}{R} e^{\Phi(v)} / \Phi'(v)}{\int_R^v e^{\Phi(t)} \frac{t}{R} dt} = 1 \quad (6.32)$$

and likewise (up to a relative sign) for the function $g(z)$, so the condition for convergence

of (6.28) is that

$$\lim_{z \rightarrow \infty} \left(f_{L,R}^0(z)^2 \frac{z}{R} e^{\Phi(z)} / \Phi'(z) \right) = 0. \quad (6.33)$$

Substituting into (6.33) the form of the zero-mode profile $f_{L,R}^0(z) \sim z^{\mp c_0} \exp(\mp \frac{c_1}{\alpha} \frac{z^\alpha}{R'^\alpha})$ and $\Phi(z) = (z/R')^\nu$ we find,

$$\lim_{z \rightarrow \infty} \left(\frac{1}{\nu} z^{\mp 2c_0 + 2 - \nu} \frac{1}{R'^\nu R} \exp \left(\frac{z^\nu}{R'^\nu} \mp \frac{2c_1}{\alpha} \frac{z^\alpha}{R'^\alpha} \right) \right) = 0 \quad (6.34)$$

and bearing in mind that $c_1^R = -c_1^L$ we see (6.34) is satisfied so long as the argument of the exponential function is negative, i.e.

$$\frac{2c_1}{\alpha} \frac{z^\alpha}{R'^\alpha} \geq \frac{z^\nu}{R'^\nu}. \quad (6.35)$$

Physically, this relation expresses the requirement that the fermion profiles go to zero fast enough in the UV and IR to overwhelm any corresponding growth in the gauge modes. Recall that α and ν set the shape of the fermion mass and dilaton profile respectively. As such, they determine the nature of the interaction between the geometric background and the matter and gauge fields respectively. Hence, these parameters must be chosen so as to give finite amplitudes for the interactions of KK gauge modes and 4D fermions computed via (6.28).

6.1.12 Observables in K and B Mixing

The observables in the $K - \bar{K}$ and $B - \bar{B}$ systems are all expressible in terms of the quantities ($M = K, B_d, B_s$)

$$M_{12}^M = M_{12}^{M,\text{SM}} + M_{12}^{M,\text{NP}} \quad (6.36)$$

where $M_{12}^{M,\text{SM}}$ is the Standard Model contribution, and the BSM contribution

$$M_{12}^{\text{NP}} = \langle M | H_{\text{eff, NP}}^{\Delta F=2} | \bar{M} \rangle \quad (6.37)$$

involves the matrix elements, with $i = 1, 4, 5$

$$\langle M | Q_i^{ab}(\mu) | \bar{M} \rangle \equiv \frac{m_M f_M^2}{3} P_i^M(\mu). \quad (6.38)$$

These are evaluated at the matching scale $\mu \sim 2m_{KK}$. For the masses we take the PDG central values $m_K^0 = 497.6$ MeV, $m_{B_d^0} = 5.280$ GeV, $m_{B_s^0} = 5367$ GeV [52], and for the decay constants the FLAG 2+1 flavour averages [6], $f_K = 156.3$ MeV, $f_{B_d} = (190.5 \pm 4.2)$ MeV, $f_{B_s} = (227.7 \pm 4.5)$ MeV. In Kaon physics, we have the two observables

$$\Delta M_K = 2\text{Re}M_{12}^K \quad (6.39)$$

$$\epsilon_K = \epsilon_K = \frac{\kappa_\epsilon e^{i\varphi_\epsilon}}{\sqrt{2}(\Delta m_K)_{\text{exp}}} \text{Im} M_{12}^K \quad (6.40)$$

where $\varphi_\epsilon = 43.51^\circ$ and $\kappa_\epsilon = 0.92$ [16]. The SM contribution to $\text{Re}M_{12}^K$ is still quite uncertain due to unknown long-distance contributions, with $\text{Im}M_{12}^K$ under somewhat better control [14]. In light of this and the inherent uncertainties in our calculation, we can simply impose $2|\text{Re}M_{12}^N P| < \Delta M_K^{\text{exp}}$, ie assume the absence of large cancellations between SM and new physics in producing the measured value. Similarly, it is only required that $|\epsilon_K^{\text{NP}}| < \epsilon_K^{\text{expt}}$, where ϵ_K^{NP} is evaluated according to (6.40).

In B physics, observables include mass difference, time-dependent CP violation, and semileptonic CP asymmetries[24]. Global fits of the data are to the ratios [24]

$$\Delta_q \equiv 1 + \frac{M_{12}^{B_q, NP}}{M_{12}^{B_q, SM}}. \quad (6.41)$$

Hence, rather than comparing to the individual observables, Δ_q is evaluated in the soft wall and compared to the global fit. In doing so, the SM expressions used are

$$M_{12}^{B_q, SM} = \frac{G_F^2 M_W^2}{12\pi^2} (V_{tq}^* V_{tb})^2 S_0(x_t) B_{B_q}(\mu_b) f_{B_q}^2 M_{B_q} \hat{\eta}_B, \quad (6.42)$$

which evaluates to [44]

$$\Delta M_d = 3.304 \times 10^{-13} \text{GeV}, \quad \Delta M_s = 1.135 \times 10^{-11} \text{GeV}. \quad (6.43)$$

where $\Delta M_q = 2|M_{12}^{B_q}|$ and $\sin(2\beta) = 0.682$ and $\sin(2\beta_s) = 0.02$ [52] give the respective complex phases.

6.1.13 Bag Factors

We evaluate $M_{12}^{M,\text{NP}}$ at a renormalisation scale $\mu = 2m_{KK}$. This has the advantage that only three bag factors are then involved. The bag factors are calculated by various lattice QCD collaborations [6, 21, 43] at low renormalisation scales and need to be RG-evolved up to the scale μ . For P_i^K we perform the evolution and flavour threshold matching up to the top mass scale according at next-to-leading order [17], and onward at leading-logarithmic order. This has the advantage of taking the known NLO corrections from low scales, where α_s is relatively large, into account, while being of leading order in $\alpha_s(\mu)$ as appropriate for our tree-level computation of the BSM effects. For B physics we perform the evolution at leading logarithmic order throughout. For Kaons, we employ the bag factor calculation of [10] up to μ_0 . Representative numerical values are given in Table 6.1.

	1 TeV	3 TeV	10 TeV	30 TeV
P_1^K	0.432576	0.419731	0.407458	0.397565
P_4^K	87.955	99.226	111.733	123.277
P_5^K	34.2583	37.9415	42.0386	45.828
$P_1^{B_d}$	0.714509	0.693293	0.67302,	0.656679
$P_4^{B_d}$	4.13435	4.66415	5.25202	5.79465
$P_5^{B_d}$	1.85466	2.02413	2.21318	2.3884
$P_1^{B_s}$	0.722915	0.701449	0.680938	0.664404
$P_4^{B_s}$	4.05558	4.57529	5.15196	5.68425
$P_5^{B_s}$	1.85696	2.02264	2.20753	2.37898

Table 6.1: “Bag” factors $P_i(\mu)$ for the relevant hadronic matrix elements at representative renormalisation scales.

6.2 Numerical Results and Analysis

Presented here are numerical results showing the impact of soft wall models on flavour physics. We will focus on $\Delta F = 2$ processes, which provide generic probes of all the FCNC couplings discussed above. We consider CP violation in $K - \bar{K}$ mixing, the most stringent generic flavour observable, as a function of a 2-parameter parameterisation of generic soft walls. We proceed to analysing the constraining impact of the combined data on $B_d - \bar{B}_d$ mixing and on $B_s - \bar{B}_s$ mixing on soft wall models and compare with the ϵ_K constraint [52]. We will be interested in the cases $(a, b) = (1, 2) = (d, s)$ ($K - \bar{K}$ mixing), $(a, b) = (1, 3) = (d, b)$ ($B_d^0 - \bar{B}_d^0$ mixing), and $(a, b) = (2, 3) = (s, b)$ ($B_s - \bar{B}_s$ mixing). We recall that these expression precisely contain the leading terms in an expansion m_M^2/M^2 from the entire tower of KK excitations, where m_M is the meson mass and M the KK mass scale.

6.2.1 $K - \bar{K}$ Mixing

Since the most stringent existing flavour constraints for warped models come from ϵ_K [8, 12] this provides a logical starting point for studying the flavour phenomenology across the $\alpha - \nu$ theory space. A further consistency check of the method presented in section 3.5 comes in the form of reproducing Figure 5 of [8], in which the boson propagators were approximated by the first 20 KK modes. Figure 6.2 provides such a comparison, although it turns out there are in fact some noticeable discrepancies. In particular, configuration E appears to be suppressed in [8] relative to the results presented here. It has, unfortunately, not been possible to completely account for this, but one can analyse the physics at play to gain some insight into the results shown in

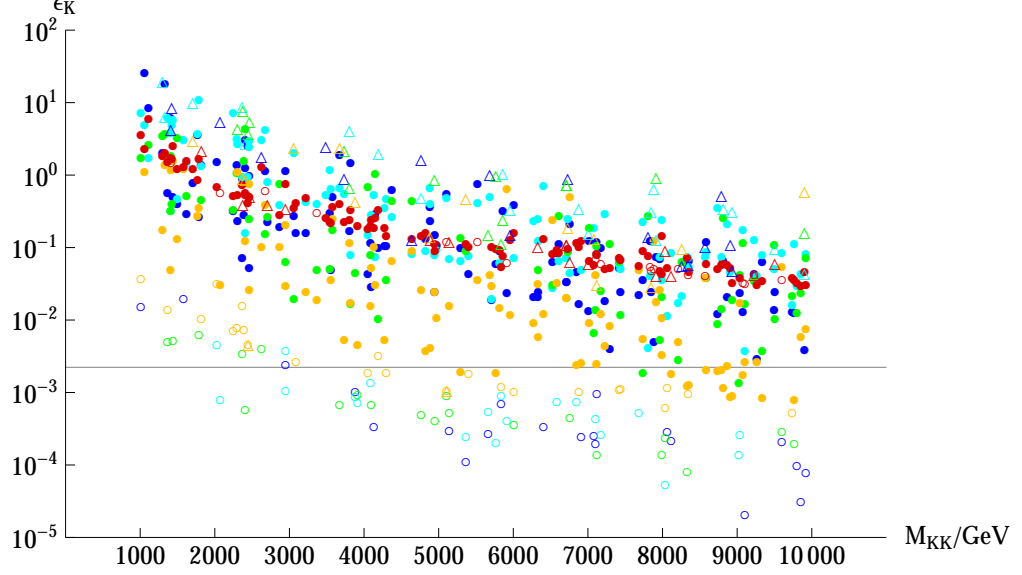


Figure 6.2: $\nu = 2$, $\alpha = 2$. Triangles (hollow circles) show points with generations 1 and 2 (2 and 3) with equal localisations, solid circles show points with all three generations having different localisations. Configurations A, B, C, D, E are shown in blue, cyan, green, orange and red respectively. The black line shows the experimental bounds [52]

Figure 6.2.

For all five sets of c_0^L values, the first and second generations are localised in the RS-GIM suppressed region, but as the fields are shifted towards the IR, the non-universality in the coupling of the heavy third generation increases. A converse effect is at play in the right-handed sector, namely that in order to give the correct quark masses for the zero-modes, the right-handed fields must fall further into the IR for more UV localised left-handed partners. For this reason, left-handed contributions dominate for configurations E and D and become increasingly less important through C and B to configuration A, where the right-handed contributions are typically at least as significant, or slightly dominant (see Figure 6.3). As one shifts the left-handed fields into the IR, the suppression of the right-handed fields leads to an overall reduction in the value of ϵ_K , until eventually the left-handed effects take over as the second

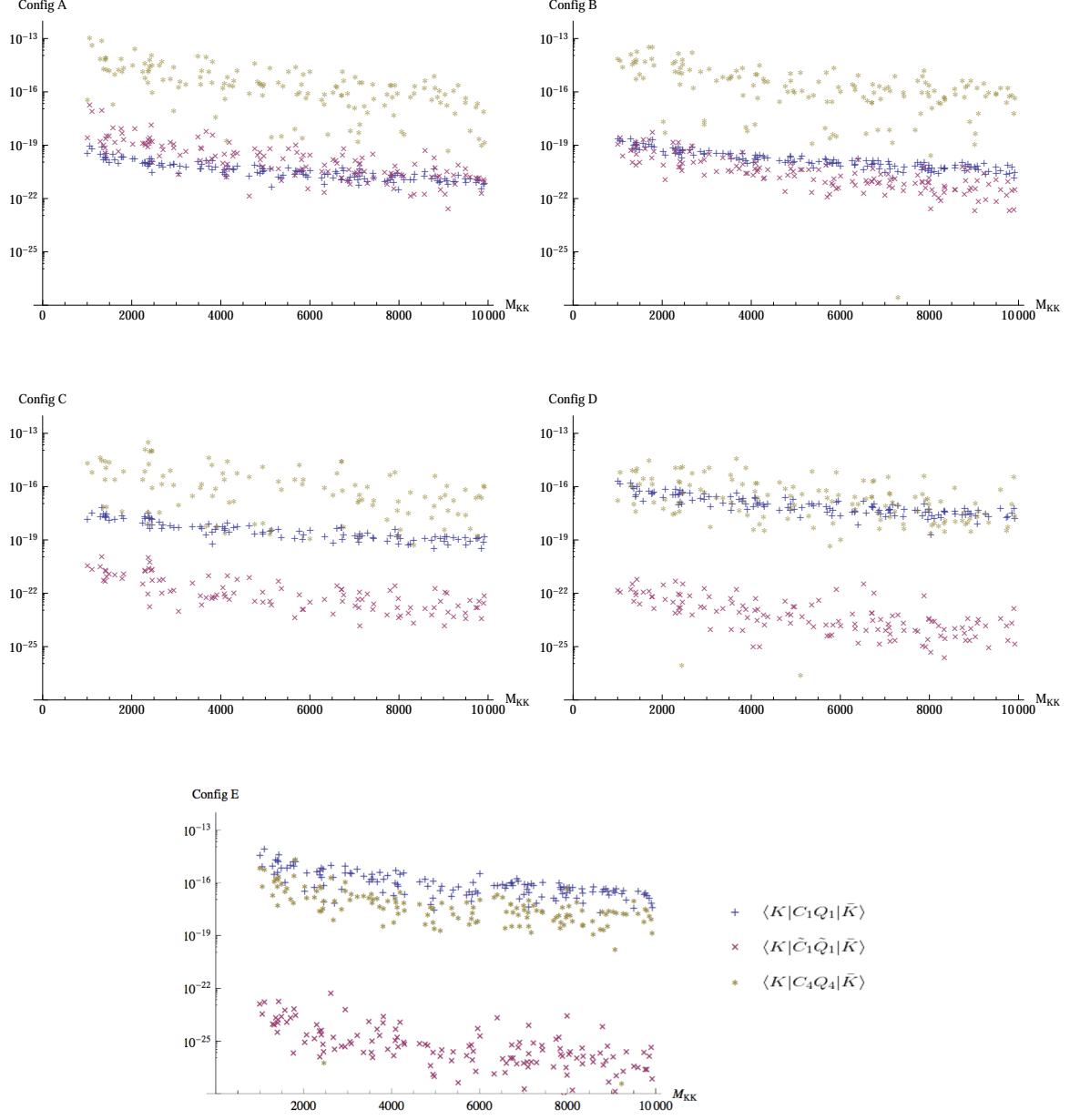


Figure 6.3: The relative sizes of terms in the absolute values of the amplitude for $K - \bar{K}$ mixing from operators Q_1 , \tilde{Q}_1 and Q_4 , giving the dominant LL, RR and RL contributions respectively, for $\nu = 2, \alpha = 2$.

generation enters the region of non-universal couplings. In light of this, one could posit some additional, unidentified suppression mechanism affecting specifically the LL contributions to explain the apparent reduction in flavour violation in configuration E, visible in [8]. Precisely what this could be, however, is not completely clear.

Figure 6.2 also shows results with an $SU(2)$ imposed flavour symmetry between the first and second generations or the second and third generations of the right-handed quarks, specifically $c_0^{R1} = c_0^{R2}$ and $c_0^{R2} = c_0^{R3}$ respectively. In the latter case, the value of ϵ_K is found to be several orders of magnitude below the rest in the configurations which are not dominated by LL contributions. One therefore sees the effect of removing completely right-handed flavour violating neutral currents from the theory. Since for the more UV localised left-handed configurations, the right-handed fields are more IR localised, these configurations are more sensitive to effects due to mixing with the third generation, and hence are suppressed to a more significant degree. In the case that first and second right-handed generations have equal localisations, this occurs in the already flavour universal region, so there is no additional suppression of the contributions to ϵ_K .

The question to be addressed is whether flavour constraints can be ameliorated modifying the background and/or the shape of the fermion mass function. To this end, we look at a sample of points across the parameter space. Figure 6.4 shows the median value of ϵ_K for 12 points with $M_{KK} = 8000, 8500, 9000, 9100, 9200, 9300, 9400, 9500, 9600, 9700, 9800, 9900$. Shown is the result of interpolating between values at $\alpha = 1.5, 2.0, 2.5, 3.0, 3.5, 4.0$ and $\nu = 1, 1.25, 1.5, 1.75, 2.0, 2.25, 2.5, 2.75, 3.0$, this range being based on arguments of Section 6.1.11. This gives an indication of which values of the two parameters give the most flavour suppression, although it should not be taken

as anything more than a guideline for which data sets to explore in more detail, and to demonstrate visually the kind of effects the dilaton and fermion mass dependence can have on the flavour phenomenology. Note that it is straightforward to do numerical computations for various forms of the dilaton using (5.56) and (5.63) just by changing the value of ν , i.e. the form of $\Phi(z)$, which would have been both analytically and computationally very challenging using a sum over modes approximation.

One can see that potentially interesting points lie at $(\nu, \alpha) = (1.5, 2), (2, 2.5)$ and $(1.5, 1.5)$ with most suppression occurring towards small values of the two parameters. Once lowest lying points are isolated, one can do more detailed scans in these regions. Of course, this is far from exhaustive, given the limited resolution of the scan along both α and ν directions. There could well, therefore, be additional interesting points that have not been discovered in this plot. Furthermore, one could also consider such plots for the other left handed configurations and perhaps include more points in the average for each pair of co-ordinates. At present, we leave this to further work. Nevertheless, more detailed studies for ϵ_K for $(1.5, 2)$ and $(2, 2.5)$ and $(1.5, 1.5)$ are shown in Figures 6.5, 6.6 and 6.10 respectively, which serve as a further demonstration of the relevant effects. In particular, Figure 6.5 shows significant reduction of ϵ_K particularly in the case of configuration A, localised relatively further towards the IR. This suggests a suppression in the right-handed sector due to this particular modification of the background. Thus we see that constraints, namely the left handed localisations in this case, coming from ϵ_K can be to some extent relaxed by modifying the geometry. With $\nu = 2, \alpha = 2.5$ or $\nu = 1.5, \alpha = 2$ one does not see much improvement on Figure 6.2 with regards to satisfying Kaon constraints. The results are similar to $\nu = 2, \alpha = 2$, i.e. still typically falling lower than RS [8]. However, for the case of $\nu = 1.5, \alpha = 1.5$, one does see a

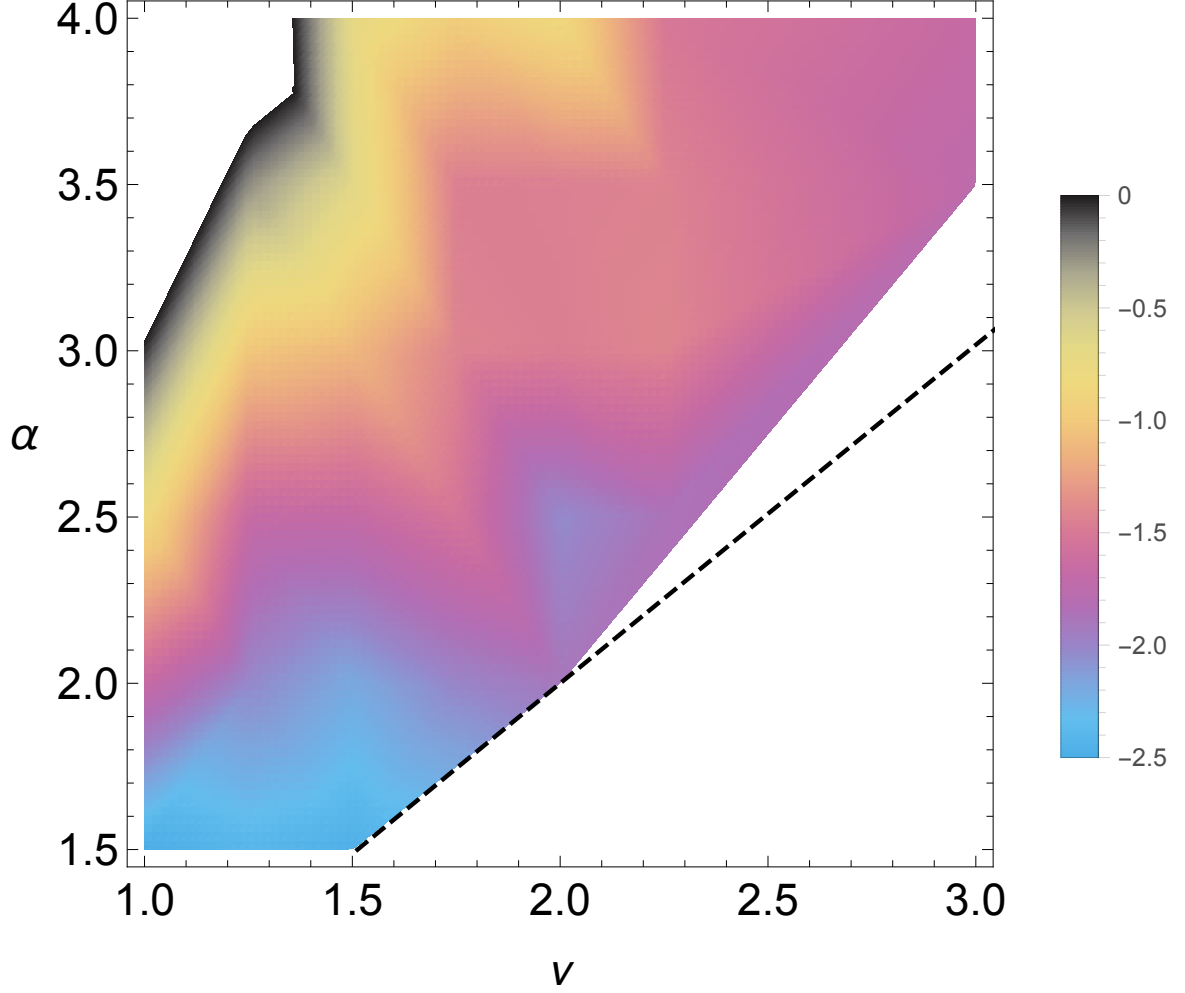


Figure 6.4: $\log_{10}(\epsilon_K)$ for configuration D and varied α and ν . The white region at the top left takes values greater than the black points on the legend. The dashed line indicates the line of equality of (6.35) for $z \gg R'$. Below the line is numerically inaccessible for the reasons explained in 6.1.11. The resolution of the scan is such that there is a small region above the line which is viable but in which there were no calculated points.

significant suppression relative to the quadratic-quadratic case, in all but configuration E. Thus for future flavour studies of SW models, such as hadronic and semi-leptonic decays, it is indeed worth extending beyond the case of $\nu = 2, \alpha = 2$.

It is not completely clear why smaller values of ν and α seem to give less flavour violation. The most likely explanation is that for smaller values of these parameters,

the fermions tend to fall in regions of the extra dimension where the gauge profile is relatively flat once fitted to the masses and mixing angles. To show this explicitly however, one would have to compute the gauge profiles for specific values of $\nu \neq 2$ which, as already emphasised in this thesis, (particularly in Section 3.5.4) is analytically troublesome.

Nevertheless, in the case $\nu = 1.5$, $\alpha = 1.5$, we see that without the $SU(2)$ flavour symmetry, one requires a KK scale of around 3-4TeV or higher to satisfy the bounds from ϵ_K . However, imposing the $SU(2)$ symmetry one can lower the bounds as far as 1-2TeV.

6.2.2 $B - \bar{B}$ Mixing

The $\Delta F = 2$ NP effects in $\bar{B}_{d,s} - B_{d,s}$ mixing from the same selection of SW geometries and fermion mass behaviour as presented above for ϵ_K are shown in Figures 6.8-6.10. The contours show constraints from combined fits from experimental values, including $a_{SL}^{d,s}$ and the semi-leptonic dimuon asymmetry A_{SL} and both $\Delta\Gamma_{d,s}$ and $\Delta m_{d,s}$ (see Section 4.3) [24]. In the B_d and B_s systems, the significant source of flavour violation is predominantly the left-handed sector, such that the most significant effects are in configurations D and E. The IR localised third generation still governs the degree of flavour violation for left handed fields, with this effect now suppressed only by one small mixing angle (4.51). Since we calculate ratios $(M_{12}^{d/sNP} - M_{12}^{d/sSM})/M_{12}^{d/sSM}$, one sees similar size effects for both B_d and B_s , as equivalent hierarchies M_{12}^d/M_{12}^s are present in both the SM and NP values.

It is immediately clear that one can satisfy observational constraints coming from both Δ_d and Δ_s . In fact these are considerably less stringent than constraints on ϵ_K in

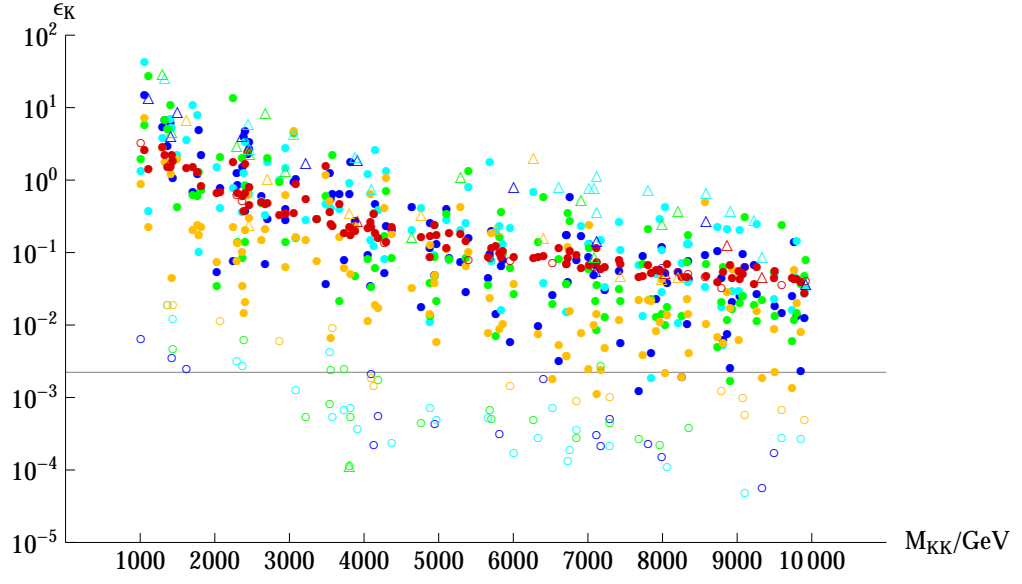


Figure 6.5: $\nu = 1.5$, $\alpha = 2$. Conventions match those of Figure 6.2

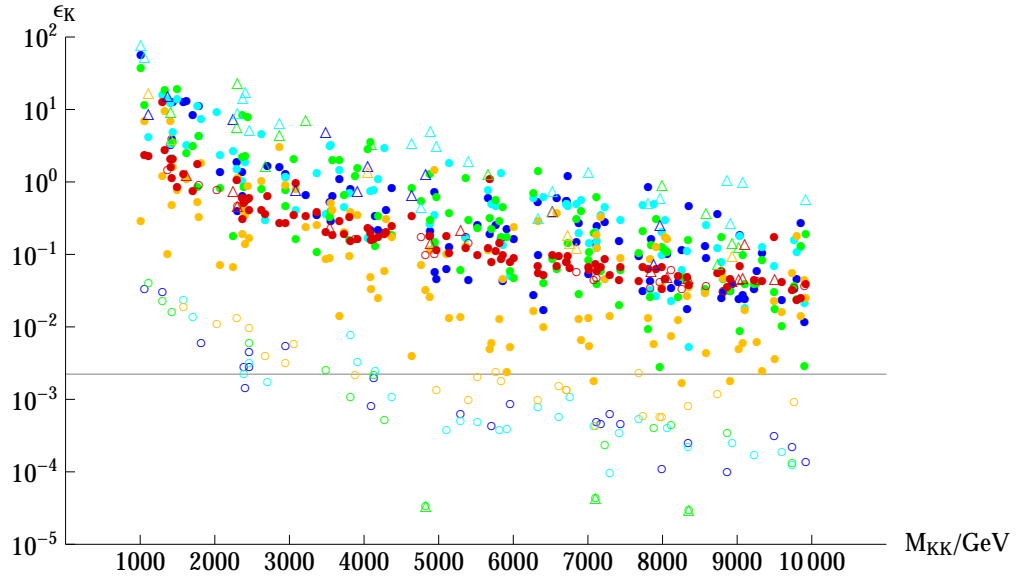


Figure 6.6: $\nu = 2$, $\alpha = 2.5$. Conventions match those of Figure 6.2

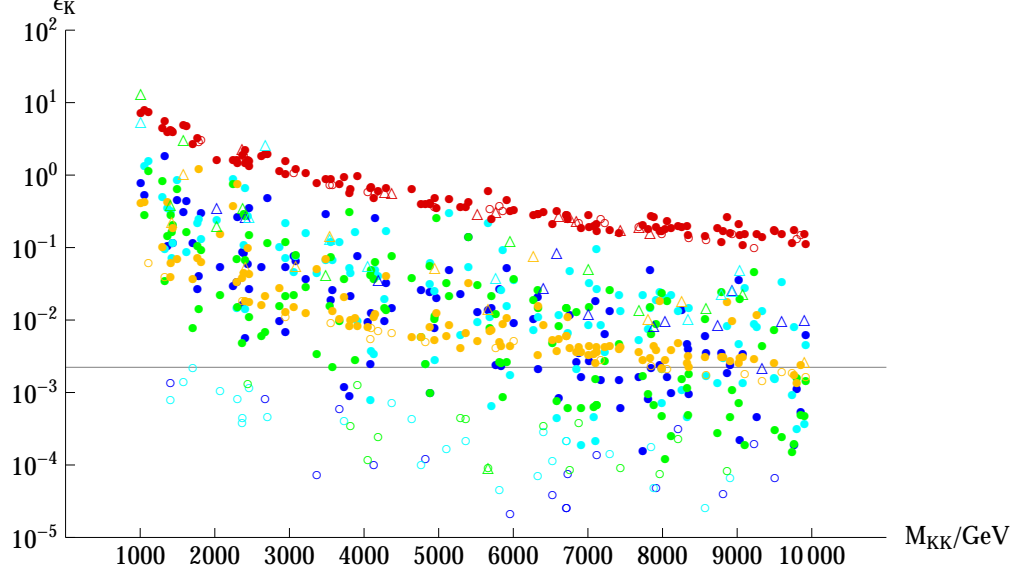


Figure 6.7: $\nu = 1.5$, $\alpha = 1.5$. Conventions match those of Figure 6.2

the kaon sector. Only a very small sample of the points shown in Figures 6.8-6.10 satisfy the bounds from ϵ_K , with all of these points lying very close to the SM prediction. The size of such effects are no greater than 0.05 in $|\Delta_d|$ and 0.025 in $|\Delta_s|$.

Worth noting is that the SM value for Δ_d already has a 1σ tension with combined observational constraints. While this is currently too small to be interesting, we find that the SW model could accommodate deviations of 3σ and beyond in both the B_d and B_s systems, since the effect size varies over several orders of magnitude between differently localised sets of left-handed fields. However, this flexibility is not present in the kaon system, so while one may also expect widely varying $\Delta F = 1$ phenomenology, constraints on ϵ_K would have to be further ameliorated before attempting to explain B physics effects via the KK bosons of the SW theory.

Drilling down to the level of the effective operators, one sees from Figures 6.11 and 6.12 that the gluon-dominated Q4 operator provides the largest contribution to $\Delta_{d,s}$ for the more UV localised left-handed configurations, although less so than in the kaon

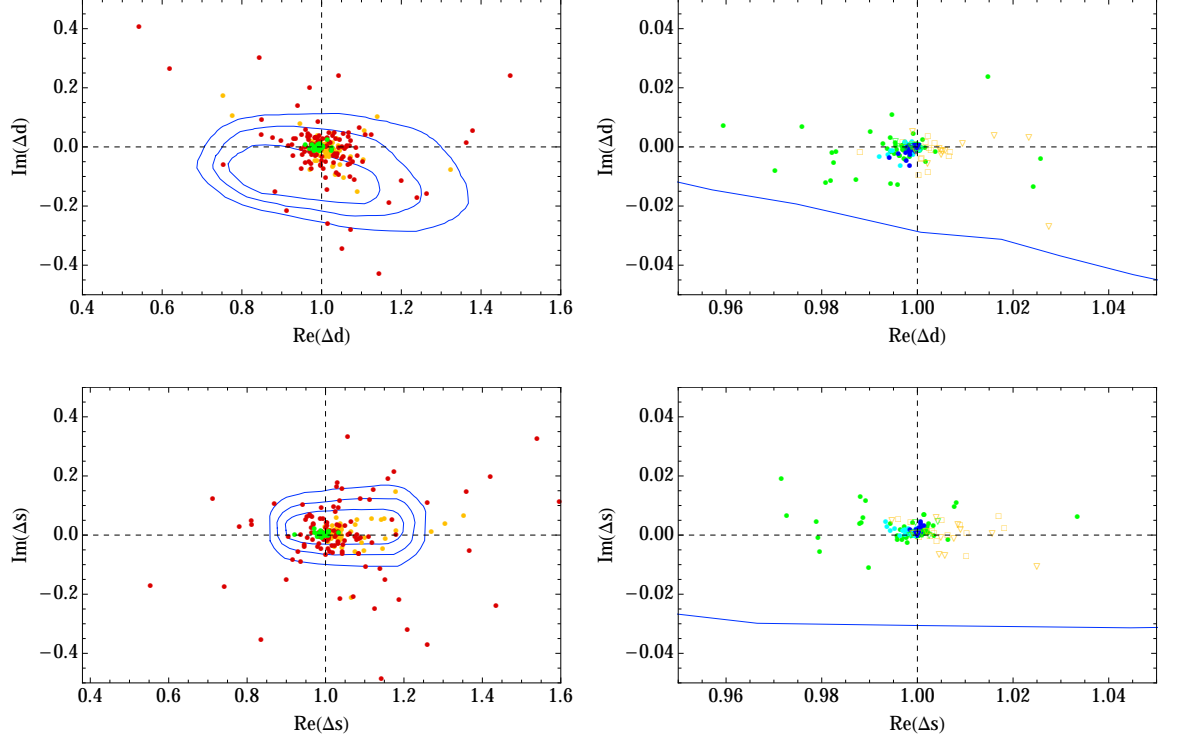


Figure 6.8: $\nu = 2$, $\alpha = 2$, for B_d and B_s . The right column shows a zoomed in view around the SM value. Again, configuration A, B, C, D and E are shown in blue, cyan, green, orange and red respectively. Points with generations 2 and 3 having equal (unequal) right handed localisations and satisfying the the ϵ_K constraints are shown as squares (triangles). Contours show 1σ , 2σ and 3σ deviation from experimental values [24]

sector, but with the LL contribution still taking over as one shifts the left-handed fields into the IR. Hadronic effects expressed in the form of the enhanced P_4 bag factor are thus overcome by RS-GIM suppression, at least in the configurations C-E. This result holds in both the B_d and B_s systems. The smallness of the RR contribution explains the trend visible in the plots, with the red points (lower RS-GIM suppression for LL) showing the largest deviations from the SM, through to the blue points showing the smallest (higher RS-GIM suppression for LL).

With regards to the α - ν space, one sees that the largest NP effects are typically found in the case of $\nu = 1.5$, $\alpha = 1.5$ (Figure 6.10), although this effect is again not significant

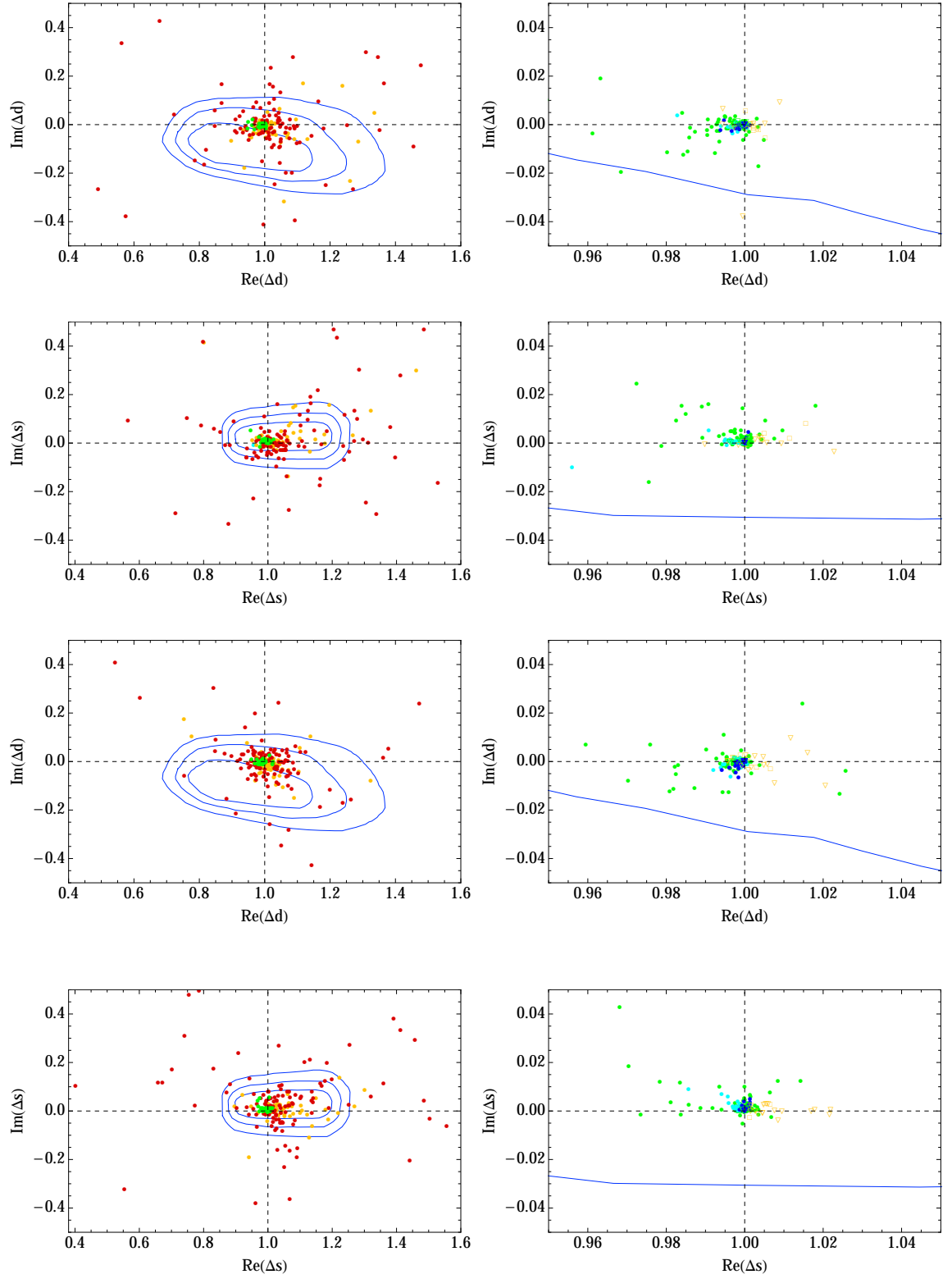


Figure 6.9: B_d and B_s with $\nu = 2$, $\alpha = 2.5$ top and $\nu = 1.5$, $\alpha = 2$ bottom. Conventions match Figure 6.8

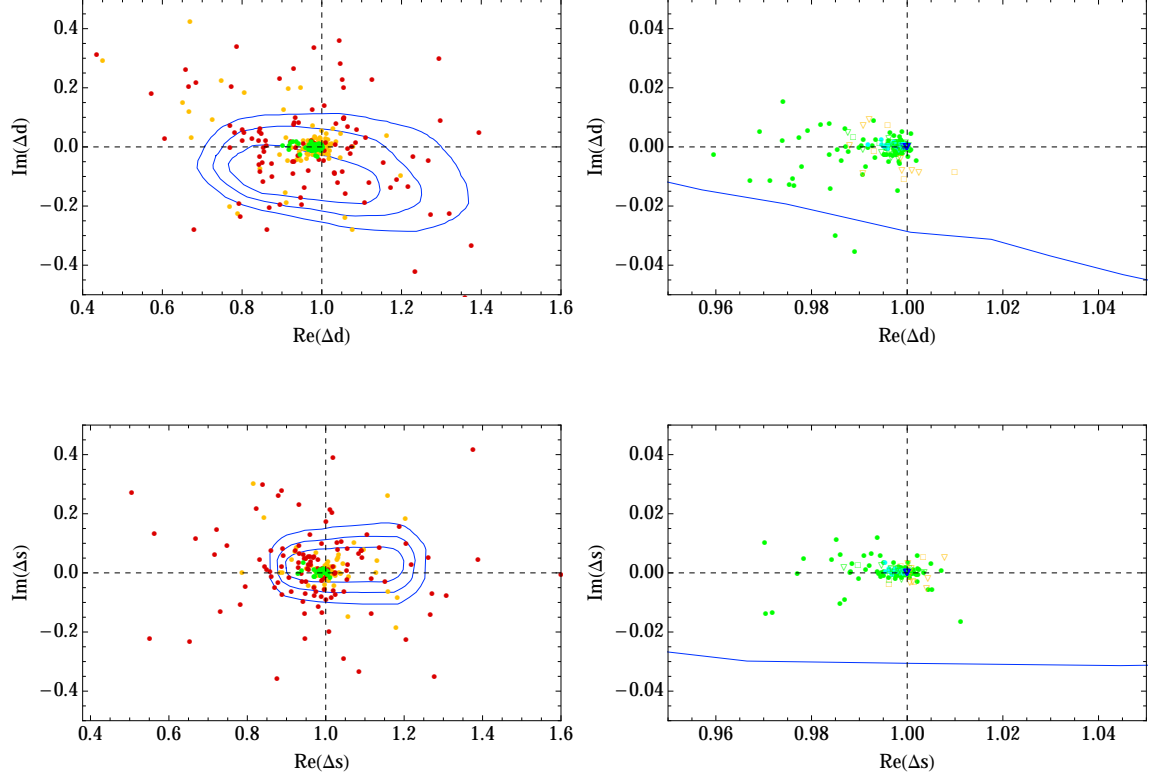


Figure 6.10: $\nu = 1.5$, $\alpha = 1.5$, for B_d and B_s . Conventions match Figure 6.8

in light of the kaon constraints. Interestingly, due to the enhanced significance of the LL operators to $\Delta_{d,s}$ compared to ϵ_K , one sees that the constraints from the B sector are most significant for smaller values of $\nu = 1.5$, $\alpha = 1.5$.

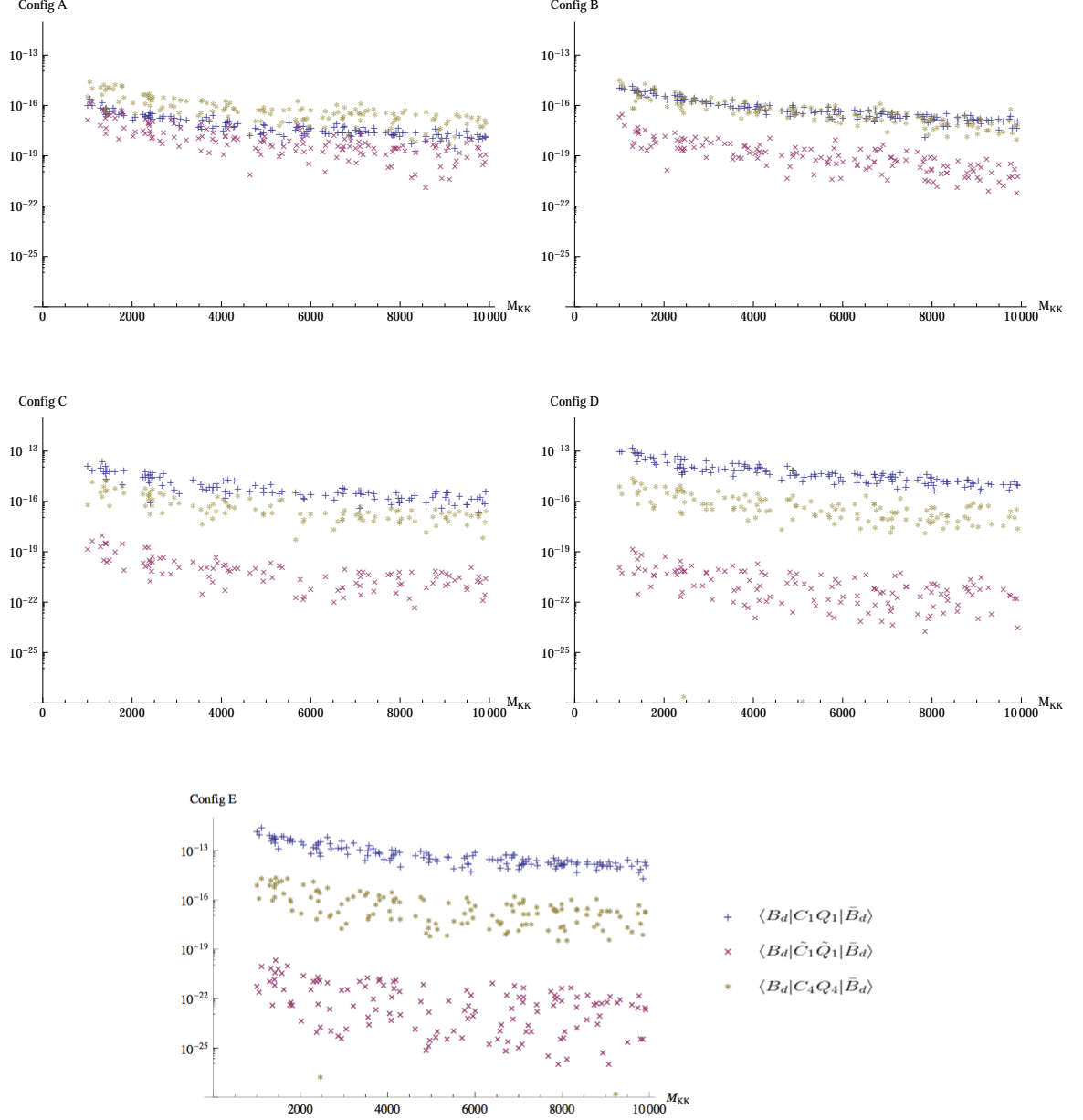


Figure 6.11: The relative sizes of terms in the absolute values of the amplitude for $B_d - \bar{B}_d$ mixing from operators Q_1 , \tilde{Q}_1 and Q_4 , giving the dominant LL, RR and RL contributions respectively, $\nu = 2, \alpha = 2$.

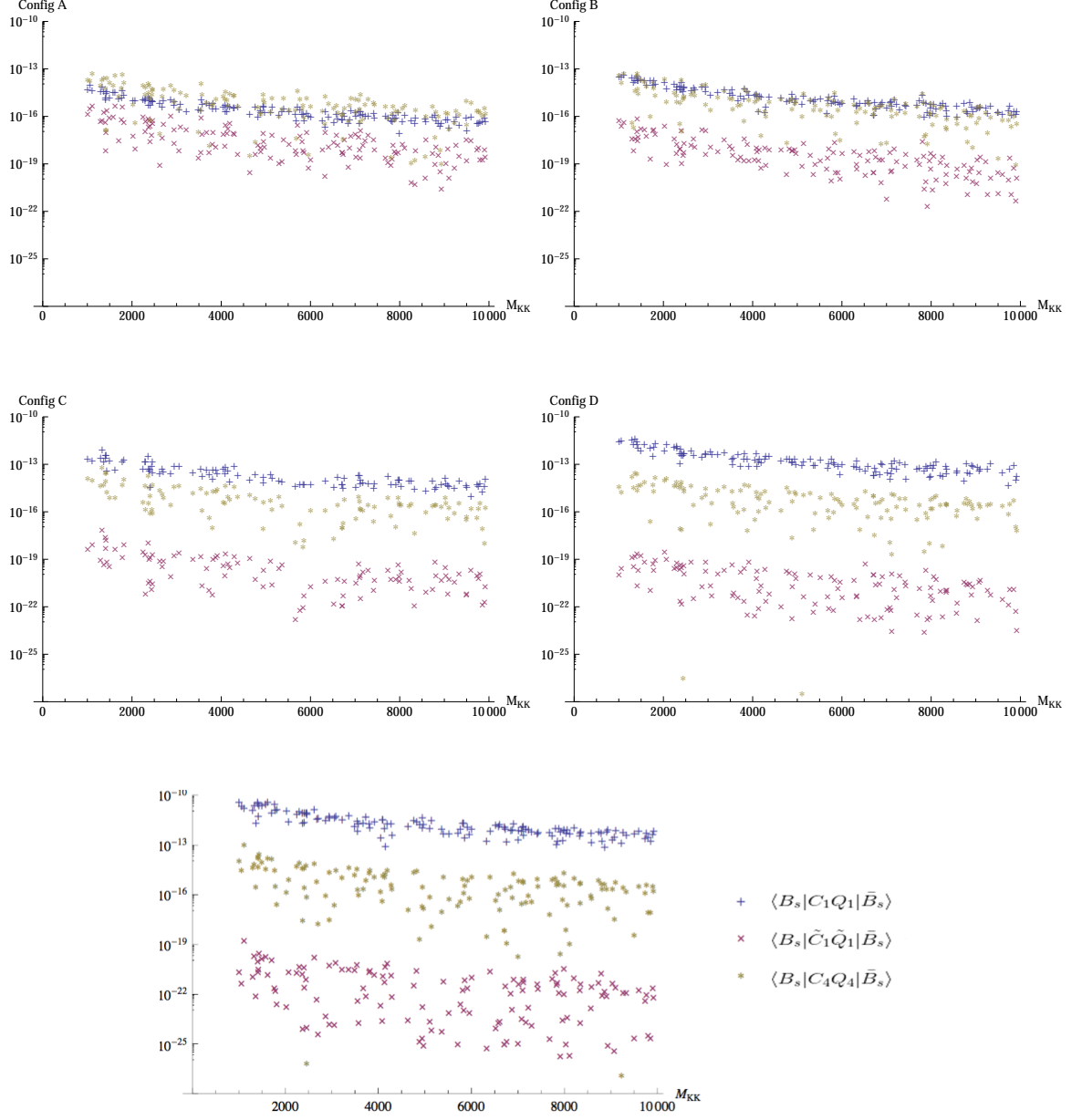


Figure 6.12: The relative sizes of terms in the absolute values of the amplitude for $B_s - \bar{B}_s$ mixing from operators Q_1 , \tilde{Q}_1 and Q_4 , giving the dominant LL, RR and RL contributions respectively, for $\nu = 2, \alpha = 2$.

Chapter 7

Summary and Conclusions

Warped extra dimensions provide a natural explanation of several of the observed features of nature which have not yet been explained by the standard model of particle physics. In particular, the large hierarchy between the Planck and EW scales and the pattern of fermion masses, can be generated through the geometrical mechanism proposed by Randall and Sundrum, without the need for significant fine-tuning of parameters. It is plausible that such a 5D model could be realised in nature, either as a standalone theory of EW scale physics up to M_{Pl} , or perhaps within the framework of some larger more fundamental theory, as part of a product manifold in a Type-II string theory[46], for example.

In any case, it is clear that there are phenomenological constraints on WED theories, notably those on the generation of tree-level FCNCs. It is also clear, however, that there are viable regions of the parameter space, and that it is certainly possible to satisfy constraints on flavour violation in both the kaon and B-meson mixing systems, in the presence of the naturally arising RS-GIM mechanism. The challenge is to employ this mechanism to balance the flavour constraints against the requirement of producing the

correct SM fermion masses and mixing angles with anarchic 4D Yukawas. It had been shown previously that this may be accomplished in the RS scenario, but more easily in the SW scenario [8] and we have now explored a two-parameter family of warped 5D geometries and elucidated the relationship between the precise geometry of the dimension and the degree of flavour violation in both the K and B meson sectors. One could certainly, however, go further and deeper into this study. The path to doing so is now clear, particularly regarding the computation of the bosonic propagators for arbitrary dilaton in a soft-wall context. We have seen that by employing a power series expansion in the square of the momentum in the massless case, or the square of the ratio of the EW to KK scale in the massless case, one can isolate the dominant contribution in calculating the effective couplings of local vertices for flavour changing quark processes. It has been demonstrated in this work, that such a methodology is practicable not only analytically, but also numerically, for studying flavour phenomenology - or indeed any processes mediated by KK gauge bosons - across the two parameter family. This has taken shape in the form of real predictions of TeV scale effects in $\Delta F = 2$ meson processes.

The outcome is that, in the scope of the examined phenomenology, there is indeed a significant interplay between the “shape” of the extra dimension and the flavour physics. It seems, extending the logic of [8], that although the quadratic case turns out to lie in a fairly optimal region of the parameter space, the constraints can be further ameliorated by varying either the dilaton power ν or the fermion mass power α away from the values $\nu, \alpha = 2$ which had previously been studied in some detail. We have also seen that B-physics is less tightly constrained than kaon physics, and that neutral KK bosons mediating flavour-changing interactions between SM quarks could indeed give

rise to significant effects in the B-meson sector, although one would have to be artful in somehow relaxing the kaon constraints. We have seen that the introduction of an ad hoc $SU(2)$ flavour symmetry, in the form of aligning the right-handed fields in the extra dimension can greatly suppress the value of ϵ_K , although this has not been enough to permit very sizeable effects in the B system. The possibility of an $SU(3)$ symmetry has not been considered here in detail, so this could be an interesting avenue of further study. An alternative could be to raise the KK scale well beyond 10TeV, although this starts to push the physics outside the probable range of current accelerator capability, and is thus less interesting from a phenomenological point of view.

Bibliography

- [1] Georges Aad et al. Observation of a new particle in the search for the Standard Model Higgs boson with the ATLAS detector at the LHC. *Phys. Lett.*, B716:1–29, 2012.
- [2] Kaustubh Agashe, Aleksandr Azatov, and Lijun Zhu. Flavor Violation Tests of Warped/Composite SM in the Two-Site Approach. *Phys. Rev.*, D79:056006, 2009.
- [3] Kaustubh Agashe, Andrew E. Blechman, and Frank Petriello. Probing the Randall-Sundrum geometric origin of flavor with lepton flavor violation. *Phys. Rev.*, D74:053011, 2006.
- [4] Kaustubh Agashe, Gilad Perez, and Amarjit Soni. B-factory signals for a warped extra dimension. *Phys.Rev.Lett.*, 93:201804, 2004.
- [5] Kaustubh Agashe, Gilad Perez, and Amarjit Soni. Flavor structure of warped extra dimension models. *Phys.Rev.*, D71:016002, 2005.
- [6] Sinya Aoki, Yasumichi Aoki, Claude Bernard, Tom Blum, Gilberto Colangelo, et al. Review of lattice results concerning low-energy particle physics. *Eur.Phys.J.*, C74:2890, 2014.
- [7] Paul R. Archer. *Constraints on Models with Warped Extra Dimensions*. PhD thesis, Sussex U., 2011.
- [8] Paul R. Archer, Stephan J. Huber, and Sebastian Jager. Flavour Physics in the Soft Wall Model. *JHEP*, 1112:101, 2011.

- [9] Michael Atkins and Stephan J. Huber. Suppressing Lepton Flavour Violation in a Soft-Wall Extra Dimension. *Phys.Rev.*, D82:056007, 2010.
- [10] Ronald Babich, Nicolas Garron, Christian Hoelbling, Joseph Howard, Laurent Lelouch, and Claudio Rebbi. K^0 - \bar{K}^0 mixing beyond the standard model and CP-violating electroweak penguins in quenched QCD with exact chiral symmetry. *Phys. Rev.*, D74:073009, 2006.
- [11] Brian Batell, Tony Gherghetta, and Daniel Sword. The Soft-Wall Standard Model. *Phys.Rev.*, D78:116011, 2008.
- [12] M. Bauer, S. Casagrande, U. Haisch, and M. Neubert. Flavor Physics in the Randall-Sundrum Model: II. Tree-Level Weak-Interaction Processes. *JHEP*, 1009:017, 2010.
- [13] Monika Blanke, Andrzej J. Buras, Bjoern Duling, Stefania Gori, and Andreas Weiler. $\Delta F=2$ Observables and Fine-Tuning in a Warped Extra Dimension with Custodial Protection. *JHEP*, 03:001, 2009.
- [14] Joachim Brod and Martin Gorbahn. Next-to-Next-to-Leading-Order Charm-Quark Contribution to the CP Violation Parameter ϵ_K and ΔM_K . *Phys. Rev. Lett.*, 108:121801, 2012.
- [15] Andrzej J. Buras. Weak Hamiltonian, CP violation and rare decays. pages 281–539, 1998.
- [16] Andrzej J. Buras and Diego Guadagnoli. Correlations among new CP violating effects in $\Delta F = 2$ observables. *Phys. Rev.*, D78:033005, 2008.
- [17] Andrzej J. Buras, Sebastian Jager, and Jorg Urban. Master formulae for $\Delta F=2$ NLO QCD factors in the standard model and beyond. *Nucl. Phys.*, B605:600–624, 2001.
- [18] Joan A. Cabrer, Gero von Gersdorff, and Mariano Quiros. Soft-Wall Stabilization. *New J.Phys.*, 12:075012, 2010.

- [19] Joan A. Cabrer, Gero von Gersdorff, and Mariano Quiros. Suppressing Electroweak Precision Observables in 5D Warped Models. *JHEP*, 1105:083, 2011.
- [20] Joan A. Cabrer, Gero von Gersdorff, and Mariano Quiros. Flavor Phenomenology in General 5D Warped Spaces. *JHEP*, 1201:033, 2012.
- [21] N. Carrasco, P. Dimopoulos, R. Frezzotti, V. Lubicz, G. C Rossi, S. Simula, and C. Tarantino. Delta S=2 and Delta C=2 bag parameters in the SM and beyond from Nf=2+1+1 twisted-mass LQCD. *Phys. Rev.*, D92(3):034516, 2015.
- [22] S. Casagrande, F. Goertz, U. Haisch, M. Neubert, and T. Pfoh. Flavor Physics in the Randall-Sundrum Model: I. Theoretical Setup and Electroweak Precision Tests. *JHEP*, 10:094, 2008.
- [23] We-Fu Chang, John N. Ng, and Jackson M. S. Wu. Flavour Changing Neutral Current Constraints from Kaluza-Klein Gluons and Quark Mass Matrices in RS1. *Phys. Rev.*, D79:056007, 2009.
- [24] J. Charles et al. Current status of the Standard Model CKM fit and constraints on $\Delta F = 2$ New Physics. *Phys. Rev.*, D91(7):073007, 2015.
- [25] Serguei Chatrchyan et al. Observation of a new boson at a mass of 125 GeV with the CMS experiment at the LHC. *Phys. Lett.*, B716:30–61, 2012.
- [26] T.P. Cheng and L.F. Li. *Gauge Theory of Elementary Particle Physics*. Oxford science publications. Clarendon Press, 1984.
- [27] J.H. Christenson, J.W. Cronin, V.L. Fitch, and R. Turlay. Evidence for the 2 pi Decay of the $k(2)0$ Meson. *Phys.Rev.Lett.*, 13:138–140, 1964.
- [28] Csaba Csaki and David Curtin. A Flavor Protection for Warped Higgsless Models. *Phys. Rev.*, D80:015027, 2009.
- [29] Csaba Csaki, Adam Falkowski, and Andreas Weiler. The Flavor of the Composite Pseudo-Goldstone Higgs. *JHEP*, 0809:008, 2008.

- [30] A. Delgado, A. Pomarol, and M. Quiros. Electroweak and flavor physics in extensions of the standard model with large extra dimensions. *JHEP*, 01:030, 2000.
- [31] Adam Falkowski and Manuel Perez-Victoria. Electroweak Breaking on a Soft Wall. *JHEP*, 0812:107, 2008.
- [32] V. Faraoni and E. Gunzig. Einstein frame or Jordan frame? *Int. J. Theor. Phys.*, 38:217–225, 1999.
- [33] Maxime Gabella. The randall-sundrum model, 2006.
- [34] Tony Gherghetta and Alex Pomarol. Bulk fields and supersymmetry in a slice of AdS. *Nucl.Phys.*, B586:141–162, 2000.
- [35] S. L. Glashow, J. Iliopoulos, and L. Maiani. Weak interactions with lepton - hadron symmetry. *Phys. Rev.*, D2:1285–1292, 1970.
- [36] Walter D. Goldberger and Mark B. Wise. Modulus stabilization with bulk fields. *Phys. Rev. Lett.*, 83:4922–4925, 1999.
- [37] Stephan J. Huber. Flavor physics and warped extra dimensions. In *Supersymmetry and unification of fundamental interactions. Proceedings, 10th International Conference, SUSY’02, Hamburg, Germany, June 17-23, 2002*, pages 1533–1538, 2002.
- [38] Stephan J. Huber. Flavor violation and warped geometry. *Nucl.Phys.*, B666:269–288, 2003.
- [39] Stephan J. Huber and Qaisar Shafi. Fermion masses, mixings and proton decay in a Randall-Sundrum model. *Phys.Lett.*, B498:256–262, 2001.
- [40] Alfredo Iorio, L. O’Raifeartaigh, I. Sachs, and C. Wiesendanger. Weyl gauging and conformal invariance. *Nucl. Phys.*, B495:433–450, 1997.
- [41] C. Itzykson and J. B. Zuber. Quantum field theory. 1980. New York, Usa: Mcgraw-hill (1980) 705 P.(International Series In Pure and Applied Physics).

- [42] Andreas Karch, Emanuel Katz, Dam T. Son, and Mikhail A. Stephanov. Linear confinement and AdS/QCD. *Phys.Rev.*, D74:015005, 2006.
- [43] Jaehoon Leem et al. Calculation of BSM Kaon B-parameters using Staggered Quarks. *PoS, LATTICE2014*:370, 2014.
- [44] A. Lenz, U. Nierste, J. Charles, S. Descotes-Genon, A. Jantsch, et al. Anatomy of New Physics in $B - \bar{B}$ mixing. *Phys.Rev.*, D83:036004, 2011.
- [45] Alexander Lenz. B -mixing in and beyond the Standard model. In *8th International Workshop on the CKM Unitarity Triangle (CKM2014) Vienna, Austria, September 8-12, 2014*, 2014.
- [46] Juan Martin Maldacena. The Large N limit of superconformal field theories and supergravity. *Int. J. Theor. Phys.*, 38:1113–1133, 1999. [Adv. Theor. Math. Phys.2,231(1998)].
- [47] Stephen P. Martin. A Supersymmetry primer. 1997. [Adv. Ser. Direct. High Energy Phys.18,1(1998)].
- [48] S. Mert Aybat and Jose Santiago. Bulk Fermions in Warped Models with a Soft Wall. *Phys.Rev.*, D80:035005, 2009.
- [49] Peter J. Mohr, Barry N. Taylor, and David B. Newell. CODATA Recommended Values of the Fundamental Physical Constants: 2010. *Rev. Mod. Phys.*, 84:1527–1605, 2012.
- [50] G. Moreau and J. I. Silva-Marcos. Flavor physics of the RS model with KK masses reachable at LHC. *JHEP*, 03:090, 2006.
- [51] Ulrich Nierste. Three Lectures on Meson Mixing and CKM phenomenology. In *Heavy quark physics. Proceedings, Helmholtz International School, HQP08, Dubna, Russia, August 11-21, 2008*, pages 1–38, 2009.
- [52] K.A. Olive et al. Review of Particle Physics. *Chin.Phys.*, C38:090001, 2014.

- [53] Antonio Pich. Effective field theory: Course. In *Probing the standard model of particle interactions. Proceedings, Summer School in Theoretical Physics, NATO Advanced Study Institute, 68th session, Les Houches, France, July 28-September 5, 1997. Pt. 1, 2*, pages 949–1049, 1998.
- [54] Pierre Ramond. *Field theory: a modern primer*. Frontiers in Physics. Benjamin-Cummings, Reading, MA, 1981.
- [55] Lisa Randall and Matthew D. Schwartz. Quantum field theory and unification in AdS5. *JHEP*, 0111:003, 2001.
- [56] Lisa Randall and Raman Sundrum. A Large mass hierarchy from a small extra dimension. *Phys.Rev.Lett.*, 83:3370–3373, 1999.
- [57] Lisa Randall and Raman Sundrum. An Alternative to compactification. *Phys.Rev.Lett.*, 83:4690–4693, 1999.
- [58] Gero von Gersdorff. From Soft Walls to Infrared Branes. *Phys.Rev.*, D82:086010, 2010.
- [59] Gero von Gersdorff. Flavor Physics in Warped Space. *Mod. Phys. Lett.*, A30(15):1540013, 2015.